FROM SMALL WATERSHEDS TO REGIONS: VARIATION IN HYDROLOGIC RESPONSE TO URBANIZATION

by

Kristina Gina Hopkins

Bachelors of Science in Biology and Environmental Science, Syracuse University, 2007

Bachelors of Arts in Geography, Syracuse University, 2007

Submitted to the Graduate Faculty of the

Kenneth P. Dietrich School of Arts and Sciences in partial fulfillment

of the requirements for the degree of

Doctor of Philosophy

University of Pittsburgh

2014

UNIVERSITY OF PITTSBURGH

Kenneth P. Dietrich School of Arts and Sciences

This dissertation was presented

by

Kristina Gina Hopkins

It was defended on

July 10, 2014

and approved by

Emily Elliott, Assistant Professor, Department of Geology and Planetary Science

Michael Ramsey, Professor, Department of Geology and Planetary Science

Jorge Abad, Assistant Professor, Water Resources Engineering

Molly Mehling, Assistant Professor, Ecology and Sustainability

Dissertation Advisor: Daniel Bain, Assistant Professor, Department of Geology and Planetary Science

FROM SMALL WATERSHEDS TO REGIONS: VARIATION IN HYDROLOGIC RESPONSE TO URBANIZATION

Kristina G. Hopkins, PhD

University of Pittsburgh, 2014

Urbanization leads to a decline in the quality of aquatic ecosystems through the alteration of the natural hydrologic cycle. Existing conceptual models specify impervious surfaces as the dominant driver of hydrologic changes because impervious surfaces significantly alter the amount and timing of water flowing through aquatic ecosystems. However, existing models oversimplify how a natural watershed becomes degraded during urbanization, minimizing the spatiotemporal variability of urban stressors.

Urbanization gradients and long-term watershed studies are two approaches used to characterize hydrologic changes associated with development. Both approaches were used to quantify variability in the type of hydrologic changes among nine U.S. cities and to assess the human- and natural-factors driving regional differences in hydrologic response. Hydrologic analysis indicated an increase in the frequency of high flow events across all nine urbanization gradients. However, the severity of hydrologic change varied among cities and was not driven by inter-city differences in developed land-cover or impervious surfaces among gradients. Instead, physiographic setting best explained inter-city variability. Cities with glacial histories had less hydrologic change relative to development intensity when compared to cities without glacial histories. Glacial history sets a template of physical features (i.e., low relief and high water-storage) that can provide hydrologic buffering to dampen the runoff signature of high flow events. In conjunction with gradients, long-term watershed studies were used to identify the timing of flow alterations. Hydrologic and development datasets were used to reconstruct the dynamics of urbanization in seven study watersheds in three U.S. cities. In a Pittsburgh watershed, a hydrologic model indicated urbanization lead to a 50% reduction in water yield through the inter-basin transfer of stream water and urban runoff. Additional long-term watershed studies demonstrated abrupt shifts in stream flow and temporal lags in hydrologic response. The magnitude of hydrologic shifts was proportional to development intensity, whereas the timing of hydrologic shifts depended on interactions with perturbations such as extreme weather events and construction projects. The results from both approaches were used to construct a framework describing the range of physical and hydrologic changes associated with development, as well as major mechanisms that drive hydrologic change.

TABLE OF CONTENTS

LIST OF TABLES

LIST OF FIGURES

PREFACE

Funding for this research was provided by the University of Pittsburgh, Heinz Foundations, the Richard King Mellon Foundation, and the Long-Term Ecological Research program's Network Office (NSF #0832652 and #0936498) via the Urban Aquatics Working Group.

This work would not have been possible without the help from collaborators in Pittsburgh including, Erin Copeland (Pittsburgh Parks Conservancy) and Joe Fedor (ALCOSAN), as well as members of the Urban Aquatic Working Group including, Nat Morse (UNH), Nancy Grimm (ASU), Jen Morse (PSU), Monica Palta (ASU), Neil Bettez (Cary Inst.), Anika Bratt (UMN), Amanda Suchy (ASU), and Rose Smith (UMD).

I would like to acknowledge all those at the University of Pittsburgh who helped with data collection and analysis. This includes Mark Christopher Scott, Bob Gradeck, Tom Antonacci, and Jess Bobryznski. I would also like to thank members of the Bain and Elliott lab groups all their support over the years, particularly for feedback on manuscript drafts, presentations, and fellowship applications, including Marion Divers, Erin Pfeil-McCullough, Rob Rossi, Lucy Rose, Katherine Redling, Sarah Lavin, Kassia Groszewski, and Zhongjie Yu.

I would like to thank my committee members for the wealth of guidance and all of their comments. Thank you to William Shuster at the Environmental Protection Agency, for his support and thoughtful comments on manuscript drafts and my dissertation chapters. His feedback helped strengthen the quality of the work presented in my dissertation. A special thanks to my advisor, Dan Bain for guiding through the past four years and for providing me with countless ideas and feedback on anything I would send his way, pictures of sewers included. Thank you for sharing your experiences and knowledge with me and for encouraging me to apply for any and all opportunities to expand my graduate experience beyond the opportunities at the University of Pittsburgh. You truly broadened my horizon and helped me grow as a scientist.

Finally, I would like to thank my parents and sister for supporting me through my time in graduate school. I couldn’t have done this without your encouragement. I would like to give a special thank you to my husband, Justin Hynicka for his support, encouragement, and help figuring out statistics in R.

1.0 INTRODUCTION

As urban populations continue to grow, urban land-cover is expected to nearly triple in extent by the year 2030 [*Seto et al.*, 2012]. The growth of cities requires the conversion of lands from agricultural and natural areas into urban areas including the construction of buildings, roadways, and sewer/water lines. These infrastructure are fundamental to urban populations, allowing the import of resources for consumptive uses and the export of wastes [*Grimm et al.*, 2008]. The conversion of land to urban land-cover has led to a consistent decline in the quality of urban aquatic ecosystems, termed the “urban stream syndrome” [*Walsh et al.*, 2005a; *Meyer et al.*, 2005]. A growing body of research documents the symptoms of urban stream syndrome, which include altered hydrologic regimes [*Konrad and Booth*, 2005; *DeGasperi et al.*, 2009], elevated nutrient and contaminant concentrations [*Klein*, 1979; *Driscoll et al.*, 2003], geomorphic changes in stream channels [*Wolman*, 1967; *Leopold et al.*, 2005], and declines in aquatic plant and animal communities [*Fitzpatrick et al.*, 2005]. Many of these studies conclude that the dominant factor driving changes in urban aquatic ecosystems is the connection of impervious surfaces to the stream network and the generation of urban stormwater runoff [*Schueler*, 1994; *Schueler et al.*, 2009]. The impervious cover model predicts that stream quality will decline as watershed impervious cover increases, with a 10% impervious cover threshold above which aquatic ecosystems become impacted by development (Figure 1-1).

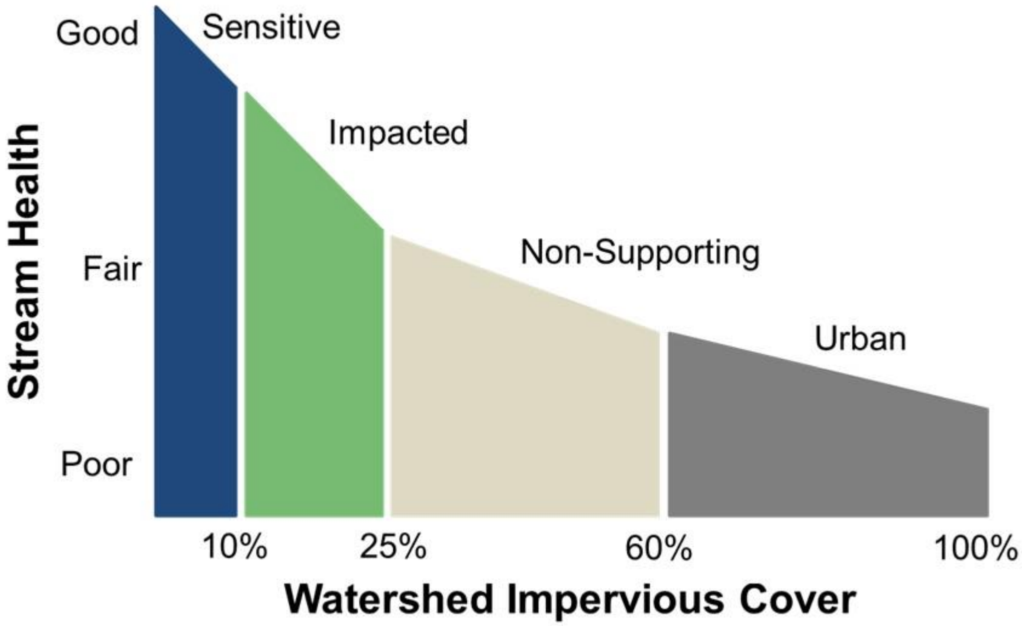

Figure 1-1: Relationship between watershed impervious cover and stream health. Previous studies have found stream quality typically declines as watershed impervious cover increases. Adapted from *Schueler et al.* [2009].

This dissertation focuses on how urbanization alters hydrologic regimes. The hydrologic regime describes the distribution of water among water cycle components and is particularly important because it controls the form and function of aquatic ecosystems by regulating the amount, timing, and delivery of water, nutrients, and contaminants to stream ecosystems [*Poff et al.*, 1997]. Existing conceptual models link the growth of impervious surfaces to changes in water balance components, such as runoff, infiltration, and evapotranspiration [*Arnold and Gibbons*, 1996]. The expansion of impervious surfaces re-routes water from infiltration dominated pathways to runoff dominated pathways (Figure 1-2). In forested watersheds, the majority of precipitation is infiltrated into the soil and runoff generation is low. As impervious surfaces expand the proportion of precipitation routed to runoff increases, leading to an increase in the frequency and magnitude of high flow events [*Konrad and Booth*, 2005].

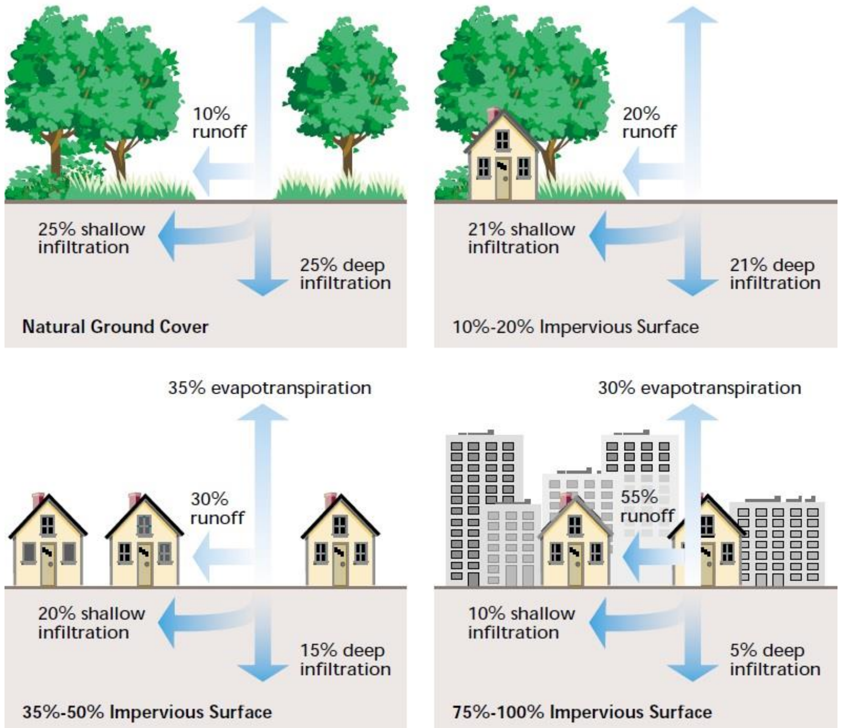

Figure 1-2: Conceptual model of the relationship between impervious surfaces and the proportion of precipitation distributed among water balance components. Figure from FISRWG [1998].

Existing conceptual models (e.g., urban stream syndrome) identify general processes linking impervious surfaces to altered hydrologic regimes. However, existing models oversimplify the process of how a natural watershed becomes degraded during the process of urbanization and minimize the spatial and temporal variability in watershed stressors during urbanization. In addition, existing models often negate heterogeneity in development patterns and water management styles, that can vary widely among urban watersheds and metropolitan areas [*Brown et al.*, 2009a]. Furthermore, variability in the phase of urban development and underlying differences in precipitation, physiographic setting, and geology likely drive variability in stream flow response to urbanization [*Roy et al.*, 2009].

This dissertation examines stormwater runoff and impervious surfaces as the drivers of aquatic ecosystem declines in a wider context. The process of urbanization and alterations to the physical landscape in different physiographic settings (i.e., glaciated and non-glaciated) are characterized. In addition, the type, timing, and magnitude of hydrologic changes during urbanization in nine U.S. cities are assessed. Clarifying regional variability in stream flow changes during urbanization is particularly important because the hydrologic regime is considered one of the primary drivers of physiochemical changes in aquatic ecosystems [*Power et al.*, 1995; *Poff et al.*, 1997]. Further, spatiotemporal dynamics in development patterns, temporal trends in hydrologic alterations during urbanization, and how these factors vary among cities are explicitly quantified. This research refines the existing conceptual model of urban stream syndrome by incorporating spatiotemporal dynamics and clarifies additional water cycle components influencing the syndrome.

The first study, (Chapter 2) characterizes long-term changes in human infrastructure during the urbanization of a small watershed in Pittsburgh, PA and human-induced alterations to natural watershed hydrology. This work was published in *Landscape Ecology* in 2014 [*Hopkins et al.*, 2014]. The study integrates a spatiotemporal reconstruction of human- (i.e., sewers and housing) and natural-infrastructure (i.e., tree canopy) changes during urbanization into a hydrologic model to quantify coincident changes in annual water yield, as well as alterations in runoff routing, infiltration processes, and evapotranspiration. Results from Chapter 2 were used to refine and integrate three additional human and hydrologic components into existing conceptual frameworks, including the integration of (1) the arrangement and connectivity of sewer and drainage infrastructure to assess potential water transfers, (2) the age of sewer infrastructure to assess groundwater subsidies from leaking pipes, and (3) the extent of tree canopy cover to assess changes in rainfall interception and evapotranspiration. Integrating these three factors into the hydrologic model improved the model's estimate of changes in annual water yield within the study watershed. The spatial arrangement and density of combined sewer pipes in the watershed was used to identify changes to drainage patterns over time and coincident impacts on annual water yield. The infrastructure reconstruction was also used to integrate the hydrologic impacts of the growth of the urban tree canopy cover and the deterioration of sewer infrastructure into the water yield model. Overall, examining the evolution of human- and natural-infrastructure allowed for the characterization of explicit connections between upstream development and downstream hydrologic effects during the last century. Moreover, this approach provides a contextual understanding of urban stream degradation within the Panther Hollow watershed that clarifies additional important components influencing urban stream syndrome, including inter-basin transfers and changes in evapotranspiration and groundwater subsidies.

Integrating a broader context into our conceptual frameworks is particularly important because hydrologic changes are not consistent among watersheds within the same city or among different cities. Inter-city variability in urban hydrologic alterations are recognized in a limited number of studies [*Brown et al.*, 2009b; *Utz et al.*, 2011]. However, these studies did not propose frameworks to explain inter-city variability in hydrologic regime shifts and only suggest potential contributing factors. Given that a vast amount of hydrologic data is collected by the U.S. Geological Survey (USGS) stream-gaging network it is possible to characterize hydrologic changes among a large study set of watersheds spanning multiple cities across physiographic regions. Chapter 3 used existing data sources to quantify changes in a suite of hydrologic metrics calculated from stream flow records in 76 watersheds in nine U.S. cities. Watersheds were selected to span an urbanization gradient in each study city and each stream flow record was used to characterize the magnitude and direction (i.e., increase or decrease) of changes in high flow frequency, high flow duration, the magnitude of maximum flows, and baseflow across each city's urbanization gradient. These data allow for the evaluation of hydrologic changes in each city using a single, standardized method to clarify the drivers of inter-city differences in hydrologic response to urbanization. Chapter 3 demonstrated the importance of physiographic region, specifically glaciation history, which sets a template of physical characteristics (e.g., topography and water storage capacity). The physical template strongly influences the type and magnitude of hydrologic changes within a city and can explain larger-scale hydrologic patterns identified in the study cities. Overall, adding physiographic context to our conceptual framework can reveal mechanisms important to hydrologic response in cities across the globe.

The urbanization gradient approach is widely used to assess the effects of urbanization on aquatic ecosystems. However, the gradient approach cannot be used to identify when flow alterations began or if the timing of hydrologic alterations coincided with a certain threshold level of development. Chapter 4 utilized a long-term watershed approach to characterize variability in hydrologic alterations as a watershed urbanizes. The availability of long-term hydrologic datasets is limited, especially datasets spanning both pre- and post-urbanization periods. This study identified six watersheds with stream flow records spanning a time period that bounded watershed urbanization. Methods for this study built upon the historical reconstruction approach utilized in Chapter 2, focusing on a subset of cities (Baltimore, MA, Boston, MA, and Pittsburgh, PA) from Chapter 3. Property tax assessment records were used to characterize the timing and intensity of development in each watershed. Stream flow records were used to calculate annual statistics for two common hydrologic metrics: (1) high flow frequency and (2) runoff efficiency. Results from Chapter 4 revealed the extreme alteration of flows in urban watersheds, including abrupt shifts in flow metrics that lag behind the period of peak watershed development. As far as I know, no previous study has identified hydrologic lags in urbanizing watersheds. Chapter 4 explored potential drivers of variability in the magnitude of stream flow shifts among watersheds and potential explanations for why flow shifts lagged behind the period of intense watershed development. Understanding the timing of hydrologic impairment relative to urban development can clarify the relative importance of short-term events (i.e., floods) and long-term processes (i.e. watershed development) in explaining observed hydrologic changes.

This dissertation refines the existing conceptual model of urban stream syndrome, incorporating the arrangement and age of infrastructure, urban tree canopy cover, and baseline hydrologic conditions that depend on physiographic setting, particularly recent glacial history. This refined framework can be used to better assess the magnitude, timing, and drivers of hydrologic changes during urbanization in other watershed and regions across the globe. Further, studies using spatiotemporal reconstructions of development and hydrologic changes can better inform restoration planning efforts, particularly by characterizing pre-development baselines and the type and severity of hydrologic changes. In addition, the methods presented in this dissertation can be used to evaluate the function of sustainable stormwater management practices in efforts to return flow regimes closer to pre-urban conditions.

2.0 RECONSTURCTION OF A CENTURY OF LANDSCAPE MODIFICATION AND HYDROLOGIC CHANGE IN A SMALL URBAN WATERSHED

2.1 INTRODUCTION

Conceptual models provide a powerful framework for predicting the impacts of urbanization on aquatic ecosystems from both ecological [*Walsh et al.*, 2005a; *Groffman et al.*, 2003] and geomorphological [*Wolman*, 1967] perspectives. Prevailing models attribute aquatic degradation primarily to impervious surfaces, such as roadways and rooftops, which reduce infiltration and transport water and pollutants quickly to receiving streams [*Schueler*, 1994; *Arnold and Gibbons*, 1996]. Degraded urban streams experience elevated nutrient and contaminant concentrations, flashy hydrographs, incised and widened stream channels, and altered plant and animal communities [*Paul and Meyer*, 2001; *Meyer et al.*, 2005].

Landscape connectivity, particularly the connection of impervious surfaces and stormwater pipe networks to surface waterways, affects the quantity and quality of surface runoff contributions to a waterway. Refined frameworks such as "effective impervious cover" begin to account for the importance of infrastructure connectivity by examining only impervious surfaces connected directly to the stream [*Walsh et al.*, 2005a]. This metric is more strongly correlated with runoff volume [*Alley and Veenhuis*, 1983; *Driver and Troutman*, 1989] and stream health [*Lee and Hearney*, 2003] than total impervious cover. While impervious based landscape metrics are used as management tools to evaluate the relative impairment of streams, they provide limited perspective on the history of the stressors that drive aquatic ecosystem decline.

Recent advances in conceptual frameworks expand our understanding of urban aquatic ecosystems by incorporating the importance of human infrastructure evolution through time and space. The urban watershed continuum provides a foundation to integrate watershed land use history into assessments of aquatic ecosystem decline [*Kaushal and Belt*, 2012]. The framework recognizes the impacts of short-term pulses and long-term stressors on aquatic ecosystems [*Bain et al.*, 2012a; *Collins et al.*, 2011]. Short-term pulses include rapid events that input pollutants to a stream, whereas long-term stressors can span centuries and encompass the history of human landscape modifications and changes in development patterns.

This study focused on the long-term impacts of urbanization on aquatic ecosystems, hypothesizing that the legacy of human landscape modifications, particularly the spatial arrangement of sewer infrastructure and neighborhood age, imparts lasting and unique impacts on urban aquatic ecosystems. Urban neighborhoods have unique development histories. For example, the timing of urbanization influences the type of sewer and water infrastructure constructed. Older cities that built sewer systems in the early 20th century typically designed systems as combined sewers, with stormwater and sanitary sewage sharing the same pipes, while newer cities designed separate sanitary and storm sewers [*Tarr et al.*, 1984]. Many of the original brick sewer mains remain in use today and communities throughout the United States utilize sewers pipes that are over 50 years old [*Wirahadikusumah et al.*, 2001]. Evaluation of variations in watershed infrastructure age and arrangement can strengthen traditional analyses based on urban to rural gradients [*Bhaskar and Welty*, 2012] and detect additional drivers of aquatic ecosystem decline.

Despite the importance of landscape change through time and space, retrospective assessments that include reconstructions of human water infrastructure expansion remain too rare. Retrospective assessments can uncover when human built infrastructure began disrupting natural hydrologic regimes and the rates of landscape conversion through time [*Jennings and Jarnagin*, 2002]. Long-term records are challenging to reconstruct. However, examining datasets that span the period of landscape urbanization can strengthen our understanding of the cumulative factors that lead to stream impairment and improve our ability to manage water resources in the future [*Bain et al.*, 2011]. This chapter assessed the implications of long-term landscape modification on aquatic ecosystems by examining the evolution of human infrastructure patterns in a small catchment in Pittsburgh, Pennsylvania throughout the last century.

Research questions included, when and where were the buildings, roadways and sewers installed in the watershed? How does the spatial arrangement and connectivity of human infrastructure networks affect drainage patterns in the watershed throughout the last century? What are the relative impacts of deteriorating sewer infrastructure and changing tree canopy cover on the water balance? Particular attention was given to interactions among road, sewer, and stream networks and the resulting impacts on annual water yield. This study evaluated the ability of two water yield models to predict hydrologic conditions; one model based on changes in impervious cover and one based on infrastructure connectivity. Examining the evolution of infrastructure and land use transitions allows for the characterization of connections between upstream development and downstream hydrologic effects. Moreover, this approach provides a contextual understanding of urban stream degradation that may guide and increase the success of restoration projects and improve decisions made during the repair and replacement of existing infrastructure.

2.2 METHODS

2.2.1 Study area

The Panther Hollow watershed (147 ha) is a sub-basin in the Four Mile Run watershed (877 ha) located in Pittsburgh, Pennsylvania (Figure 2-1). The Panther Hollow watershed was selected to inform ongoing efforts to improve the health of the streams in the watershed through the installation of stormwater management practices [*PPC*, 2011]. The Panther Hollow watershed lies in the Western Allegheny Plateau and is underlain by the Casselman Formation, comprised of alternating layers of limestone, sandstone, and shale [*Wagner*, 1970]. Soils are predominantly formed from weathered shale and sandstone and are typically silty, clay loams [*Newbury et al.*, 1981]. Rainfall is evenly distributed throughout the year, averaging 970 mm per year.

The Panther Hollow watershed has 27% impervious cover, with the eastern half of the watershed composed of a dense residential neighborhood (14 houses/ha) and business district, while the western half is parkland containing forest land and managed lawn areas including a golf course. Two small streams flow through the parkland portion of the watershed and drain into a human-made lake (Figure 2-1). The stream network historically flowed to the Monongahela River. However, half of the reaches upstream of Panther Hollow Lake were buried and streams downstream of the lake were connected to the combined sewer system (Figure 2-1). The residential neighborhood is serviced by a combined sewer system with an overflow outfall to the Monongahela River. In 2010, 1.6 billion liters of sewage and stormwater were discharged into the Monongahela River from this outfall [*ALCOSAN* 2010].

The two streams that flow through the catchment are listed on the EPA's 303 (d) list of impaired waterways. The cause of impairment is sedimentation resulting from stream bank modification and slope destabilization. Elevated *E. coli* levels, ranging from 1,000 to 3,000 cfu/100 ml, were found in both streams during 2006 and 2007 [*VanBriessen and Schoen*, 2007]. Potential sources for *E. coli* include pet waste, goose and deer feces, and leaking sewer infrastructure.

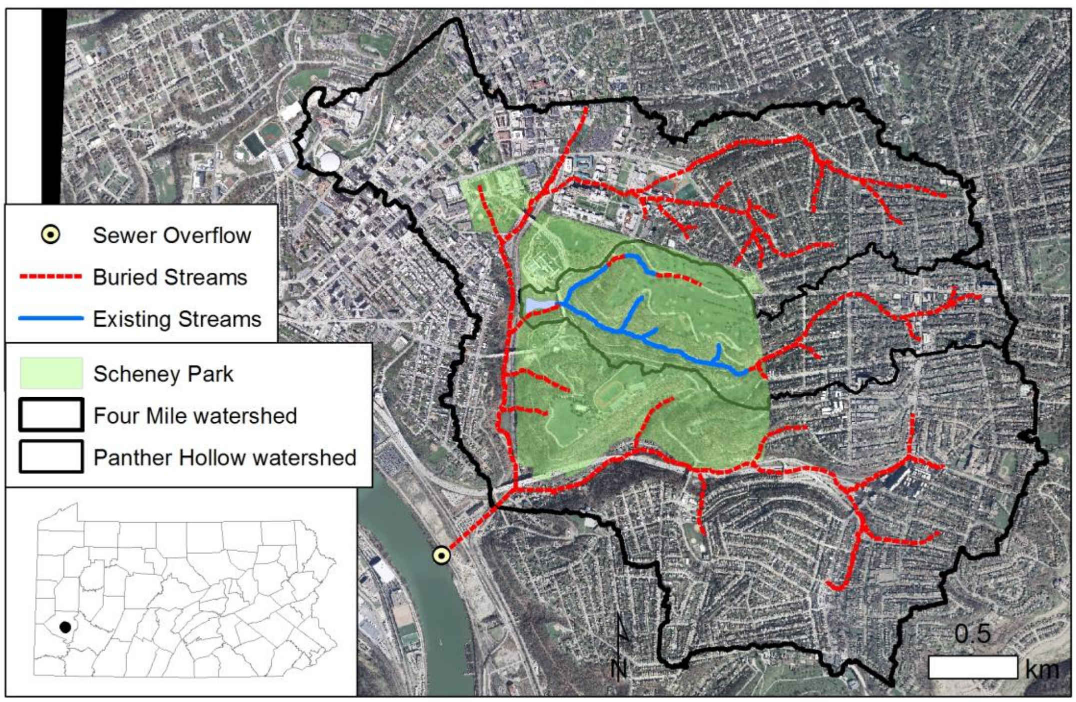

Figure 2-1: Map of the Panther Hollow sub-basin nested within the Four Mile watershed. The majority of the historical stream network is buried and piped (red lines), except for two streams in Schenley Park (blue lines). During wet weather, a mixture of stormwater runoff and sewage from the Four Mile Run watershed is discharged into the Monongahela River at the combined sewer overflow point indicated on the map. The inset shows the location of the Four Mile watershed in the state of Pennsylvania (USA).

2.2.2 Human infrastructure reconstruction

Historical maps and aerial photography were used to reconstruct the expansion of roads and sewers and the loss of stream length in the Panther Hollow watershed (Figure 2-2). Aerial photographs and historical maps were rectified to 2010 USGS digital orthophoto quarter quads using image-to-image recognition techniques and a first order polynomial transformation in ArcMap10 (ESRI). Road, sewer, and stream networks shown on G. M. Hopkins Company Maps (1872, 1882, 1890, 1898, 1904, 1911, 1923, and 1939) were digitized and attributed with the earliest depiction of each segment [*UPitt*, 2012]. In addition, infrastructure removed during reorganization were digitized and similarly attributed with the earliest indication of abandonment. Reorganizations include the removal of streets to allow for additional housing construction. Human infrastructure networks were clipped to the watershed area and totaled to provide an estimate of road, sewer, and stream length for each digitized map. Linear interpolation was used to estimate road and sewer length for years not included in map coverage.

Housing growth was reconstructed using a building description database obtained from the Pittsburgh Neighborhood and Community Information System (PNCIS) and Allegheny County Property Tax Assessment records from 2010. Parcels in the watershed were joined by map block number to the inventory of building descriptions. A housing construction date was assigned to each parcel in the basin. Building construction dates during the early 1900s appeared to assign uncertain housing construction dates to the start of the nearest decade. Therefore, our building inventory was generalized to decadal time steps from 1900 to 2010. To confirm housing estimates, trends in neighborhood growth were compared with watershed population estimates obtained from tract-level United States Census records. Linear interpolation was used to estimate annual changes in building densities and population between decades.

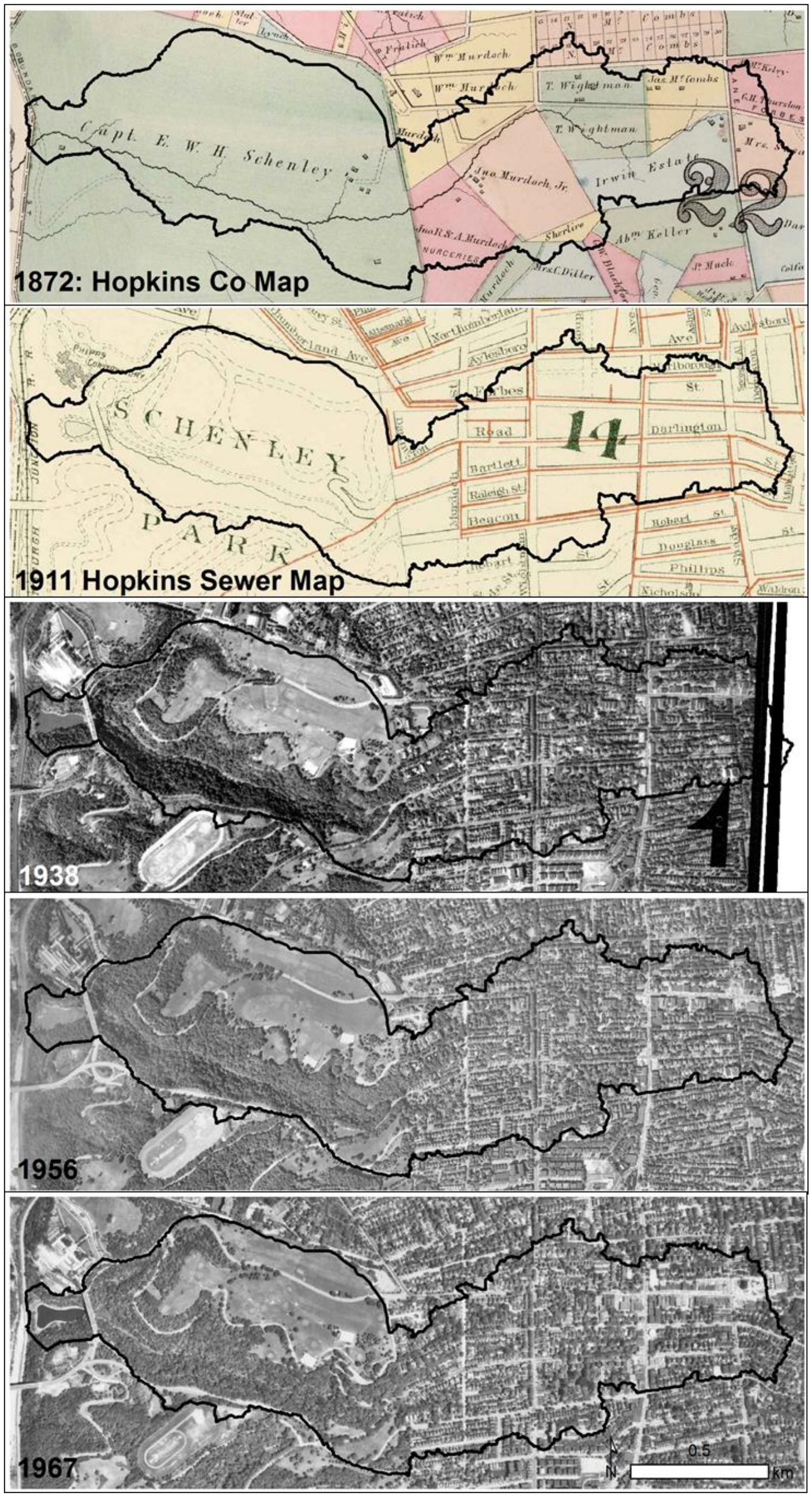

Figure 2-2: Historical maps and aerial photographs used for infrastructure reconstructions.

2.2.3 Impervious cover reconstruction

Historical datasets were used to reconstruct changes in watershed impervious cover since 1870. Impervious cover was estimated using total roof and road area. Roads and roofs are the dominant hard surfaces in the watershed, comprising 82% of present day impervious cover. Total roof area was estimated for each time interval by multiplying average roof area (164 m^2) by the total number of buildings. Total road area was estimated for each time interval by multiplying average road width (10 m) by total road length. Roof and road area were summed and divided by watershed area to determine percent impervious cover for each time interval. Impervious cover in 2010 was estimated using current PNCIS datasets for building footprints, edge of street pavement, and parking lots. In addition, effective impervious cover was estimated by only counting impervious surfaces directly connected to the existing stream network.

2.2.4 Tree canopy reconstruction

Tree canopy cover was reconstructed in the commercial and residential portions of the watershed using aerial photography from 1939 to 2010. To conduct this analysis, 15% of the parcels in the watershed were randomly selected. From this subset, parcels smaller than 200 m^2 were eliminated to ensure that the sample included parcels with the majority of the area within the watershed boundary and excluded small parcels such as condominium units. Additionally, the resolution (1:20000) of the aerial photographs limited canopy delineation in small parcels (Figure 2-2). From the initial selection of 15% of the total parcels, 27 parcels were smaller than 200 m^2, leaving 145 parcels or 13% of the total number of parcels for the analysis. The parcel subset composed 25% of the total commercial parcel area and 21% of the total residential parcel area. Parcel area averaged 1,010 m^2 and 714 m^2 (parcels > 200 m^2) in the commercial and residential portions of the watershed, respectively. In the subset parcel areas averaged 1,669 m^2 (range 258 – 7,673 m^2) and 842 m^2 (range 209 – 6,720 m^2) for the commercial and residential sections, respectively. Within each zoning category the sample included both large and small parcels.

Three aerial photographs taken during the growing season in 1938, 1956, and 1967 were obtained from the Penn State University Penn Pilot archive (Figure 2-2). Aerial photographs were rectified using image-to-image recognition techniques and a first order polynomial transformation in ArcMap10 (ESRI). All transformations had root mean square errors of 35 m or less. To quantify tree canopy cover in each photograph, parcel subset boundaries were overlain on the historical photographs. The tree canopy in each parcel for each of the three photographs was visually interpreted and digitized in GIS. Overall canopy cover was estimated by summing tree canopy area in the parcel subset and dividing by total parcel subset area. Percent canopy cover was also calculated for the commercial and residential zoning groups for each year.

Canopy cover for 2010 was derived from canopy area data supplied by the Pittsburgh Urban Tree Canopy Cover (UTC) Assessment [*UTC*, 2012]. The UTC derived canopy cover from high-resolution aerial imagery from 2010 and LiDAR acquired in 2006. Parcel subset boundaries were overlain on the 2010 UTC tree canopy layer and tree canopy was clipped to the parcel boundaries. Overall canopy cover was estimated by summing tree canopy area in the parcel subset and dividing by total parcel subset area. The UTC was also used to estimate canopy cover in the entire watershed, and in residential and commercial areas.

Rectification error was assessed by spot checking twenty current building footprints in each aerial photograph. Corner-to-corner distance errors between aerial photograph buildings and building footprints averaged 6.9 m (s.d. = 2.4 m). The boundaries of parcels in each photograph may vary slightly due to rectification error. However, estimated rates of canopy area expansion were consistent, with an average expansion of the canopy area of 0.22% per year. Additionally, parcel subset estimates were cross-checked with watershed-wide estimates from 2010. Parcel subset canopy cover estimates were 1.6% higher than watershed-wide canopy cover for commercial areas and 1.7% lower for residential areas. Overall, the subset estimate was 1.7% lower than watershed canopy cover. This consistency suggested that the sample subset captures the larger watershed-wide trend.

2.2.5 Water yield model methodology

A simple water balance approach was used to reconstruct runoff proportions and annual water yield in the Panther Hollow watershed. Two models were developed to predict annual water yield, (1) one based on runoff proportions associated with varying degrees of watershed impervious cover and (2) one based on stream flow monitoring results, infrastructure connectivity, changes in tree canopy cover, and groundwater subsidies from leaking sewerlines.

The first model, the impervious cover model, estimated annual water yield using runoff proportions associated with impervious cover in the watershed. Runoff proportion is defined as the proportion of annual precipitation routed to the stream channel and is composed of baseflow contributions from shallow infiltration and storm flow contributions from direct runoff. The total water yield estimate assumed shallow infiltration would emerge in the stream as baseflow on an annual time-step. Runoff and shallow infiltration contributions, commonly relied upon when estimating impervious impacts [*Arnold and Gibbons*, 1996], were used to derive an equation to predict runoff proportion based on percent impervious cover. Average runoff estimates from

Figure 1 in Arnold and Gibbons [1996] were used to derive a relationship between runoff contributions and impervious cover:

$$R = 0.0032\ IC + 0.34 \qquad \text{(Equation 1)}$$

Runoff proportion (R) was a function of impervious cover (IC), expressed as a percentage. For each year between 1870 and 2012, annual runoff proportion in the Panther Hollow watershed was estimated using the historical impervious cover reconstruction and Equation 1. Annual yield was then predicted by applying annual estimates of runoff proportion to the annual precipitation record (1870 to 2012) from the National Weather Service Pittsburgh Station. Annual yield in mm was calculated as,

$$Y = R * P \qquad \text{(Equation 2)}$$

Where water yield (Y) equals the runoff proportion (R) times annual precipitation (P) in mm. This equation assumes the entire watershed area is contributing water to the streams (Figure 2-3A).

The foundation for the second water yield model, the infrastructure model, was Panther Hollow's contemporary runoff proportion. Contemporary annual runoff proportions were determined using five years of stream flow and precipitation records from January 2008 to December 2012. Flow data was provided by the Allegheny County Sanitary Authority (ALCOSAN) from a discharge monitoring station at the bottom of the watershed, below Panther Hollow Lake (Figure 2-3B). Discharge was recorded at 15-minute intervals using an area-velocity flow meter (American Sigma 920) installed in a 38.1 cm diameter overflow pipeline below the lake. Annual water yield was calculated by summing annual stream flow volume and dividing by the watershed area. Annual runoff proportions were determined for each year by dividing annual yield by precipitation depth obtained from the Three Rivers Wet Weather Rain

Gage Network from rain gage located within 1 km of the watershed. Annual runoff proportions averaged 0.209 (s.d. = 0.036) and the overall runoff proportion during the five year monitoring period was 0.213.

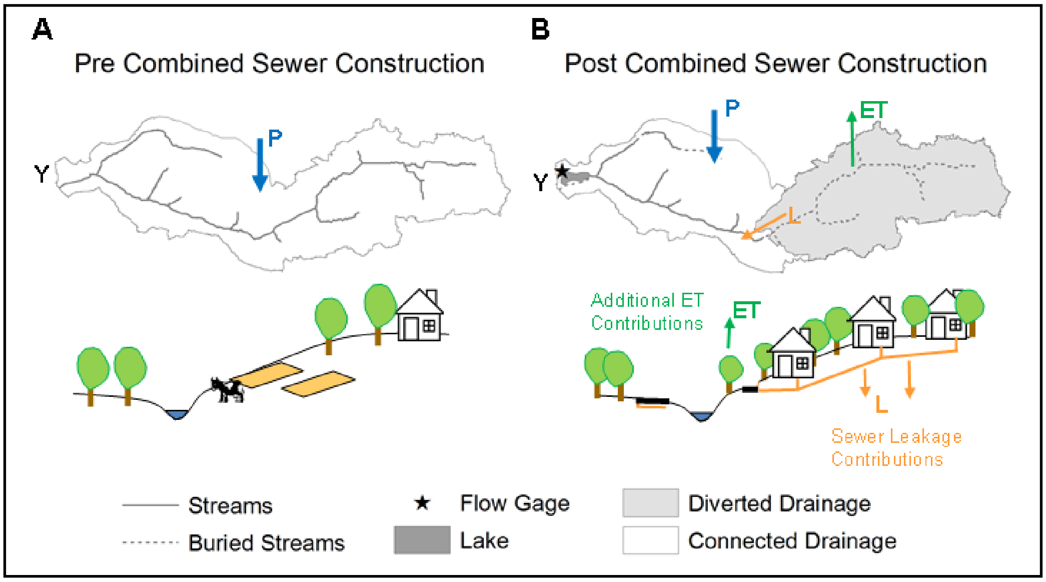

Figure 2-3: Important water balance components during pre- (A) and post-urbanization (B). Annual precipitation inputs (P) where multiplied by the runoff proportion to determine annual water yield (Y). Panel A shows the watershed prior to urbanization (pre-1900) when the entire watershed contributed drainage to the streams. Panel B shows the watershed post urbanization (post-1911) when the upper half of the watershed was connected to the combined sewer system. The infrastructure model also explored groundwater subsidies from leaking sewer lines (L) and additional exports from increased evapotranspiration (ET).

For the infrastructure water yield model, the contemporary runoff proportion of 0.21was applied to the annual precipitation record from 1911 to 2012. This runoff proportion reflected water inputs from groundwater sources and runoff from impervious surfaces directly connected to the stream from the western portion of the watershed (Figure 2-3B). A constant runoff proportion was applied because impervious surfaces directly connected to the streams during this time period remained around 10% of the directly connected watershed area. Runoff contributions from increased impervious cover in the upper, eastern portion of the watershed were routed out of the Panther Hollow watershed to an adjacent basin. Therefore, annual water yield from 1911 to 2012 was estimated using Equation 2, where $R = 0.21$ and P is annual precipitation in mm.

From 1872 to 1911, the infrastructure model incorporated changes in watershed drainage patterns during the construction of the combined sewer system. During this time period this study assumed the main factor influencing water yield in the watershed was the disconnection of the upper-basin drainage during the eleven year period between 1900 and 1911 when the combined sewer was constructed. The infrastructure reconstruction revealed ~50% of the upper-watershed was disconnected from the lower-watershed during the construction of the combined sewer system (Figure 2-3B). Impervious surfaces in the upper-watershed were connected directly to the combined sewer system and runoff from these surfaces was routed out of the Panther Hollow watershed. To account for the transfer of water draining from 50% of the basin, the runoff proportion was incrementally doubled from 0.21 to 0.42 over the course of eleven years spanning the construction of the sewer network from 1900 to 1911 and fixed at 0.42 prior to 1900. Annual water yield was then estimated using Equation 2, reconstructed runoff proportions, and annual precipitation.

2.2.6 Infrastructure model: Imported and exported water

To understand the role of other processes, the infrastructure model included estimates of increased evapotranspiration due to the growth of the urban tree canopy and additional water imports from leaking sewer lines due to deteriorating infrastructure (Figure 2-3B). Additional annual evapotranspiration was estimated from 1938 to present using the historical tree canopy reconstruction. Percent canopy increase was calculated for each year since 1938, using canopy cover in 1938 as the baseline. Additional water contributions from evapotranspiration were estimated for each year assuming that a 1% increase in tree canopy cover would reduce the total water yield by 2.2 mm [*Hibbert*, 1966]. Sewer leakage was quantified by first estimating annual sewer flow and then applying a leakage factor between 0% and 5% depending on pipe age [*Ellis et al.*, 2004]. Most of the combined sewer lines were installed in the watershed by 1910, making them 100 years old. Therefore, this study applied a leakage factor starting with 0% leakage in 1910 and adding 0.5% leakage more leakage each decade since 1910, ending with 5% leakage in 2010. Annual sewer flow was estimated by multiplying watershed population by average daily water consumption, assuming water use of 379 liters/person/day [*Gleick*, 1996] and that residential water use was the main component of sewer flow. To determine annual leakage yield, the leakage factor was applied to total annual sewer flow and divided by the watershed area. These additional water balance components were incorporated into the infrastructure model by adding and subtracting evapotranspiration and leakage contributions, respectively, to the annual yield record. The bounds of this range in estimated yield provided a measure of infrastructure yield uncertainty.

2.3 RESULTS

2.3.1 Road and sewer growth

Prior to 1900, road and sewer infrastructure was limited in the Panther Hollow watershed (Figure 2-4). Historical maps from 1872 show the Panther Hollow watershed as an agricultural landscape, with seven large parcels containing 29 structures (Figure 2-5). The two main roads that ran through the upper-basin were likely surfaced with dirt, gravel, or macadam since widespread asphalt paving did not occur until the 1920s [*McShane*, 1979]. Residents disposed of sewage on-site in privy vaults or pit-style outhouses [*Buchan*, 1948]. Households obtained water from wells, surface water, or precipitation harvesting with cisterns [*Ogle*, 1996; *Tarr*, 2005].

The transition from agriculture to urban land use occurred between 1890 and 1920. Development was concentrated in the upper-half of the watershed, while the lower-watershed remained mostly forest parkland with the exception of an eighteen-hole golf course that opened in 1902 (Figure 2-5). Between 1890 and 1911, approximately 16.7 km of brick and vitrified clay sewer pipes were installed in the watershed. Sewer infrastructure diverted water drainage from the upper-half of the watershed to an adjacent watershed (Figure 2-5). The road network expanded from 4.5 km of dirt roads to 15 km of asphalt, brick, and block surfaces [*Hopkins*, 1911]. A network of curbs, gutters, and storm drains were installed during road construction, channeling runoff to the combined sewer [*Tarr et al.*, 1984]. Approximately 2.8 km of streams (42% total stream length) were buried and piped during urbanization (Figure 2-4). A 0.9 ha lake was constructed at the mouth of the watershed around 1904. The lake outfall was connected to the newly constructed combined sewer and discharged water to the Monongahela River (Figure 2-1). The rapid installation of road, sewer, and stormwater infrastructure during the urban transition significantly altered natural drainage patterns. Half of the natural drainage area was disconnected from surface water drainage and re-routed through the combined sewer to the Monongahela River. Raw sewage and stormwater flowed into the Monongahela River until 1959 when ALCOSAN installed sewer interceptors along the river to convey sewage to a centralized treatment facility [*Tarr*, 2005].

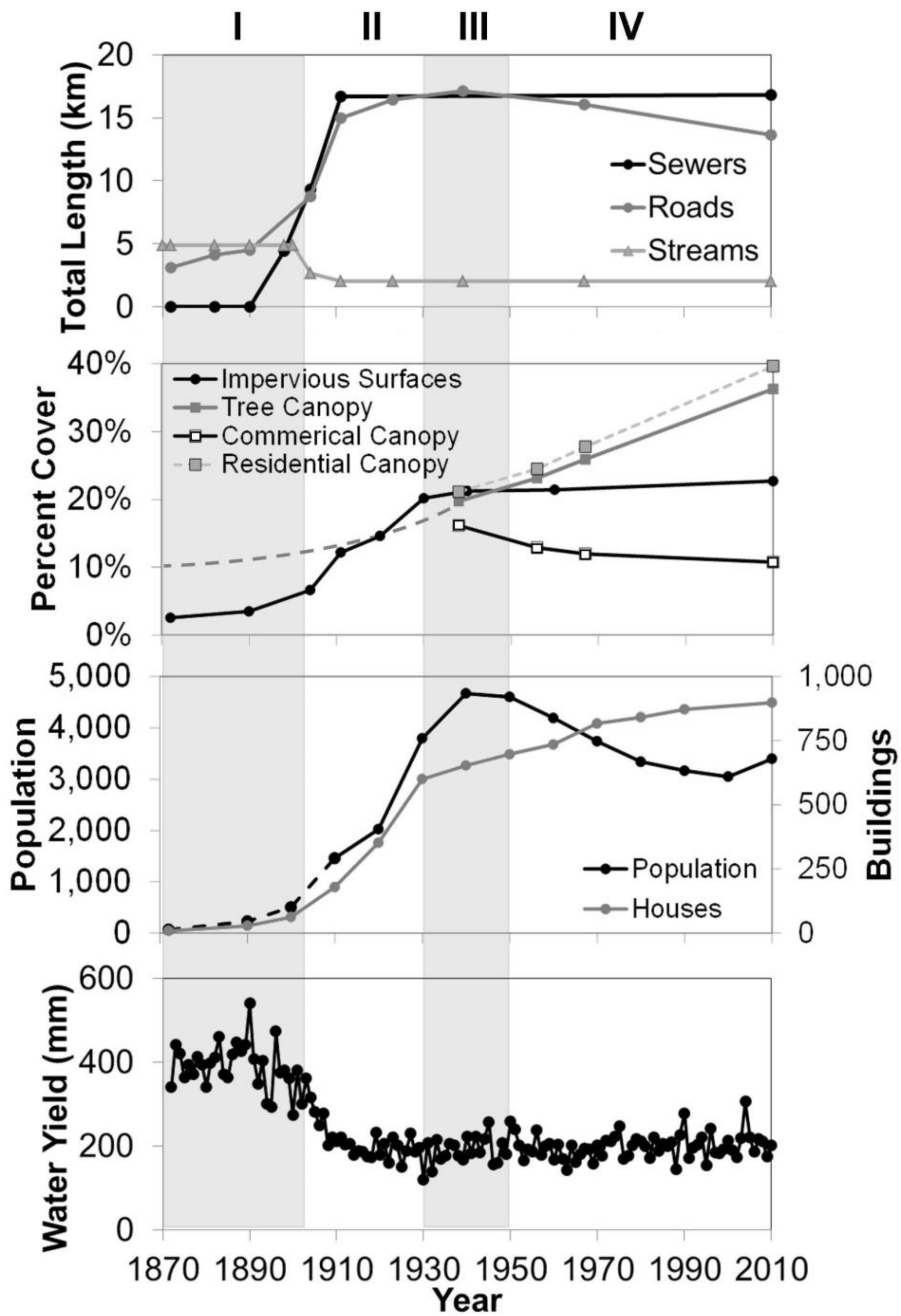

Figure 2-4: Four infrastructural phases identified in the Panther Hollow watershed. Phase I was dominated by agriculture, with a limited road network and low population. Phase II was marked by the rapid expansion of the sewer and road networks, the loss of headwater streams and a decline in annual water yield (infrastructure model). Phase III included the growth and stabilization of the watershed population. Phase IV spanned the decline of the watershed population and the growth of the urban tree canopy.

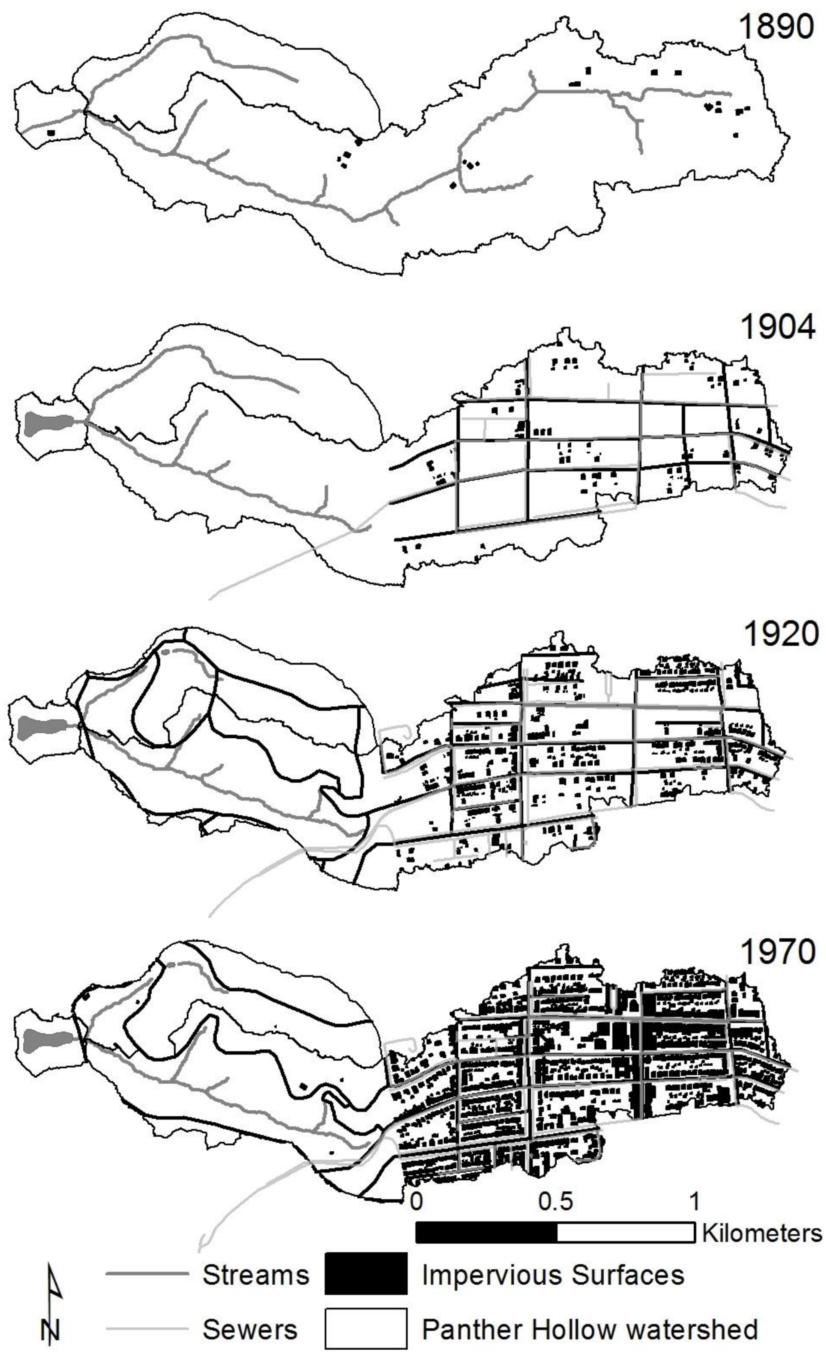

Figure 2-5: Infrastructure reconstruction in the Panther Hollow watershed. Prior to 1900 the watershed was dominated by agriculture and contained very few impervious surfaces. Between 1900 and 1910 road and sewer networks expanded in the eastern portion of the catchment and a lake was constructed at the bottom of the catchment. From the 1920s to 1940s the majority of houses were constructed, with development concentrated in the eastern half of the catchment, while the western portion was preserved as parkland.

2.3.2 Housing growth

The main road and sewer infrastructure in the basin was largely completed by 1911. However, the watershed contained only 179 residential houses, just 20% of the current number (Figure 2-4). The completion of the road network connected the eastern half of the watershed with economic activity to the north and west, making parcels in the Panther Hollow watershed attractive to potential buyers. Housing construction increased dramatically between 1920 and 1930, with 248 houses constructed in a single decade (Figure 2-4). The western portion of the watershed remained forested parkland or part of the golf course. Minor structures built in the park included picnic shelters, a boathouse, and golf clubhouse.

2.3.3 Expanding residential tree canopy cover

Historical photographs indicate that much of the watershed's forests were cleared during early agricultural activity, leaving the eastern half of the basin mostly devoid of trees [*UPitt*, 2012]. Parcel analysis revealed that overall tree canopy cover increased from 20% canopy cover in 1938 to 36% canopy cover in 2010 (Figure 2-4). In residential parcels, canopy cover expanded from 21% in 1938 to 40% in 2010. However, commercial parcel canopy cover declined from 16% in 1938 to 11% in 2010. Between 1938 and 2010, overall average increases in canopy cover of 17% per lot were observed, with an average canopy cover increases of 18% in residential parcels and average losses of 4% in commercial parcels. The entire Panther Hollow watershed, including the parkland, had 47% tree canopy cover in 2010 [*UTC*, 2012].

2.3.4 Water yield model comparison

Monitored annual yield in Panther Hollow is roughly half that of yield predicted by the impervious model (Figure 2-6). The impervious model predicted an increase in water yield over the past century, whereas the infrastructure model indicated a decline in water yield starting in 1901. In the infrastructure model, contributions from increased evapotranspiration from tree canopy growth and water inputs from leaking sewer infrastructure were relatively modest and offsetting. Since 1990, leaking sewer lines could be contributing an average annual input of 14 mm into the catchment, thereby subsidizing on average 7% of total annual water yield. Since 1938, additional evapotranspiration from tree canopy growth is potentially removing an average of 18 mm of water annually (9% of total yield) from the watershed (Figure 2-6).

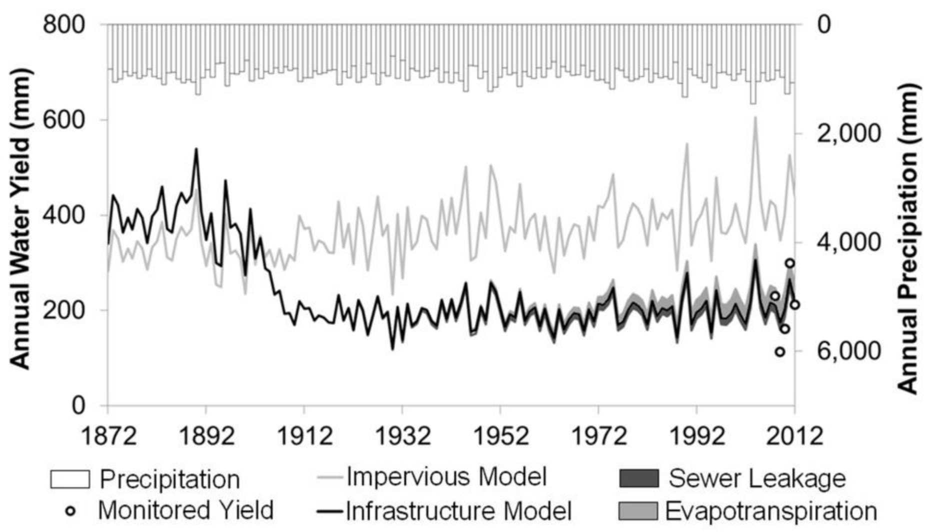

Figure 2-6: Yield reconstructions for the Panther Hollow watershed. The impervious model predicted 50% higher yield than the infrastructure model from 1910 to present. The dark grey shading indicates the potential contributions of leaking sewer lines, composing on average 7% (14 mm) of total water yield since 1990. Similarly, the growing tree canopy transpires increasing amounts of water out of the catchment and removes on average 9% (18 mm) total water yield since 1990.

2.4 DISCUSSION

Effective restoration planning to improve aquatic health requires a complete understanding of how historical and contemporary infrastructure interacts with stream ecosystems. The reconstruction of a century of urbanization in the Panther Hollow watershed reveals fundamental lessons about the effects of human infrastructure networks on urban stream hydrology. This historical perspective allows for the identification of when urbanization began altering natural drainage networks and the onset of hydrologic changes that lead to aquatic ecosystem decline.

2.4.1 Clarifying discrepancies in annual water yield

Both yield models predicted similar pre-development water yields (Figure 2-6). However, the impervious model predicts annual yield in Panther Hollow's streams increased over the last century, while the infrastructure model indicated a decline in annual yield beginning in 1901. For example, the impervious model predicted that contemporary yields in Panther Hollow were twice that of the monitored and infrastructure model yields. This discrepancy occurred because the impervious model did not incorporate interactions between the sewer and stream networks. Sewer infrastructure installed in the early 20th century hydrologically disconnected much of the upper-watershed, transferring stream water and urban runoff through the combined sewer to an adjacent watershed (Figure 2-3B). While this may seem a unique case, the importance of inter-basin transfer in urban areas is recognized in catchments throughout the United States [*Brandes et al.*, 2005; *Claessens et al.*, 2006; *Lookingbill et al.*, 2009].

Interactions among sewer and water infrastructure and stream networks may be much more common and significant than recognized in urban systems. The effects of inter-basin transfer can be particularly dramatic at the small basin scale, a scale roughly equivalent to many urban neighborhoods [*Bain et al.*, 2012b]. Refined urban water budgeting can clarify additions from municipal water from leaking water lines and exfiltration of sewage [*Bhaskar and Welty*, 2012; *Kaushal and Belt*, 2012]. This case emphasizes the continued need to refine urban water budgets to include and characterize interactions between sewershed and watershed areas.

2.4.2 Human infrastructure histories and watershed metrics

Results from this retrospective assessment reveal the importance of integrating human infrastructure histories into urban catchment models. Without this evaluation, traditional impervious-based models over-estimate water yield in Panther Hollow's streams. Further, additional landscape metrics, such as infrastructure connectivity and development age, can clarify when urbanization began altering watershed hydrology and degrading aquatic ecosystems.

The application of general urban growth models results in the assumed associations between the growth of urban areas, impervious cover expansion, and the existence of identifiable thresholds [*Arnold and Gibbons*, 1996; *Booth and Jackson*, 1997]. Initial studies hypothesized that stream impairment would be minimal in watersheds with less than 10% impervious cover [*Booth and Jackson*, 1997]. However, recent work has refined linear thresholds to a continuous but variable gradient of impairment as impervious cover increases [*Schueler et al.*, 2009]. The examination of infrastructure history in Panther Hollow agrees with this impairment continuum and corroborates urbanization's non-linear impact on aquatic ecosystems.

In Panther Hollow, the onset of urbanization occurred around 1910 and the progression of infrastructure growth was non-linear, peaking in the 1930s. This non-linearity is exhibited in the four phases of Panther Hollow's development history (Figure 2-4). During the Phase I, the watershed was an agriculture landscape with a small population and little impervious cover (< 3%). Large family farms were connected by a sparse network of dirt roadways and headwater streams remained intact (Figure 2-5). Water yield in the streams was double that of contemporary yields.

Phase II, the construction phase, spanned 1905 to 1930. During this phase, large parcels were subdivided into residential lots, around which the road and sewer network were built (Figure 2-5). Housing development then in-filled the established street network and the watershed's population nearly doubled between 1920 and 1930. The construction of the street network and houses effectively created present day impervious cover in one step during the two decades between 1910 and 1930. This period of peak development had significant impacts on the aquatic ecosystem. Headwater streams were buried and piped into the new combined sewer system (Figure 2-5). The diversion of headwater streams marks the onset of urbanization's impact on the aquatic ecosystems because it significantly reduced water yield through the catchment. Downstream aquatic ecosystems likely experienced reduced baseflow, nutrient and sediment inputs from surrounding roads, and a decline in aquatic communities.

Phase III spanned 1930-1950 and was characterized by a plateau in watershed population and a slower rate of infrastructure construction. Increased population led to an increase in water use and flux through sewer networks. Estimated water use at the height of Panther Hollow's population (4,700 residents in 1940) was roughly 645 million liters/yr. This volume of water, combined with stormwater draining from the road network likely tested the capacity of early

1900s era sewer lines and increased the occurrence of sewer overflows [*Tarr*, 2005]. However, infrastructure arrangement focused these impacts along the Monongahela River, not the streams in Panther Hollow.

Phase IV encompassed a decline in watershed population, continued deterioration of infrastructure networks, and the growth of the residential urban tree canopy (Figure 2-4). While our historical estimates do not quantitatively incorporate these processes, I estimate that between 1950 and 2010, sewer leakage and additional evapotranspiration fluxes constitute on average 6% and 10% of total yield, respectively (Figure 2-6).

These results suggest that the evolution of neighborhoods, particularly sewer infrastructure deterioration and tree canopy recovery, is not well incorporated into conceptual models of urban stream impairment. In addition, patterns of infrastructure development can result in surprising changes in stream hydrology. In this case, development has actually reduced, not increased annual water yield. Even though impervious cover in the upper portion of the catchment is substantial, the arrangement of sewer infrastructure routes stormwater runoff from 90% of the impervious surfaces out of the catchment. Clarifying the interactions among these human and natural drainage networks can aid in assessing the causes of stream impairments and in prioritizing restoration efforts.

2.4.3 Integrating landscape evolution into urban watershed frameworks

With stream restoration and stormwater management projects quickly becoming a multi-million dollar industry [*Lavendel*, 2002], it is vital that interactions among road, sewer and stream networks be incorporated into planning processes. Consider the impacts of leaking sewer lines. Many brick and clay combined sewer lines in Panther Hollow were installed 100 years ago, and remain far beyond design lifetimes. As maintenance of sewer lines is deferred, deterioration rates increase [*Micevski et al.*, 2002]. Though not necessarily surprisingly with hindsight, sewer leakage is a potentially large and relatively under-characterized catchment input. Given data availability, it is impossible to trace the exact amount of water leaking from Panther Hollow's sewer lines. However, estimates from this study reveal that sewage exports to the streams should be characterized for accurate water and material budgeting. Leaking sewer lines subsidize baseflow and nutrients to downstream reaches. In Baltimore City, lawn irrigation and pipe leakage accounted for 14% of catchment inputs, whereas infiltration of groundwater into sewer lines accounted for 41% of catchment outflows [*Bhaskar and Welty*, 2012]. Without a clear understanding of this system's evolution, material budgeting approaches are prone to large uncertainty (e.g. [*Divers et al.*, 2013]).

Changes in the tree canopy also have implications for assessing the quality of urban streams. During the late 1800s much of Panther Hollow's watershed was deforested. Residents and the city reforested portions of the watershed by planting trees during the 1930s and 1940s (Figure 2-4). As the neighborhood matured, newly planted trees grew into a canopy covering 36% of the upper-watershed and covering a growing portion of impervious surfaces. The dramatic increase in tree canopy cover over the last century provides numerous hydrologic benefits to the catchment, including increased interception and evapotranspiration. However, impervious-based models do not fully incorporate the benefits of increased canopy cover, though these benefits are recognized in the literature [*Sanders*, 1986; *Xiao et al.*, 1998]. During smaller precipitation events water is likely intercepted on tree leaves and evaporated before it becomes runoff [*Xiao et al.*, 1998]. For example, in Panther Hollow the current tree canopy covers 13.6% of the total road area and 3.7% of the total roof area, both the dominant impervious surfaces. In cities with extensive urban forests, the contribution of trees to stormwater reduction is likely substantial. Just as impervious models have addressed connectivity with effective imperviousness, incorporation of inter-basin transfer, deteriorating infrastructure, and changing tree cover into conceptual models will enhance available approaches to assess hydrologic impairments. Additionally, effective planning for urban stream restoration often requires site history and infrastructure interaction data in addition to impervious cover.

2.5 IMPLICATIONS

The importance of watershed history is clear. Understanding legacy impacts and interactions can help target watershed restoration to achieve goals that provide multiple benefits. For example, in Pittsburgh and Panther Hollow, focusing repair on deteriorating infrastructure and installing stormwater practices to slow down and store water in the eastern portion of the watershed will likely provide substantially more benefits to the aquatic ecosystem than riparian restoration [*Walsh et al.*, 2005b]. Implementing stormwater management practices (e.g., rain gardens) in the upper-catchment could provide the neighborhood with multiple benefits including increased green space, reduced flooding, and increased infiltration. These improvements may also benefit downstream reaches by reducing peak flow events, increasing baseflow, and reducing sediment and pollutant inputs, thereby protecting any future investments in the stream channel. Effective restoration planning recognizes the limitations associated with site history and prioritizes practice placement within the broader context of the watershed as a whole [*Bernhardt and Palmer*, 2007]. This study demonstrates the fundamental importance of also incorporating watershed history into restoration planning efforts.

3.0 CROSS-CITY VARIATION IN STREAM FLOW RESPONSE TO URBANIZATION: USING A GRADIENT-RESPONSE APPROACH

3.1 INTRODUCTION

By 2030, 87% of the U.S. population will reside in urban centers [UNPD 2009], with urban land cover expected to nearly triple compared to the urban extent in 2000 [*Seto et al.*, 2012]. Given urban growth projections, resource consumption by city residents will continue to be one of the primary drivers of environmental change [*Grimm et al.*, 2008]. Urban growth generally impairs aquatic ecosystems by altering hydrologic regimes, nutrient and contaminant chemistry, and the structure of plant and animal communities [*Walsh et al.*, 2005a; *Konrad and Booth*, 2005; *Meyer et al.*, 2005]. The alteration of hydrologic regimes is particularly important as hydrology fundamentally drives the form and function of aquatic ecosystems [*Poff et al.*, 1997] and regulates the amount, timing, and delivery of water runoff, pollutants, and nutrients to aquatic ecosystems [*Deletic*, 1998]. The most significant hydrologic changes associated with urban development include: increased occurrence of high-flow events, reduced baseflow, and increased variability in certain flow recurrence intervals [*Konrad and Booth*, 2005; *Poff et al.*, 2006]. More generally, urbanization shifts watershed hydrology from infiltration- to runoff-dominated processes, creating a broad range of disturbances in aquatic ecosystems [*Schueler*, 1994; *Booth and Jackson*, 1997].

General hydrologic changes are evident in urban watersheds. However, there is wide variability in the magnitude and direction (i.e., increase or decrease) of hydrologic changes among watersheds due to heterogeneity in processes mediating interactions among hydrologic cycle components. For example, baseflow yield varies widely among urban watersheds because of uncertainty in water imports and exports and site-specific differences in soils conditions that regulate subsurface storage and infiltration processes [*Price*, 2011]. Baseflow in urban areas can be reduced because of decreased infiltration after soils are paved over [*Scalenghe and Marsan*, 2009]. In contrast, urban areas can also subsidize local water cycles via intentional and unintentional inputs. Inputs that may augment groundwater and surface water include wastewater effluent, stormwater outfalls, lawn watering, and leaking septic, sewer, and water infrastructure [*Lerner*, 2002; *Fitzpatrick et al.*, 2005; *Bhaskar and Welty*, 2012].

Recent work has identified regional variability in hydrologic response to urbanization and attempted to link this variability to land cover at the scale of metropolitan areas [*Brown et al.*, 2009b] and large regional watersheds [*Poff et al.*, 2006]. However, there is uncertainty in the relative role of the drivers of regional hydrologic variability. Incorporating heterogeneity in development patterns and physical constraints (e.g., climate and geology) into assessments of hydrologic change across cities can clarify the relative importance of these factors and identify appropriate indicators for management targets.

Heterogeneity in hydrologic response to urbanization can also be driven by differences in watershed management styles and other social and economic factors. For example, differences in development styles, water management strategies, and vegetation type can arise from diversity in social characteristics such as lifestyle behavior, that includes the desire to uphold the prestige of the community and belong to a specific lifestyle group [*Grove et al.*, 2006a, 2006b]. *Grove et al.*

[2006a] found that lifestyle behavior was the strongest predictor of vegetation type on private land and in the public right of way in Baltimore, MD. Urban development style differences also occur because the human decision-making process is organized across scales from metropolitan regions, to neighborhoods, down to individual parcels [*Bain et al.*, 2012b]. Across these scales, human history and physical constraints shape the type, arrangement, and age of development and infrastructure within a city [*Bain and Brush*, 2008; *Schneider and Woodcock*, 2008; *Seto et al.*, 2010]. Some human-built structures, such as dams and reservoirs, control and regulate the movement of water, thus providing consistent water supplies in areas with too much or too little water. The regulating function of dams homogenizes stream flow, stabilizing changes in flow duration and frequency by providing consistent streamflow above a specified threshold [*Williams and Wolman*, 1984; *Poff et al.*, 2007].Yet there are negative biological responses associated with stabilized flow regimes, including life-cycle disruption and aseasonal reproduction, that can further lead to altered ecological relationships among communities and the species that constitute them [*Poff and Zimmerman*, 2010]. In contrast, other human-built structures can prevent flooding by quickly moving water out of the city. Stream culvert and stormwater drainage networks minimize flooding in urban centers, but quicken and magnify the delivery of runoff volume to receiving waters and downstream communities [*Alley and Veenhuis*, 1983]. Ecological responses to increased frequency of high flow events include loss of sensitive species, life cycle disruption, and reduced species richness [*Walsh et al.*, 2005a].

To characterize regional variability in hydrologic response, this study identified inter-city differences in development intensity across urbanization, climatic, and geologic gradients in nine U.S. cities. Differences in hydrologic response to urbanization within metropolitan areas and among the cities were compared. The two main research questions are (1) Is hydrologic response to urbanization consistent among cities? and, (2) To what extent do climatic, geologic, and human factors drive any observed hydrologic variability? It is expected that development intensity and precipitation amount are the main drivers of regional differences in hydrologic responses to urbanization, with more profound hydrologic changes in humid cities compared to arid cities.

3.2 METHODS

3.2.1 Approach and study area

This study utilized urbanization gradients in each study city to discern relationships between land cover and hydrologic metrics. The urbanization gradient approach is widely used to assess the effects of urbanization on aquatic ecosystems by comparing how ecological, hydrological, or geochemical response metrics vary among watersheds at different urban development stages [*Walsh et al.*, 2005a; *McDonnell and Pickett*, 1990; *Paul and Meyer*, 2001]. Gradient studies are typically based on simple urbanization metrics, such as impervious cover, assuming that the effect of urbanization increases in the watersheds composing the gradient [*Carter et al.*, 2009]. However, watershed stressors vary among watersheds and regions, leading to unique pathways of ecosystem change [*Wenger et al.*, 2009]. Therefore, this study also explored variability in stressors across each urbanization gradient by characterizing differences in developed land use, impervious cover, and sewerage across the gradients.

This study identified urbanization gradients spanning from rural to urban watersheds in nine cities in the U.S., including Atlanta, GA, Baltimore, MD, Boston, MA, Detroit, MI, Raleigh, NC, St. Paul, MN, Pittsburgh, PA, Phoenix, AZ, and Portland, OR (Figure 3-1). Cities were selected based on the availability of stream flow records and relative climate and geology (Table 3-1). Study cities spanned a mean annual precipitation gradient from 46 to 195 cm/yr and a mean watershed soil permeability gradient of 3 to 17 cm/hr.

Cities were grouped into two broad physiographic categories defined by whether a city had a glacial legacy (Table 3-1). Cities with glacial legacies include Boston, MA, Detroit, MI, St. Paul, MN, and Portland, OR. The topography of glaciated watersheds tends to be flatter, with less relief compared to non-glaciated cities (Table 3-1). In addition, glacial deposits impart soils with higher permeability compared to unglaciated soils in other cities (Table 3-1). More specifically, watersheds in Boston are underlain by sandy, glaciofluvial deposits derived from granite and gneiss mantled by friable loamy eolian deposits [SSURGO 2.2]. Watersheds around Detroit are underlain with glacial sediment ranging from 50-300 feet thick, including lacustrine deposits composed of well-sorted fine particles [*Thomas*, 2000]. Surficial sediments around Detroit are predominately clay-till, including layers of sand and gravel within the till. Surficial soils around St. Paul are glacial outwash composed of sand, gravelly sand, and gravel underlain by 2-5 feet of loess [*Meyer*, 2007]. Surrounding Portland, surface geology is dominated by poorly sorted, compacted glacial till underlain by volcanic bedrock.

The unglaciated cities were characterized by a different set of topographic and geologic conditions (Table 3-1). Watersheds composing the Atlanta and Raleigh gradients are in the Piedmont physiographic province characterized by hilly topography and underlain by late Palaeozoic metamorphic rock mantled by an average of 20 m of regolith, including ultisols, sandy clay, and alluvium [*Heath*, 1984]. Watersheds composing the Baltimore gradient are in the North Piedmont and Southeastern Coastal Plain characterized by ridges and valleys and relatively flat topography, respectively. The Piedmont is underlain by gneiss–schist and shale–sandstone crystalline mantled with 1-2 m of soil, while the Coastal Plain is underlain by crystalline rock mantled by a wedge with more than 10 m of unconsolidated sediments [*Markewich et al.*, 1990]. Watersheds in Pittsburgh lie in the Western Allegheny Plateau and are underlain by alternating layers of limestone, sandstone, and shale mantled silt- and clay-loam soils [*Newbury et al.*, 1981]. Soils in Phoenix are typically sandy, coarse-loam with a subsurface caliche horizon composed of calcium carbonate accumulations that are underlain by Proterozoic low-grade metamorphic rocks [SSURGO 2.2].

Within each metropolitan area, all USGS stream flow gages with discharge records spanning the years 2000 to 2012 were identified. This time period was selected to overlap with available land use datasets (2000 and 2006) and to encompass a range of annual precipitation events, capturing flow variability in each watershed. Due to limited gage records in urban Pittsburgh and St. Paul watersheds, some of the stream flow records in these watersheds spanned a shorter time period. The location of USGS stream flow gages was used to identify a subset of watersheds spanning an urbanization gradient in each city, yielding a total of 76 watersheds across the nine study cities (Figure 3-1). Each city's gradient was composed of five to fifteen watersheds. All watersheds selected had less than 33% agricultural land, dam storage less than 75 Megaliters/km^2, and drainage areas smaller than 200 km^2, except for Phoenix watersheds which had drainage areas less than 450 km^2. The intensity of urbanization was determined using road density (Tiger 2000) and population density (2000 Census) from the USGS Gages II database [*Falcone*, 2011]. Among all the watersheds, road density and population density ranged from 0 – 15 km/km^2 and 2 – 3,200 people/km^2, respectively. The Baltimore, Boston, Portland, and Raleigh gradients were the most complete, spanning rural to ultra-urban land use (Figure 3-

1). The Pittsburgh urbanization gradient spanned suburban to ultra-urban land use. The Atlanta, Detroit, and Phoenix gradients spanned rural to urban land use, whereas the St. Paul gradient included only ultra-urban land use. The Phoenix and Detroit gradients lacked highly urbanized watersheds.

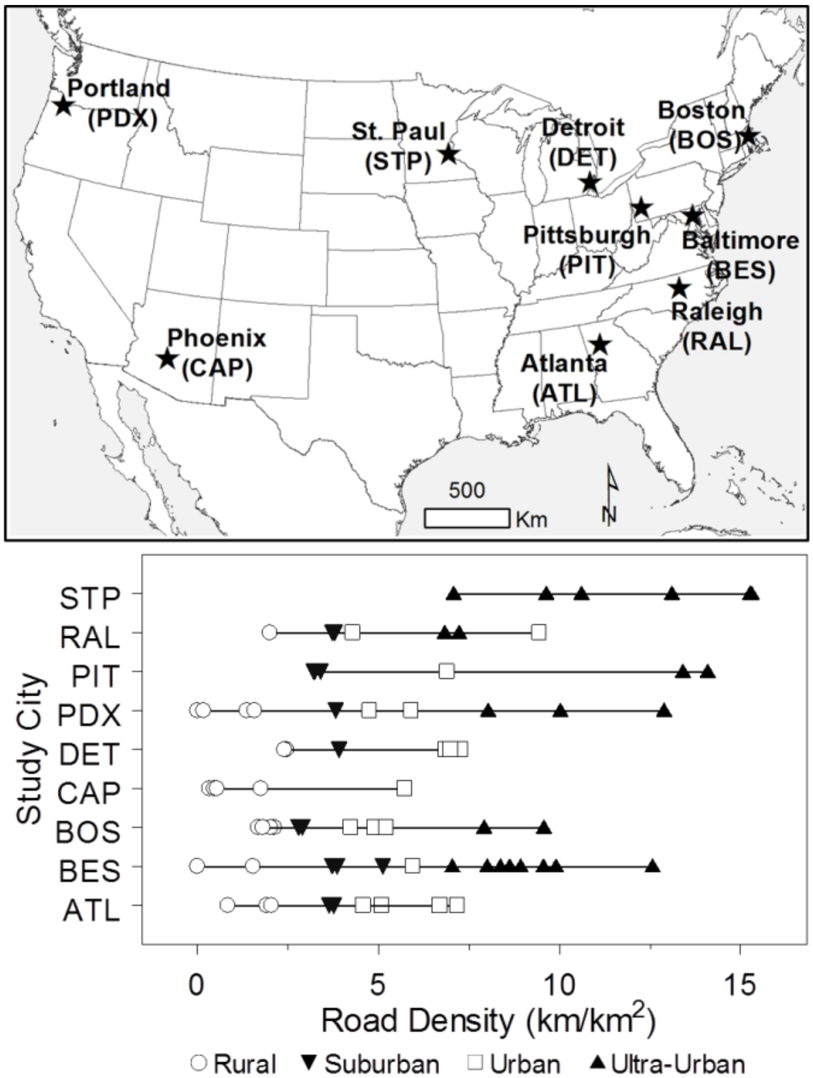

Figure 3-1: Location of study cities in the U.S. and the composition of watersheds included in each city's urbanization gradient. Urbanization gradients were composed of rural (< 100 people/km^2), suburban (100 – 350 people/km^2), urban (350 – 1,000 people/km^2), and ultra-urban (> 1,000 people/km^2) watersheds.

Table 3-1: Description of study city gradient climates, topography, and soils.

Site	City Code	Number of Watersheds	Watershed Areas (km^2)	Average Annual Precip (cm)	Average Annual Temperature (°C)	Average Soil Permeability (cm/hr)	Average Watershed Slope (%)	Glacial History (Yes/No)	Eco Region (Level II)
Atlanta, GA	ATL	9	66 - 191	136	15	4	4.3	N	Piedmont
Baltimore, MD	BES	15	0.5 - 159	117	13	5	3.8	N	Northern Piedmont & SE Plains
Boston, MA	BOS	12	11 - 173	121	9	17	3.2	Y	Northeastern Coastal Zone
Phoenix, AZ	CAP	5	170 - 425	46	19	9	15.9	N	Sonoran Desert & Arizona Mnts
Detroit, MI	DET	6	46 - 186	81	9	9	1.6	Y	S. Michigan Drift Plains
Portland, OR	PDX	10	2 - 137	195	11	5	14.2	Y	Willamette Valley & Cascades
Pittsburgh, PA	PIT	6	15 - 191	102	11	5	9.5	N	Western Allegheny Plateau
Raleigh, NC	RAL	7	3 - 197	119	15	3	2.7	N	Piedmont
St. Paul, MN	STP	6	3 - 73	81	7	16	1.2	Y	North Central Hardwood Forests

3.2.2 Land cover and sewer infrastructure data

Data from the GAGES II database were used to determine road density, population density, developed land-cover, and impervious cover in each watershed [*Falcone*, 2011]. Road density and population density were estimated for the year 2000 from U.S. Census datasets. Developed land-cover and impervious cover were characterized as a percent area from the 2006 National Land Cover Dataset. Metrics for watersheds not included in Gages II were characterized using the methods outlined in GAGES II. In addition, another metric called the "degree of impervious expansion" was quantified. The degree of impervious expansion was quantified as the slope of each city's linear fit for impervious cover as a function of road density (Figure 3-2). This metric represented the change in impervious cover across the urbanization gradient; with high values indicating more impervious surfaces relative to road density.

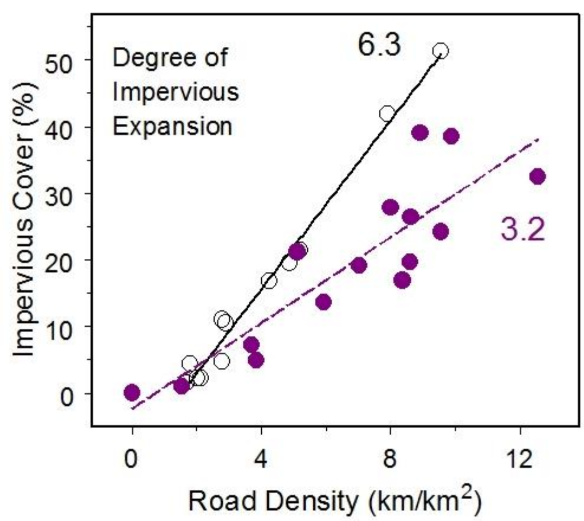

Figure 3-2: Degree of impervious expansion was calculated as the slope each city's the regression line for impervious cover as a function of road density. For this sample data, the degree of impervious expansion was 6.3 and 3.2 for the open symbols and closed symbols, respectively.

Sewage infrastructure in each watershed was characterized from block-group data for household water, plumbing, and sewage from the most recent U.S. Census Bureau Population and Housing Survey (1990). Census data were aggregated into two categories; households serviced by (1) septic systems or (2) public sewer. For each watershed, area-weighted Census block-groups were used to estimate the proportion of households in each sewage infrastructure category. Land cover and sewer infrastructure metrics were regressed with road density to characterize inter-city variability in development intensity and infrastructure among the urbanization gradients.

3.2.3 Hydrologic metrics

The Indicators of Hydrologic Alteration software (version 7.1) was used to calculate annual statistics for each hydrologic metric for the entire available daily mean discharge record [*Richter et al.*, 1996]. Daily mean stream flow data were obtained from USGS stream flow gages at the mouth of each watershed. Due to the prevalence of stream burial in St. Paul, only one USGS stream flow record was available during the study period. To complete the St. Paul urbanization gradient, five additional daily stream flow records were obtained from in-stream stormwater flow monitoring during 2006-2011. The Capital Region Watershed District and collaborators at the University of Minnesota provided these data [*Janke et al.*, 2013]. Due to limited stream flow records in Pittsburgh, three watersheds had only a three-year stream flow record and one watershed had a nine-year flow record. All of the remaining watersheds had stream flow records spanning 2000-2012.

Based on previous work, ecologically relevant hydrologic metrics were selected to assess changes in the magnitude, frequency, and rate of change of stream flow response to urbanization

[*Barringer et al.*, 1994; *Mathews and Richter*, 2007]. Hydrologic metrics included: baseflow index, high pulse frequency, high pulse length, and normalized 1-day maximum flow (Table 3-2). Daily discharge records with at least 80% of the annual record complete were used to calculate annual hydrologic metrics for each water year (i.e., Oct 1, 2000 to Sept 30, 2001). Annual values were then averaged over water years 2000 to 2012. This time period was selected to overlap with available land use datasets (2000 and 2006) and to encompass a range of annual precipitation events, capturing flow variability in each watershed. Two newly-developed hydrologic metrics were also calculated for each city using the slope and intercept for the general linear model for high pulse frequency as a function of road density (Table 3-2). "Flashiness response" was quantified as the slope of each city's linear fit between road density and high pulse frequency and represents the change in high pulse frequency across the urbanization gradient. The "flashiness baseline" was quantified as the intercept of this fit and represents the background frequency of high-pulse events at low levels of development.

Table 3-2: Hydrologic metric definitions.

Hydrologic Metric	Definition
High Pulse Frequency	Annual frequency of flow events exceeding 75th percentile flow, days in the same pulse event were counted as one distinct event.
High Pulse Length	Annual average length of high pulse events in days.
Normalized 1-day Max Flow	Annual maximum flow (m^3/sec) / watershed area (km^2).
Baseflow Index	Annual 7-day minimum flow / annual mean flow.
Flashiness Response	Linear slope of high pulse frequency as a function of road density in each city.
Flashiness Baseline	Linear intercept of high pulse frequency as a function of road density in each city.

3.2.4 Data analysis

Stream flow metrics were compared among watersheds within a city (i.e., urbanization gradients), as well as across cities (i.e., geologic and climate gradients). Pearson correlation coefficients were used to examine the association between urbanization metrics and hydrologic metrics across the entire dataset and within each city. A test for homogeneity of regression slopes (SPSS version 20) and general linear models for each study city were used to identify significant differences the degree of impervious expansion and flashiness response among the study cities. The degree of impervious expansion, flashiness response, and flashiness baseline were then used to examine the role of human infrastructure (i.e., dams), climate, geology, and topography in driving variability among cities. Inter-city differences in climate were assessed by characterizing average annual precipitation, annual temperature, and the percent of precipitation as snow in each watershed. These values were then averaged across the watersheds composing each city's gradient. In addition, average watershed slope, soil permeability, and total dam storage were quantified for the watersheds composing each city's urbanization gradient from data provided in Gages II [*Falcone*, 2011]. Average physiographic characteristics and linear regressions were used to assess the drivers of inter-city variability in the degree of impervious expansion, flashiness response, and flashiness baseline. City groupings from ANCOVA regression slope test results were used to explore the drivers of regional differences in flashiness response, particularly relative to land use, climate, topography, and geology.

3.3 RESULTS AND DISCUSSION

3.3.1 Inter-city variability in developed land and impervious cover

Along the road density gradients, developed land use consistently increased up to a road density of 8 km/km^2 at which point developed land use reached maximum coverage (Figure 3-3A). In urban watersheds, developed land cover averaged 88% (range 66% - 99%) of the watershed area. These data suggest that at a road density greater than 8 km/km^2, developed land cover as a metric of urbanization is insensitive to increasing development. Developed land cover saturates as an indicator of development intensity, supporting the choice of road density as a more effective metric of urbanization. Increased impervious cover was positively correlated ($R^2 = 0.83$, $p < 0.01$) with road density across the entire urbanization gradient (Figure 3-3B). At high levels of urbanization (road density > 8 km/km^2) impervious cover continued to increase with road density, whereas developed land cover plateaued at around 88% (Figure 3-3A). In addition, urban and suburban watersheds with road densities greater than 5 km/km^2, had greater variability in impervious cover relative to the corresponding road density, compared to watersheds with road densities less than 5 km/km^2. The variability in impervious cover is reported as mean residuals of 6.9% for watersheds with road density greater than 5 km/km^2, compared to mean residuals of 3.2% for watershed with road density less than 5 km/km^2 (Figure 3-3B). Increased variability in impervious cover was particularly evident in urban watersheds (road density > 8 km/km^2). In suburban and urban watersheds, Boston and St. Paul watersheds had notably more impervious cover for a given road density than Baltimore and Pittsburgh (Figure 3-3B).

Inter-city differences in impervious cover across each city's road density gradient were assessed by comparing each city's degree of impervious expansion (Figure 3-2). Cities with higher degrees of impervious expansion had more impervious surfaces relative to road density across the gradient. The Boston gradient had the largest degree of impervious expansion, indicating the largest increase in impervious cover relative to road density, while the Pittsburgh gradient had the lowest degree of impervious expansion (Table 3-3). While most of the study cities had similar degrees of impervious expansion, there were significant differences in the degree of impervious expansion along some of the study urbanization gradients (ANCOVA, $F = 46.78$, $p < 0.001$). The Baltimore and Portland gradients had significantly lower degrees of impervious expansion than the Boston gradient, indicating significantly more impervious cover for a given road density in Boston than Baltimore or Portland (Table 3-3). In addition, the St. Paul gradient had a significantly different degree of impervious expansion than all of the other cities except Boston. This difference is likely because the St. Paul gradient only spans watersheds at the ultra-urban end of the spectrum, with all watersheds having road density > 7 km/km^2 (Figure 3-1). Heavily weighting the gradient with ultra-urban watersheds in St. Paul may lead to a lower degree of impervious expansion compared to the other cities. Therefore, the St. Paul gradient provides insight about change at very high levels of development, but limited data on changes between rural and suburban development.

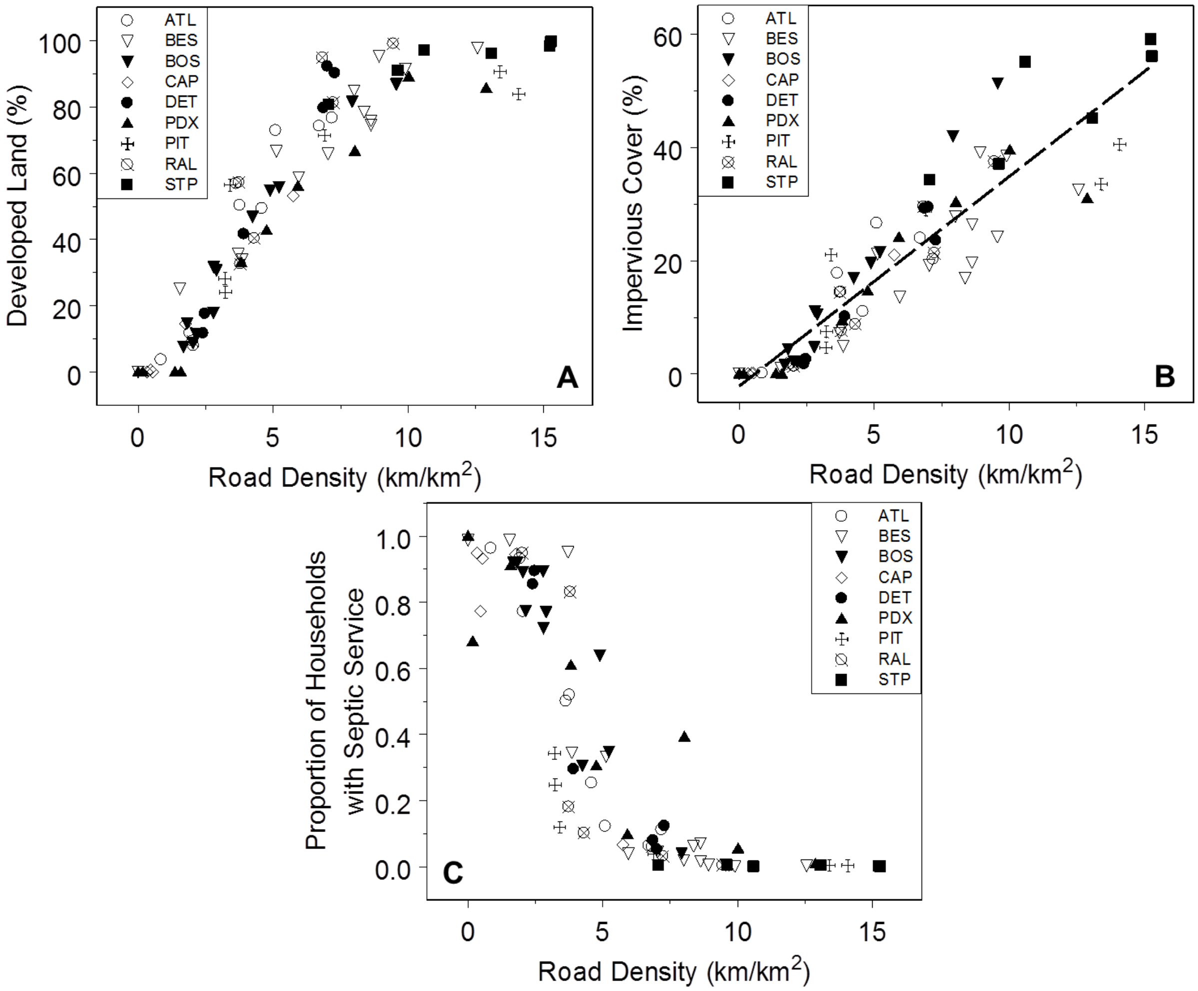

Figure 3-3: Associations between the road density gradients and (A) developed land use, (B) impervious cover, and (C) sewage disposal method. Thresholds were evident in developed land use and waste disposal method, while impervious cover increased linearly with road density (R^2 = 0.83, p < 0.01).

Table 3-3: Regressions of changes in impervious cover as a function of road density.

City	Degree of Impervious Expansion (Linear Slope)	R^2
All	3.7	0.83*
ATL	4.1[a,b]	0.72*
BES	3.2[a]	0.75*
BOS	6.3[b,c]	0.98*
CAP	3.9[a,b]	0.96*
DET	5.4[a,b]	0.94*
PDX	3.3[a]	0.86*
PIT	2.5[a,b]	0.72*
RAL	4.8[a,b]	0.89*
STP	2.6[c]	0.60*

*Significant at $p < 0.05$
[abc] Significantly different slopes based on ANCOVA slope test. Groupings indicate cities with similar slopes.

3.3.2 Shifts in sewage disposal method

In addition to other common urbanization indicators, U.S. Census data were used to characterize the proportion of households in each watershed serviced by septic systems or public sewer systems. There were surprisingly consistent thresholds in households serviced by septic systems in each study city, with a shift from septic to sewer service at a watershed road density between 2-5 km/km^2 and at a population density of 1,000 people/km^2 (Figure 3-3C). Thresholds were observed across each city's urbanization gradient except Portland, where the transition from septic to sewer was linear. The linear relationship in Portland is likely due to data gaps in the Census block-groups composing two suburban watersheds in Portland. This data gap may overestimate septic service in these areas. Study watersheds with road densities between 2 and 5 km/km^2 had average watershed impervious cover of 9% (range: 1-21%). The shift from septic service to sewer service coincided with 10% impervious cover degradation thresholds, above which stream quality is thought to decline [*Booth and Reinelt*, 1993; *Schueler*, 1994; *Booth and Jackson*, 1997]. Above this threshold, development stressors overcome the ability of aquatic ecosystems to cope with disturbances. Results indicate the characterization of sewage-disposal method is particularly important when distinguishing between exurban watersheds (i.e., rural transitioning to suburban), spanning a road density between 2 and 5 km/km^2. These watersheds straddled the transition zone from septic to sewer systems where households may be serviced by mostly septic, mostly sewer, or a mix septic and sewer.

Sewage-disposal metrics identified a consistent shift from septic to sewer service. However, there were some temporal and spatial limitations of this dataset. The sewage-disposal dataset may underestimate watershed sewer service, as data are from the 1990 Census compared to 2000 and 2006 for the other urbanization metrics. This limitation applies mostly to suburban watersheds along the urban fringe, where public sewer service likely expanded to serve additional households between 1990 and 2000. The main spatial limitation of this dataset is tied to the size of Census block-groups. The Census defines block-groups to contain between 600 and 3,000 people. In rural and low-density suburban areas, block groups were larger and therefore the estimate of sewage service was based on a fewer number of block-groups averaged over a larger area. Given the difficulty of compiling a national sewer service dataset, even with these limitations, the data provided a reasonable estimate of overall sewage service across the urbanization gradients. Further, no other existing studies use indirect methods to chart and differentiate sewer service type across urbanization gradients and for different cities. Therefore, this relationship provides a way to represent sewer infrastructure in urban ecosystem studies and potentially better constrain water, nutrient, and contaminant cycles that affect aquatic ecosystems.

3.3.3 Geologic and topographic controls on development

The inter-city variability in developed land and impervious cover identified may be driven by geologic and topographic controls on development. The study cities included four (n = 30 watersheds) with glacial legacies (e.g., Quaternary glacial deposits) and five (n = 46 watersheds) without glacial legacies (Table 3-1). The main physiographic contrasts identified between glaciated and non-glaciated watersheds were soil permeability, watershed slope, and lake density. Mean soil permeability in glaciated watersheds was two times higher than soil permeability in non-glaciated watersheds (Table 3-4). On average, watersheds with glaciation histories had twice the lake density and roughly half the slope of non-glaciated watersheds.

Table 3-4: Two sample t-tests for mean soil permeability, lake density, and watershed slope between glacial and non-glacial study watersheds.

Metrics	Non-Glaciated Mean (n = 46)	Glaciated Mean (n = 30)	t	df	p
Soil Permeability (cm/hr)	2.3	4.8	-4.47	42.2	0.0001
Lake Density (#/km^2)	0.6	1.3	-3.59	47.5	0.0008
Slope (%)	7.5	3.4	3.39	57.5	0.001

Previous work has shown that geomorphic history can constrain development in glaciated regions where level topography is generally more easily developed compared to unglaciated regions, where the variety and severity of slopes constrain development [*Bain and Brush*, 2008]. The watersheds in this study spanned a range of watershed slopes, from a mean slope of 1.2% in St. Paul to 15.9% in Phoenix (Table 3-1). Phoenix watersheds had the steepest slopes, however the gradient mean overestimated watershed slope in the urban Phoenix watershed (slope = 4.6%). In contrast, rural watersheds in Phoenix had watershed slopes ranging from 10% to 23%. In

Phoenix, urban and suburban developments typically avoid steep mountain outcrops that dot an otherwise flat landscape (Figure 3-4). Therefore, for the comparison of topographic constraints on development, this study used the mean watershed slope of the urban Phoenix watershed, instead of the overall average watershed slope of all of the watersheds composing the Phoenix gradient. Results identified a negative linear relationship ($R^2 = 0.53$, $p < 0.05$) between the mean watershed slope and the degree of impervious expansion among the urbanization gradients, indicating cities with flatter topography (e.g., Boston and Detroit) had more impervious surfaces relative to road density than cities with steep topography (Figure 3-5). St. Paul was excluded from this fit because the gradient did not include watersheds at the undeveloped end of the urbanization gradient. The lack of undeveloped watersheds may result in a lower degree of impervious expansion than expected in St. Paul.

Figure 3-4: Aerial photograph of development surrounding Phoenix, AZ. Development avoided steep mountain outcrops scattered across the extremely flat landscape. Photo credit: Kristina Hopkins.

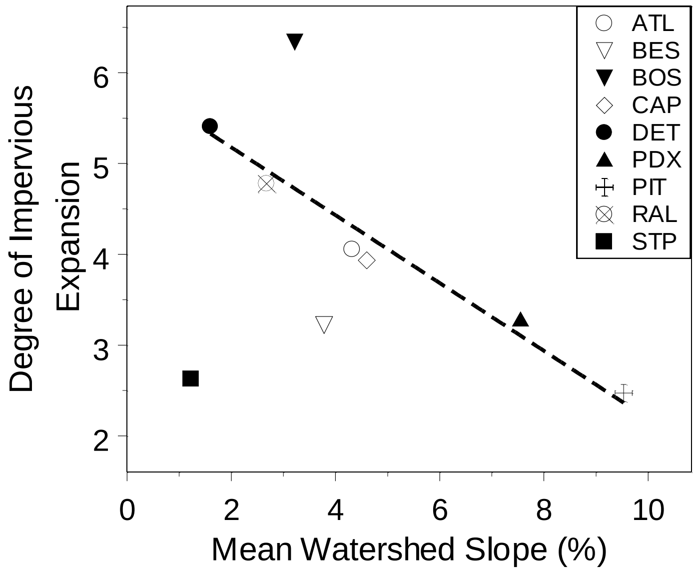

Figure 3-5: The degree of impervious expansion as a function of mean watershed slope (R^2 = 0.53, $p < 0.05$).

Along with impervious cover, other factors such as soil permeability may drive the observed variability in hydrologic response among cities. The Boston and Detroit gradients had the highest degrees of impervious expansion (Table 3-3). However, these gradients also had high average soil permeability of 17 cm/hr in Boston and 9 cm/hr in Detroit (Table 3-1). High soil permeability across these gradients may buffer some of the hydrologic effects of urbanization. Soil permeability reported here represented the average soil permeability across each city's urbanization gradient, based on USGS STATSGO data aggregated to a 1 km resolution grid [*Wolock*, 1997]. While this dataset captured inter-city differences in soil permeability, it may not capture variability across each city's urbanization gradient. Infiltration rates should be lower in urban watersheds compared to rural watersheds due to higher levels of compaction and fill in urban areas. For example, on sandy soils in North Central Florida compaction typical with urbanization reduced infiltration rates by 70 to 99% compared to near-by non-compacted sites

[*Gregory et al.*, 2006]. However, soil permeability estimates in this study may not capture variability in soil permeability across each city's urbanization gradient. For example, soil permeability in the three urban Detroit watersheds was higher than field estimated soil permeability in similar urban soils (i.e., silty, clay loam and lacustrine deposits) in Cleveland (Figure 3-6). In Cleveland, OH *Shuster et al.*, [2014] found soil infiltration rates of 1.8 cm/hr in urban soils in vacant lots. Given that soil permeability is likely lower in urban watersheds, average soil permeability reported in Table 3-1 is likely higher than actual soil permeability in urban watersheds in the study cities.

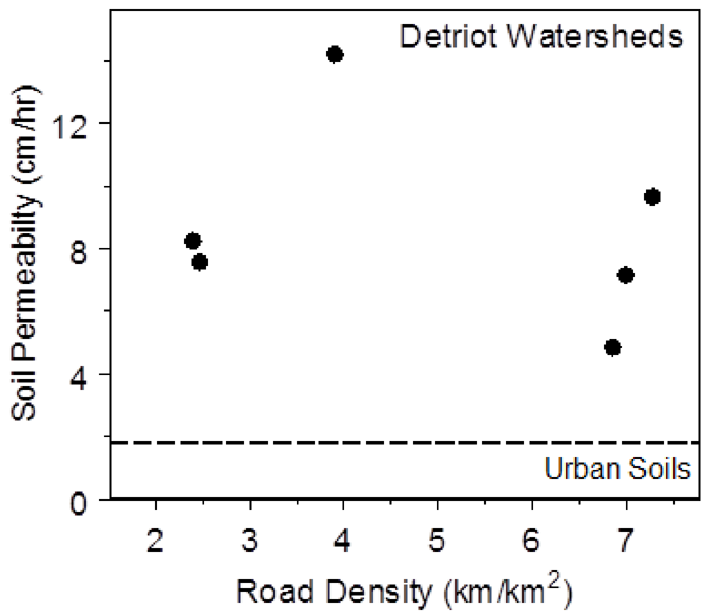

Figure 3-6: Average soil permeability across the Detroit gradient. Estimated average soil permeability in the urban Detroit watersheds (road density >6 km/km^2) were higher than *Shuster et al.* [2014] field measured infiltration of 1.8 cm/hr in similar soils in Cleveland, OH (dashed line).

3.3.4 Increased stream flashiness with urbanization

Hydrologic responses to urbanization were characterized both within (i.e., along an urbanization gradient within each city) and among cities. Stream flashiness increased across each city's urbanization gradient from rural to urban watersheds. Increased flashiness was detected as more frequent high pulse events with shorter durations during the study time period (Figure 3-7). Overall, the average annual high pulse frequency ranged from 3 to 43 events per year. A positive relationship ($R^2 = 0.48$, $p < 0.001$) between high pulse frequency and road density and a negative relationship ($R^2 = 0.37$, $p < 0.001$) between high pulse length and road density were found. Negative residuals indicated watersheds in Boston, Detroit, Portland, and St. Paul tended to have less frequent high flow events relative to road density when compared with the other cities (solid symbols, Figure 3-7A). High pulse duration was also variable across watersheds with low to moderate levels of development (road density < 8 km/km^2), but converged to an average length of 1.5 days (s.d. = 0.29) in urban watersheds (road density > 8 km/km2, Figure 3-7B). Positive residuals from the overall fit between high pulse duration and road density indicated watersheds in Boston, Detroit, Portland, and St. Paul tended to have longer high pulse events compared to similarly developed watersheds in other cities (solid symbols, Figure 3-7B).

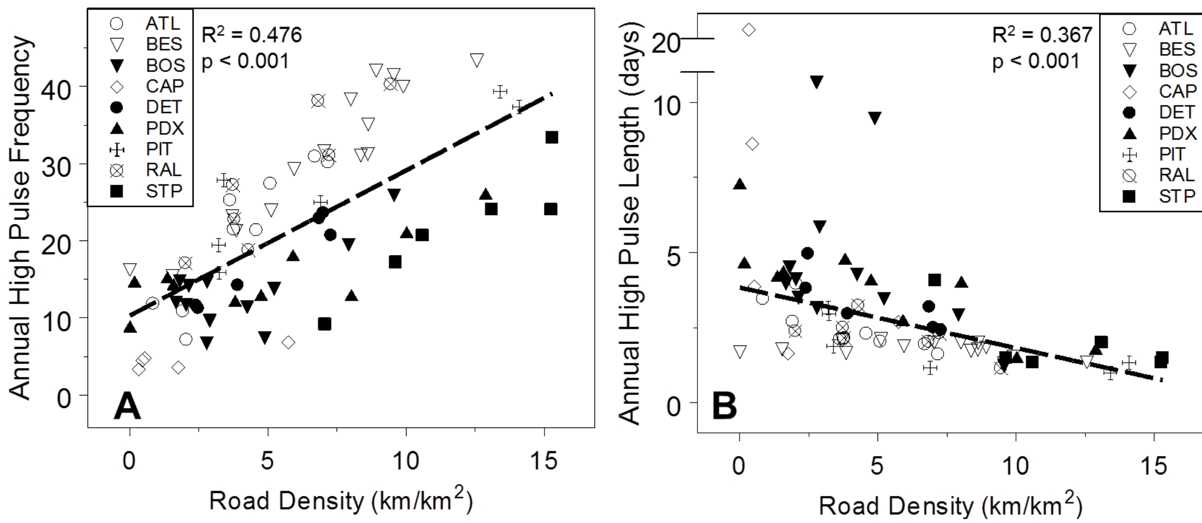

Figure 3-7: Regressions of high flow frequency (A) and high flow duration (B) with road density for nine U.S. cities. Open symbols indicate non-glaciated watersheds, whereas closed symbols indicate glaciated watersheds. Non-glaciated watersheds tended to have more frequent, shorter duration high flow events than glaciated watersheds.

Inter-city variability in high pulse frequency across the gradients was explored with two new metrics for flashiness response and flashiness baseline (Table 3-2). Higher flashiness response indicated a larger change in high pulse frequency across the urbanization gradient. Higher flashiness baseline indicated more frequent high pulse events at low levels of development. Flashiness response ranged from 0.5 in Phoenix to 3.7 in Atlanta (Table 3-5). There were significant differences (ANCOVA, $F = 40.02$, $p < 0.001$) in flashiness response among the study cities, such that Atlanta, Baltimore, Pittsburgh, and Raleigh had similar, large flashiness response compared to the other cities (Table 3-5). This city grouping had a disproportionate increase in high flows with urbanization, with more high flow events relative to road density that the other cities. Likewise St. Paul, Boston, and Phoenix were grouped together due to similar, small flashiness response, indicating similar lower flashiness response (Table 3-5).

Flashiness baseline represented the background frequency of high-pulse events at low levels of development. Flashiness baseline ranged between -5.1 in St. Paul and 15.3 in Pittsburgh (Table 3-5). The flashiness baseline in St. Paul may be an artifact of the urbanization gradient, which spanned only ultra-urban watersheds with nearly 100% buried streams (Figure 3-1). The reported data used linear regressions to determine flashiness baselines and the shape of the regression fit for St. Paul may be exponential rather than linear due to the extreme alteration of natural stream channels in the St. Paul study watersheds. Cities with lower flashiness response tended to have lower flashiness baseline, expect for Atlanta which had a high flashiness response and a lower flashiness baseline (Table 3-5). This difference may indicate that flashiness is altered to a larger degree in Atlanta relative to the other cities.

Table 3-5: Results of regressions for changes in high pulse frequency as a function of road density for each city.

City	Flashiness Response (Regression Slope)	Flashiness Baseline (Regression Intercept)	R^2
All	1.9	10.3	0.48*
ATL	3.7[a]	6.0	0.81*
BES	2.6[a]	13.4	0.89*
BOS	1.4[b,c]	7.7	0.43*
CAP	0.5[b,c]	3.7	0.06
DET	2.4[b]	5.5	0.94*
PDX‡	1.4[b]	6.4	0.77*
PIT	1.7[a]	15.3	0.77*
RAL	3.2[a]	11.0	0.78*
STP	2.2[c]	-5.1	0.81*

*Significant at $p < 0.05$
[abc] Significantly different slopes based on ANCOVA slope test. Groupings indicate cities with statistically similar slopes.
‡ Excludes sites with precipitation > 160cm

3.3.5 Regional differences in flashiness response

Regional variability in climate, geology, and topography may explain differences in flashiness response among the study cities. Separation of means groupings from the ANCOVA results indicated significant differences in flashiness response between cities and identified cities with statistically similar flashiness response (Table 3-5). The cities separated into two groupings including glaciated cities with lower flashiness response (Boston, Detroit, St. Paul, and Portland) and unglaciated cities with higher flashiness response (Atlanta, Baltimore, Pittsburgh, and Raleigh). Phoenix was excluded from the groups and analysis due to a lack of additional cities in the dataset with comparable arid climates. Based on the city groupings, two divergent relationships between flashiness response and precipitation among the cities were identified (Figure 3-8A). A positive relationship ($R^2 = 0.893$, $p < 0.05$) between annual precipitation and flashiness response in unglaciated cities was identified (open symbols Figure 3-8A). In these unglaciated cities, results suggest annual precipitation is the main driver of inter-city difference in flashiness response. Increased flashiness response with increased annual precipitation is consistent with the expectation that cities with high annual precipitation would have more frequent high flow events compared to cities with lower annual precipitation, given similar levels of development. A negative relationship ($R^2 = 0.943$, $p < 0.05$) between annual precipitation and flashiness response was identified in the glaciated cities (closed symbols, Figure 3-8A). This result was counterintuitive. Precipitation type (i.e., rain or snow) is one possible explanation for the two different responses to precipitation between the two city sets. Non-glaciated cities had less precipitation falling as snow (range = 0% to 17%), compared to glaciated cities which had between 12% and 27% of precipitation falling as snow (Figure 3-8B). Overall, flashiness response was negatively associated with the amount of precipitation falling as snow ($R^2 = 0.709$,

$p < 0.05$) (Figure 3-8B). Snow melt events likely extend the duration of high flow events resulting in an overall lower frequency of high pulse events.

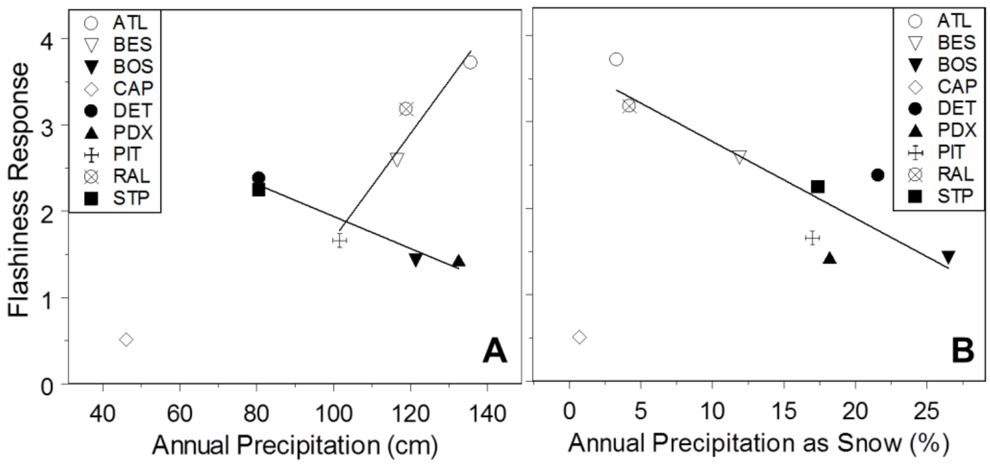

Figure 3-8: **Flashiness response as a function of annual precipitation (A) and precipitation as snow (B). Among the unglaciated cities (open symbols) flashiness response increased with annual precipitation, whereas among glaciated cities flashiness response decreased with precipitation.**

Results suggested that both the amount and type of precipitation were important drivers of inter-city variability in flashiness response among the study cities. Additional data from cities with drier climates is required to improve our understanding of urban hydrologic impacts in arid regions. The observed differences in flashiness response to urbanization also suggest potential future stream flow changes due to climate change, indicating that changes in the hydrologic regime and risks associated with changing stream flow will vary regionally. Climate change is expected to result in warmer winters and the intensification of the hydrologic cycle in the northern U.S. and drier conditions in the southern U.S. [*Grimm et al.*, 2013]. In snowy cities, such as Boston, warmer winters may lead to a larger increase in flashiness response due to shifts in the proportion of precipitation as snow. Additional work to fill in the climate gradient among the study cities, particularly in arid and semi-arid regions that cover nearly a third of the U.S., could improve our understanding of the complete range of urban hydrologic changes and better inform predictions of climate change impacts on cities.

3.3.6 Regional differences in flashiness baseline

Flashiness baseline also varied among cities, with St. Paul and Pittsburgh having the lowest and highest baseline, respectively (Table 3-5). A low flashiness baseline was interpreted as an indicator of relatively fewer high pulse events at low development levels. A weak, negative correlation (R^2 = 0.215, p = 0.1) between mean watershed soil permeability and flashiness baselines was identified (Figure 3-9). This result is consistent with the expectation that watersheds with more permeable soils will have higher infiltration rates and less overland flow [*Horton*, 1945]. This suggests that watersheds with more permeable soils may be buffered against hydrologic impacts at low levels of development. For example, Boston's Townbrook watershed averages 26 high pulse events per year, 65% fewer high pulse events than watersheds with similar development extents in Raleigh and Baltimore (Figure 3-7A). Average watershed lake density was higher in Boston (2.0 lakes/km^2), compared to in Raleigh (1.4 lakes/km^2) and Baltimore (0.4 lakes/km^2). High lake density may provide a hydrologic buffer by storing water during high flow event. Lower flashiness baselines may indicate areas that are less hydrologically-sensitive to development due landscape features such as lake density, relief, and soil permeability.

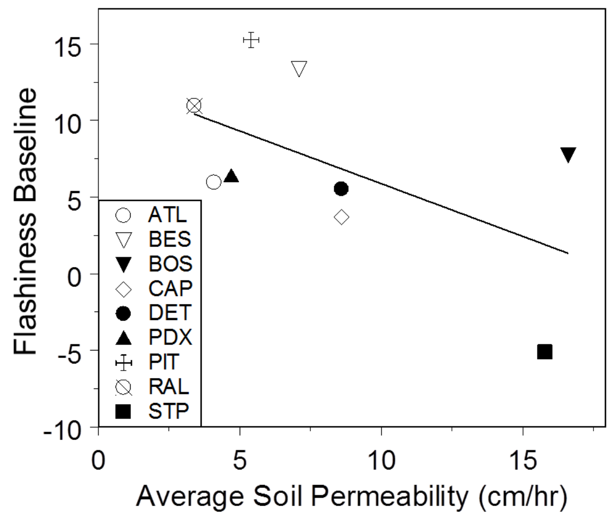

Figure 3-9: Flashiness baselines as a function of average watershed soil permeability (R^2 = 0.215, p = 0.1).

3.3.7 Glaciation history and flashiness response and baselines

Physiographic setting may explain the divergence between glaciated and non-glaciated watersheds in their respective relationships between flashiness response and precipitation. Flashiness response increased with increasing annual precipitation among the non-glaciated urbanization gradients and declined with increasing annual precipitation among the glaciated urbanization gradients (Figure 3-8A). Across the non-glaciated cities, precipitation appeared to be the main driver of inter-city differences in flashiness response. However, in glaciated watersheds, precipitation alone could not explain declines in flashiness response with increasing precipitation, other factors such as topography are likely important. For example, watersheds in Boston had some of the fewest high flow events and longest high pulse lengths despite annual precipitation inputs similar to Atlanta, Raleigh and Baltimore (Figure 3-7). Low relief and high lake storage capacity in Boston watersheds may buffer the severity of stream flow responses to rainfall events. In watersheds with glacial legacies, topographic features such as lakes and watershed slope may help further explain inter-city differences in hydrologic changes with urbanization.

3.3.8 Increase in the magnitude of extreme flow events

Along with an increase in stream flashiness, urbanization also increased the volume of 1-day maximum flow events. Annual average 1-day maximum flow normalized to watershed area was used to assess changes in extreme flow events with urbanization (Table 3-2). Normalized 1-day maximum flow events tended to be larger in non-glaciated watersheds (open symbols) compared to similarly developed glaciated watersheds (solid symbols) (Figure 3-10A). Monotonic increases in normalized 1-day maximum flows along the urbanization gradient were evident in Atlanta, Baltimore, Detroit, Raleigh, and St. Paul (Figure 3-10A). Normalized maximum flows were highest across the Atlanta and Raleigh gradients (Figure 3-10A). A slight decrease in 1-day maximum flows was evident across the Portland, Phoenix, and Boston gradients (Figure 3-10A).

In Phoenix and Portland, the negative correlation between maximum flows and urbanization may be explained by a combination of climate and topographic variability along the gradients. In Phoenix, results suggested that the declining trend in normalized 1-day maximum flows was driven by a negative trend in temperature ($R^2 = 0.737$, $p < 0.05$) and a positive trend in mean watershed slope ($R^2 = 0.723$, $p < 0.05$) across the gradient. Urban development in Phoenix occupies the valley bottom, which is warmer, flatter, and receives less precipitation than the surrounding area (Figure 3-4). These local differences likely lead to lower 1-day maximum flows compared to less developed, higher-elevation watersheds. The negative correlation in Portland was also likely driven by an underlying orographic precipitation gradient, whereby precipitation falls as air masses move up the mountainside. If Portland's less developed, higher-elevation watersheds with higher annual precipitation were removed, no significant trends between land use metrics and 1-day max flows were identified. In these two cities, climate co-variation with the road density gradient masked the effect of urbanization.

In other cases, maximum flows declined with urbanization. In Boston, negative correlation between maximum flows and urbanization seemed to be driven by dams. There was an underlying gradient in dam storage, with more dam storage in the more urban watersheds ($R^2 = 0.382$, $p < 0.05$) (Figure 3-11). As dam storage increased, maximum flow declines. This decline in maximum flow occurred in other watersheds with dam storage greater than one megaliter/km^2. In this subset of watersheds, 1-day maximum flows declined with increasing dam storage ($R^2 = 0.118$, $p < 0.05$). In watersheds with small dams, lakes, or wetlands, the effects of urbanization may be buffered, reducing the magnitude of extreme flow events. In Pittsburgh, the short duration of the data record prevented effective evaluation of extreme events and urbanization. The three most urban Pittsburgh watersheds had only three-year stream flow records, while the less urban Pittsburgh watersheds had nine- to thirteen-year periods of record. Hydrologic characterization requires long-term stream flow records to fully capture stream flow variability during both wet and dry years. Among the study cities, the magnitude of extreme events generally increased with urbanization. However, when declines in 1-day maximum flow were identified, underlying gradients in precipitation and dam storage could explain this contrasting result. Selecting urbanization gradients that limit variability in climate, topography, and water storage among the study watersheds within the same city is particularly important, as these differences can obscure hydrologic response.

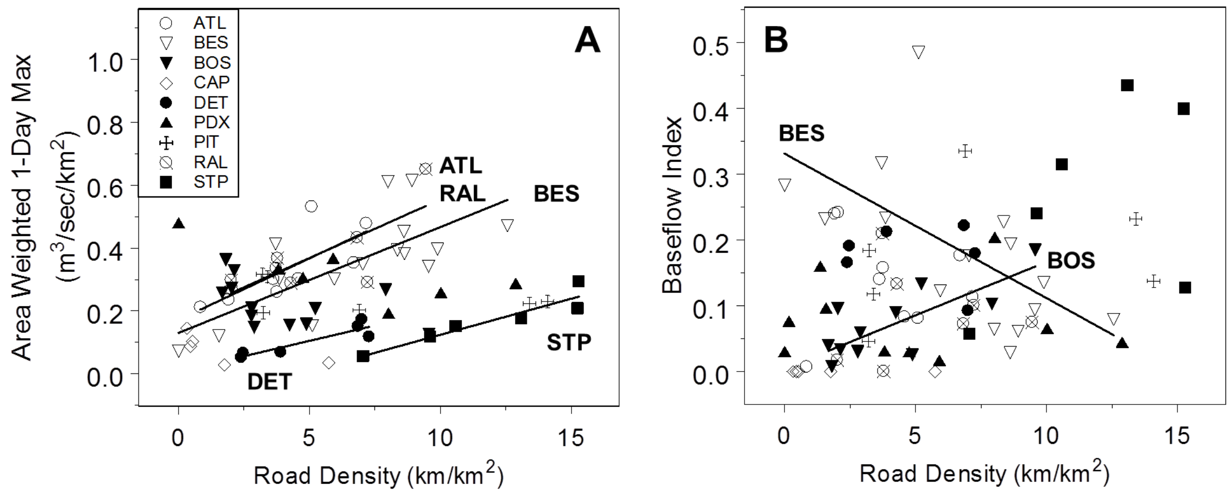

Figure 3-10: Regressions of 1-day maximum flows (A) and baseflow index (B) with road density for nine U.S. cities. Open symbols indicate unglaciated watersheds, whereas solid symbols indicate glaciated watersheds.

3.3.9 Baseflow

Baseflow index was used to evaluate alterations following urbanization, with higher values indicating more consistent baseflow [*Richter et al.*, 1996]. Baseflow index is as unitless metric defined as 7-day minimum flow divided by mean annual flow (Table 3-2). Although baseflow response to urbanization was inconsistent among cities, some trends were evident. In Baltimore, baseflow consistency declined across the gradient (R^2 = 0.34, $p < 0.05$) (Figure 3-10B). The negative relationship in Baltimore was consistent with the expectation that urbanization would reduce infiltration and therefore baseflow. In contrast, baseflow consistency increased with urbanization in Boston (R^2 = 0.56, $p < 0.01$). The increase in baseflow consistency across the Boston gradient was likely driven by the prevalence of dams in urbanized Boston watersheds. In Boston, the watersheds with road densities greater than 4 km/km^2 also had dam storage greater than 50 Megaliters/km^2 (Figure 3-11). Across these watersheds, dam storage increased linearly with road density ($R^2 = 0.38$, $p < 0.05$). The prevalence of dams in urban watersheds regulate flow, providing more consistent stream flow during low flow periods and buffering hydrologic alterations by damping the magnitude of high flow events. Ultra-urban St. Paul watersheds also had higher baseflow index values relative watersheds with similar road densities in other cities (Figure 3-10B). This difference may result from the sampling locations, since flows for the five downtown St. Paul watersheds were recorded in storm sewers rather than stream channels. In these ultra-urban watersheds, elevated baseflow consistency may arise from groundwater subsidies to storm sewer flow [*Bhaskar and Welty*, 2012; *Janke et al.*, 2013].

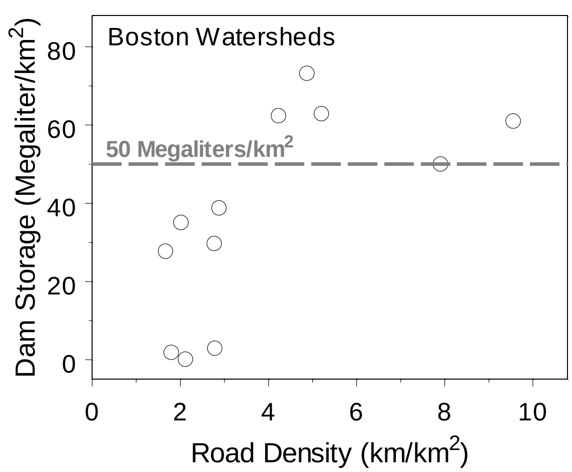

Figure 3-11: Dam storage increased across the Boston urbanization gradient, with urban watersheds having dam storage greater than 50 Megaliters/km^2.

Average annual baseflow index provided some insight on regional baseflow variability. However, annual average values may obscure seasonal differences. Seasonal fluctuations in flows may be particularly important to aquatic ecosystem function in humid regions [*Poff and Zimmerman*, 2010]. For example, in humid climates, baseflow index in the summer months may be more representative of ecologically relevant hydrologic alterations than an annual average.

Further, variation in urban baseflow may be linked to uncertainty in water balance characterization and baseline variability [*Price*, 2011]. Therefore, clarification of connections among baseflow changes and watershed characteristics, including soils and land use, are necessary to improve prediction and mitigation of urban hydrologic impacts on low flows.

3.3.10 Framework for characterizing inter-city variability in hydrologic response

Urban-induced hydrologic changes are increasingly documented in the literature. However, a framework is lacking that provides a mechanistic explanation of the wide variability in hydrologic alterations observed among watersheds and physiographic regions. Results from this study were used to develop an overarching framework to explain inter-city variability in the degree of hydrologic changes among cities. The framework uses physiographic setting, specifically glaciation history, to describe a range of pre-existing physiographic templates upon which the urban template is built (Figure 3-12). Among the cities in this study, glaciation history imparts specific features on the landscape (i.e., low relief and high water storage capacity) that hydrologically buffers and dampens the frequency and severity of high flow events and extreme flows compared to unglaciated watersheds. While this study defines only two pre-existing physical templates, watersheds across the globe can be placed along a continuum of watersheds reliefs and water storage capacities (Figure 3-12). The hydrologic effects of urbanization will then depend on where a watershed falls along these continuums. Among areas with steep relief and low water storage capacity, development intensity and precipitation amount will explain variability in the severity of hydrologic changes due to urbanization. In contrast, in watersheds with low relief and high water storage capacity, other factors such as lake density and soil permeability will better explain variability among urban watersheds. Potential hydrologic changes associated with the physical template are summarized in Figure 3-13. In addition to influencing the severity of hydrologic change, the pre-existing physical template also influences the type of urban template constructed (Figure 3-12). For example, results from this study indicated the degree of impervious cover expansion depends partially on watershed relief, with more impervious surfaces in areas with flatter topography (Figure 3-5). Other important characteristics of the urban template include water imports/exports, the density of sewer and water lines, point sources (i.e., wastewater treatment), and the urban tree canopy (Figure 3-12). The relative importance of these urban characteristics will vary depending on specific infrastructure traits including type, location, extent, connectivity, and age (Figure 3-12). For example, the importance of runoff generated from impervious surfaces will depend on the extent of impervious cover and if those impervious surfaces are directly connected to the stream. Potential hydrologic changes associated with the urban template are summarized in Figure 3-13. Together the range of physical and urban templates provide a framework to organize both natural and human features that influence the type and magnitude of hydrologic changes due to urbanization.

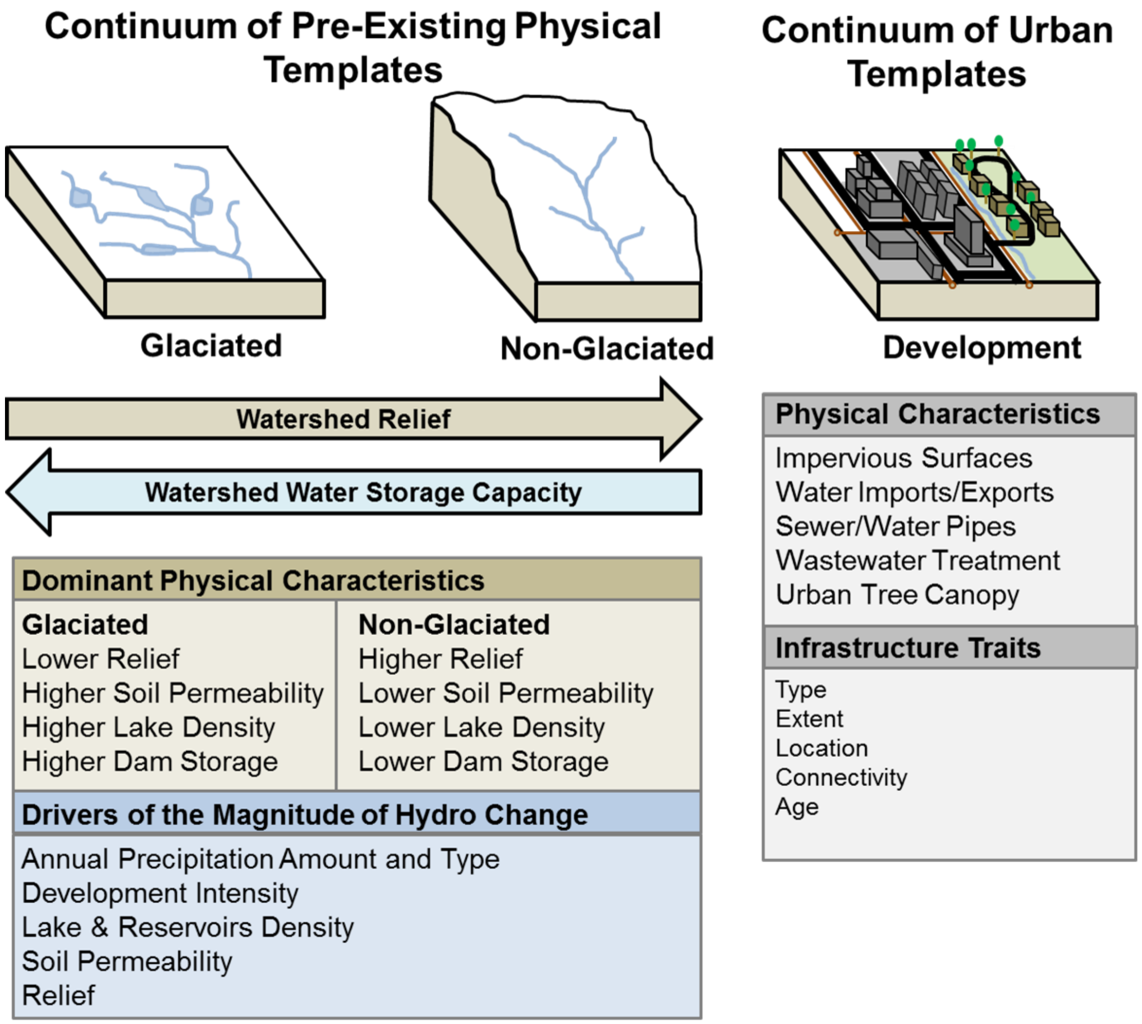

Figure 3-12: Conceptual model of continuum of pre-existing landscape templates that the urban template is built upon. Underlying physical characteristics of watershed relief and water storage capacity are two of the dominant factors influencing the type and magnitude of hydrologic changes during urbanization.

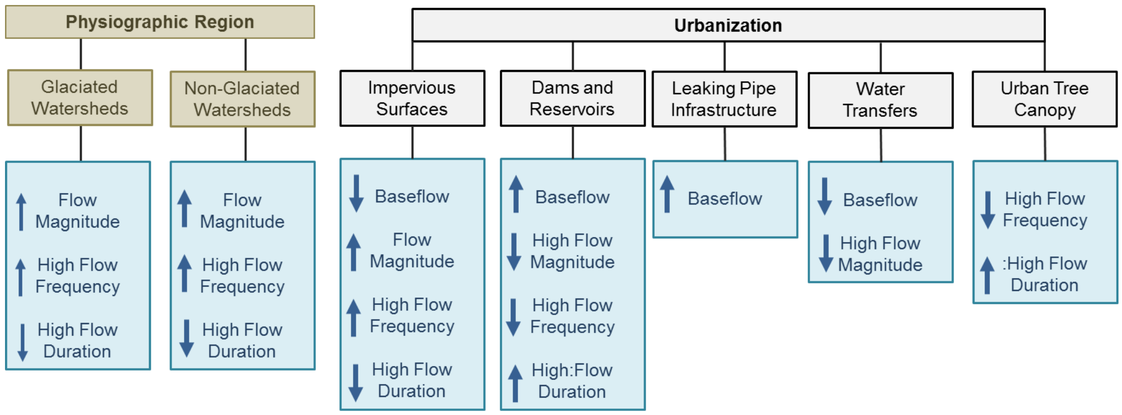

Figure 3-13: The direction of hydrologic changes (blue boxes) in based differences in physiographic region and among watershed characteristics association with urbanization (grey boxes). Hydrologic alterations associated with impervious surfaces and dams were summarized in Chapter 3, whereas the effects of pipe infrastructure, water transfers, and tree canopy were considered in Chapter 2.

3.4 CONCLUSIONS

The land cover characterization in this study revealed relatively similar development trajectories among the watersheds composing each city's urbanization gradient. Developed land cover and impervious surfaces increased with urbanization and sewage disposal methods shifted from septic to public sewer. Based on this land cover characterization, the extent of landscape urbanization was relatively consistent across each urbanization gradient. In addition, the types of hydrologic changes across all the urbanization gradients were relatively consistent, including increased frequency and shortened duration of high flow events and increased volume of 1-day maximum flows. However, the magnitude of these hydrologic changes was variable among cities, with less severe hydrologic change in Boston, Detroit, St. Paul, and Portland compared to the other cities. Results indicated the variability in severity of hydrologic changes can be explained by differences in the physical template (i.e., relief and soil) that a city is built upon (Figure 3-12). In this study, glacial history was used to group the study cities into two general physical templates; watersheds with a glacial history and watersheds without a glacial history. The study watersheds with glacial histories tended to have specific physical characteristics that provide a hydrologic buffer that dampens the severity hydrologic changes associated with urbanization, including less frequent high flow events, longer high flow durations, and lower volume of extreme flow events compared to similarly developed watersheds without glacial histories (Figures 3-13). Important physical characteristics in glaciated regions included lower watershed relief and higher water storage capacity in lakes and soils, when compared to non-glaciated watersheds (Figure 3-12).

Results from this Chapter were used to develop a framework to summarize important natural landscape and urbanization characteristics influencing the severity of hydrologic changes following urbanization (Figure 3-12). This framework can help identify additional urban research necessary to make comparisons across a larger, global set of cities and to comprehensively examine the broad range of urban impacts on aquatic ecosystems. In addition, long-term watershed studies that supplement gradient approaches may also clarify the temporal and spatial dynamics of hydrologic changes in urban watersheds. This study also identified cities and watersheds that experienced lower hydrologic changes and landscape features with higher hydrologic buffering capacity. Replicating the water storage function of landscape features, such as soils, lakes, and wetlands, via a distributed network of stormwater management strategies that promote water infiltration and storage may have similar impacts in urban watersheds. However, given the importance of the physical template upon which a city is built, addressing hydrologic alterations through the installation of new stormwater management strategies will likely require solutions tailored to the local environment and more investment in some cities than others to achieve target conditions.

4.0 LONG-TERM STREAM FLOW SHIFTS IN URBANIZING WATERSHEDS IN THE EASTERN U.S.

4.1 INTRODUCTION

The hydrologic changes associated with urbanization include increased stream flashiness, reduced evapotranspiration, reduced infiltration, and reduced baseflow (Konrad & Booth 2005; Walsh et al. 2005a; Poff et al. 2006). However, the magnitude and direction of these hydrologic changes vary across regions due to the interactions of multiple factors including climate, geology, land use, and water management [*Brown et al.*, 2009b; *O'Driscoll et al.*, 2010]. In addition, much of our current knowledge of the impact of urbanization on stream ecosystems is based on studies that assess biotic and abiotic responses across land use gradients. For example, *Brown et al.* [2009] identified regional variability in stream flow response across urbanization gradients in nine U.S. cities, including significant relationships between the frequency of high flow events and urbanization in 2/3 of the cities studied and between the magnitude of extreme flows and urbanization in five of nine cities. In the U.S., urban streams are typically flashier than rural streams, with more frequent extreme flow events, increased runoff efficiency and peak flows [*O'Driscoll et al.*, 2010]. Findings from Chapter 3 identified regional differences in the magnitude of flashiness response across urbanization gradients in nine U.S. cities. Cities with glacial legacies had lower flashiness response to urbanization compared to non-glaciated cities.

The use of urbanization gradients relies on the assumption that the effects of urbanization increase with development intensity and that a gradient of rural, suburban, and urban watersheds represents different steps in the process of watershed urbanization. However, these assumptions minimize temporal and spatial variability in development intensity and do not incorporate underlying differences in the physiographic setting among watersheds composing the gradient. Therefore, gradient studies frequently fail to arrive at mechanistic explanations of how stressors lead to aquatic declines [*Carter et al.*, 2009]. Supplementing gradient studies with long-term datasets can identify candidate mechanisms by quantifying the types and timing of hydrologic changes throughout the process of urbanization in a given watershed.

A parallel body of research utilizes long-term watershed datasets to reconstruct development patterns and to characterize changes to stream flow. Long-term stream discharge records are limited due to the substantial resources necessary to sustain them. However, a long-term monitoring approach is the only way to comprehensively characterize the timing, intensity, and effects of watershed development. Further, a long-term approach can detect interactions between urban growth based on the direction and magnitude of changes in stream flow. Examination of hydrologic changes in long-term studies can include comparison of reconstructed land cover changes with long-term observations of stream flow alterations. For example, *Jennings and Jarnagin* [2002] relate stream flow changes in an urbanizing watershed in Annandale, VA to coincident increases in watershed impervious cover from 3% to 1949 to 33% in 1994. Long-term watershed studies can also approximate the year of significant stream flow alterations. The timing of stream flow alteration can be used to isolate coincident changes to the landscape that sparked the stream flow shift. For example, in a small urban watershed in Pittsburgh, PA the construction of the combined sewer systems in 1910 routed half of the watershed's pre-development stream flow to an adjacent watershed [Chapter 2]. These studies illustrate how a long-term approach allows characterization of the expansion, arrangement, and connection of impervious surfaces to the stream network, a factor cited as one of the main causes of declines in stream health [*Shuster et al.*, 2005; *Schueler et al.*, 2009].

Some studies suggest a convergence or homogenization of landscape structure during urbanization [*Groffman et al.*, 2014; *Steele et al.*, 2014]. However, the underlying process of urbanization is a complex mix of landscape modifications and spatially distributed management practices that leads to uncountable permutations of urban pattern [*Bain et al.*, 2012b]. Urban form and growth rates are dynamic, varying spatially within and among cities and temporally with cycles of development [*Olson*, 1979; *Alberti et al.*, 2007; *Cuo et al.*, 2009]. Therefore, watersheds should be assessed within the context of overall landscape history, detailing how and when an area was developed and the sequence of long-term changes [*Bürgi et al.*, 2004].

This study reconstructed development in urbanizing watersheds surrounding three eastern U.S. cities: Baltimore, MD, Boston, MA, and Pittsburgh, PA. The study coupled development histories with long-term stream flow records to quantify the timing and magnitude of development and the alteration of the stream flow regime in each study watershed. This work focused on urban growth during the last century and stream flow changes since the 1930's and 1940's and evaluated how stream flow changes through time (i.e., gradual and linear or abrupt at a threshold) and how stream flow changes relate to development trajectories in each study watershed.

4.2 METHODS

4.2.1 Study Area

Baltimore, MD, Boston, MA, and Pittsburgh, PA were selected as study metropolitan areas due to the availability of long-term stream flow records and historical datasets for growth reconstruction, including parcel-scale property tax assessment records. A total of six watersheds with USGS stream flow records covering a period longer than 40 years were identified, including continuity through periods prior to and after watershed urbanization. Watersheds included three in Baltimore, two in Boston, and one in Pittsburgh (Table 4-1). These three cities were selected because parcel-scale property tax assessment records were available to use for the growth reconstructions. In addition, the watersheds selected were a subset of the study watersheds used in Chapter 3. All the selected stream flow gages had watersheds within the U.S. Census Bureau metropolitan statistical area (MSA) of each city (Figure 4-1). No long-term stream flow records in the highly urbanized city core were available. Baltimore watersheds were located within the Northern Piedmont, Boston watersheds were located in the Northeastern Coastal Zone, and the Pittsburgh watershed was located in the Western Allegheny Plateau. Watersheds varied in their development history, spanning rural to urban land cover, and all had drainage areas less than 100 km^2 (Table 4-1).

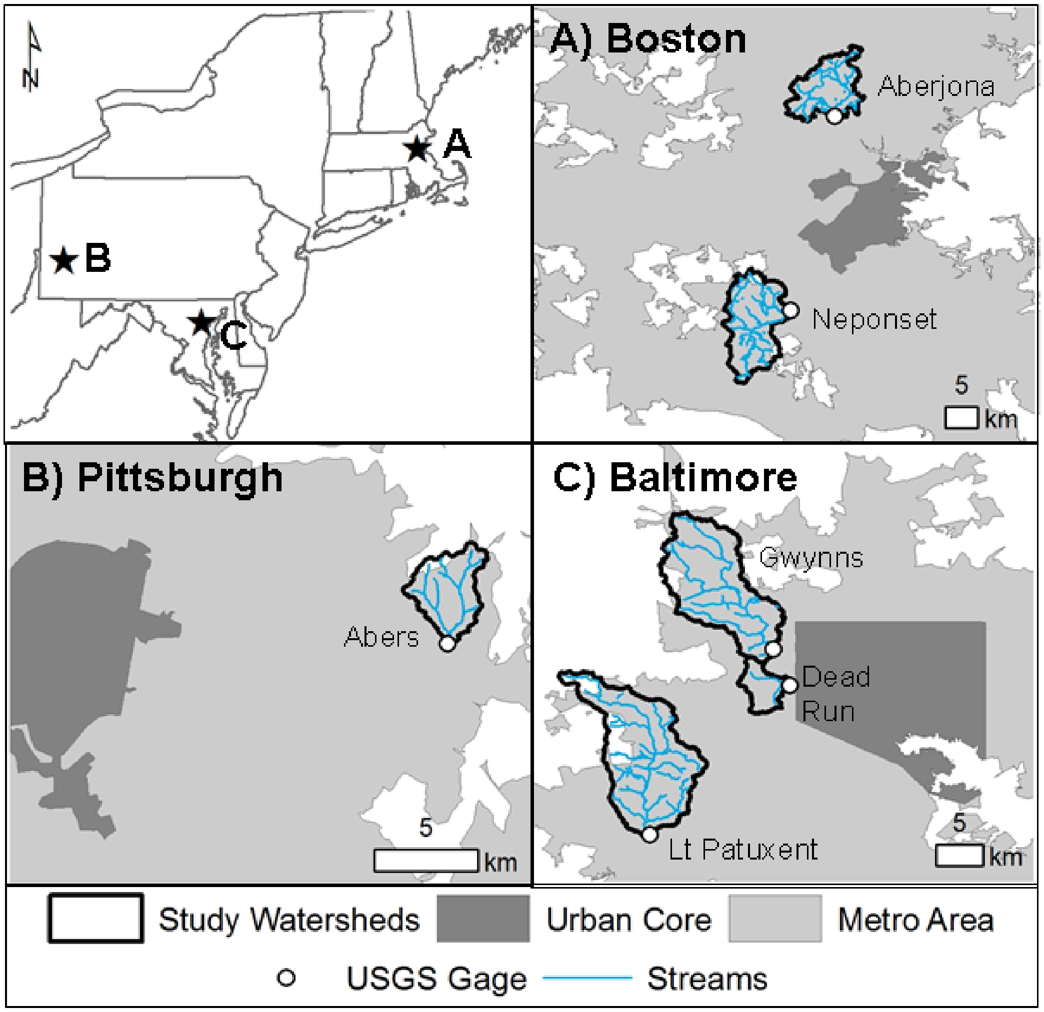

Figure 4-1: Long-term watersheds were located within the Eastern U.S. in Boston, MA (A), Pittsburgh, PA (B), and Baltimore, MD (C). Note that spatial scale varies among panels.

Table 4-1: General characteristics for long-term watersheds used in this study.

Watershed Name	USGS Gage Number	Basin Area (km^2)	Dominant Land Use	Flow Record Spans	Record Length (years)	Property Assessment Data Source	NCDC Rain Gage Location*
Baltimore, MD							
Dead Run	01589330	14.2	Suburban	1961 -2012	41	Maryland Property View	Baltimore Airport
Gwynns Falls Villa Nova	01589300	84.5	Urban	1957 - 2012	48	Maryland Property View	Baltimore Airport
Little Patuxent River	01593500	98.0	Suburban	1933 - 2012	80	Maryland Property View	Baltimore Airport
Boston, MA							
Aberjona River	01102500	59.7	Urban	1940 - 2012	73	MassGIS	Boston Logan Airport
Neponset River	01105000	84.9	Suburban	1941 - 2012	72	MassGIS	Boston Logan Airport
Pittsburgh, PA							
Abers Creek	03084000	11.4	Suburban	1950 - 1993	44	Allegheny County Property Assessment ǂ	Pittsburgh Airport

ǂ Property tax assessment records were only available for the portion of the Abers Creek watershed in Allegheny County, PA (82% of watershed). Basin area in Allegheny County was used to estimate building densities.

* NCDC station IDs for Pittsburgh (USW00094823), Baltimore (USW00093721), and Boston (USW00014739).

4.2.2 Reconstructing watershed growth

Parcel-level property tax assessments and U.S. Census records were used to reconstruct building density and population density time series for each study watershed (Table 4-1). Parcel-level property tax assessment records contained a building construction date for each parcel. Parcel boundaries in each watershed and associated building construction dates were used to estimate building densities every five years from 1900 to 2010. This study assumed each parcel contained one building, and only buildings included in the records were used in building density estimates. It is possible that building densities were underestimated in earlier decades due to replacement of historical houses during redevelopment. However, given limited data on historical housing locations and actual structure counts, these estimates are reasonable for evaluating general growth trends. In addition, the consistency in property tax records across cities was verified by cross-checking building density data with tract-level U.S. Census records [*Minnesota Population Center*, 2011]. When tract-level population data were not available, county-level data were used. This substitution was necessary for years prior to 1950 in three watersheds (Little Patuxent River, Gwynns Falls Villa Nova, and Abers Creek) and years prior to 1960 in one watershed (Neponset River). Area-weighted tract/county population records were used to calculate watershed population densities each decade from 1930 to 2010. These records provided a time series of population density and building density in each watershed over the last century.

4.2.3 Long-term hydrologic characterization

The Indicators of Hydrologic Alteration software (IHA) allows for rapid processing of daily discharge records to characterize flow conditions [*Richter et al.*, 1996]. The IHA (version 7.1) was used to characterize changes in ecologically-relevant flow conditions, including changes in the frequency of high flow events. The annual frequency of high flow events was calculated as the number of times daily mean stream flow exceeded the 75th percentile of flow. High flow events that spanned multiple days were counted as one distinct event. Since the frequency of high flow events may vary annually with precipitation, watershed runoff efficiency was also calculated. Annual runoff efficiency was estimated by dividing total annual storm flow (mm) by total annual precipitation (mm). USGS PART software (version 2.0) was used to separate daily mean discharge into annual baseflow and storm flow contributions (mm). Annual precipitation records were obtained from the National Climate Data Center using the nearest long-term weather station (Table 4-1).

4.2.4 Data analysis

The building density record was used to estimate the onset of peak development, the length of the peak development period, and the intensity of development in each long-term watershed. The onset of peak development was identified as the year coinciding with the first inflection point in the building density time series, indicating accelerated development (Figure 4-2A). The second inflection point was used to identify the year of the end of the peak development period, indicating a slowing of development (Figure 4-2A). The first and second inflection points were used to delineate years of the "peak growth period" in each watershed and the total length (years) of the peak development period (Figure 4-2A). Development intensity during the peak growth period was estimated by calculating the rate of change in building density construction from the start to the end of the peak growth period. In addition, the average year of building construction and the overall rate of change in population density and building density between 1950 and 2000 were calculated.

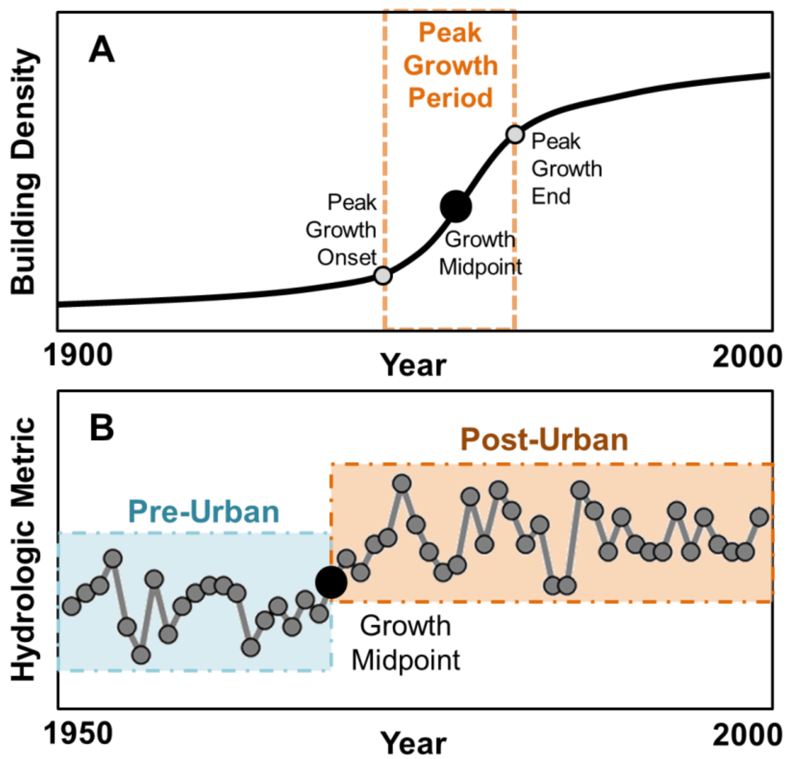

Figure 4-2: Pre- and post-development periods were defined based on the year of the building density growth midpoint.

Non-parametric Kendall tau (τ) tests were used to assess the significance of hydrologic trends across the stream flow time series. Kendall's tau is used to correct for the non-normal distributions, heterogeneous variances, and extreme events common in hydrologic datasets [*Kendall*, 1938]. The midpoint of the peak growth period was used to define the pre- and post-development time portions of the hydrologic record (Figure 4-2B). The growth midpoint provided a standardized technique to delineate growth periods in watersheds that vary in the timing and intensity of development. The pre-development period was defined as the time period prior to and inclusive of the growth midpoint, whereas the post-development period was defined as the time period after the growth midpoint. Due to limited stream flow records prior to the growth midpoint in Dead Run and Gwynns Falls at Villa Nova, the hydrologic breakpoint was used to delineate pre- and post-development time periods in these two watersheds. Annual values for each hydrologic metric during the pre- and post-development periods were averaged across the respective periods. The magnitude of change in hydrologic metrics arising from development was calculated by subtracting mean pre-development values from the mean of post-development values. Welch modified two-sample t-tests (TIBCO, Spotfire S+, version 8.2) were used to test the significance of differences between means of hydrologic metric values and precipitation amounts during the pre- and post-development periods. The mean change in hydrologic alteration metrics during pre- and post-development periods and growth metrics were used to assess if greater development intensity leads to a larger and faster change in hydrologic metrics. Linear regression analysis (TIBCO, Spotfire S+, version 8.2) was used to assess relationships between hydrologic and growth metrics.

Breakpoint analysis and piecewise linear regression were used to identify the year of any shifts in stream flow during the study period. Breakpoint and regression analysis were conducted using the segmented package in R Project version 2.15.3 [*Muggeo*, 2003]. Breakpoints were identified from the piecewise regression model with the lowest mean square error. Each breakpoint identified the year of shifts in annual high pulse frequency and runoff efficiency in the stream flow record for each study watershed. Lag times between the year of hydrologic shifts and development were calculated by subtracting the year of the hydrologic breakpoint from the year of the growth midpoint (Figure 4-3). Regression analysis was used to test associations between lag times and growth metrics.

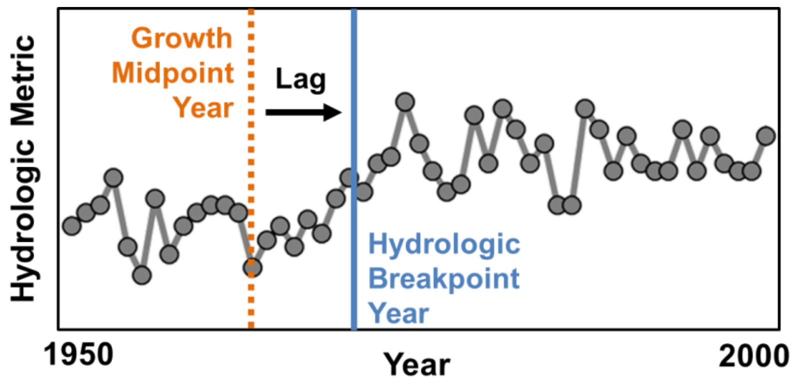

Figure 4-3: Hydrologic lags were identified as the number of years between the growth midpoint and the hydrologic breakpoint.

4.3 RESULTS

4.3.1 Long-term growth trends

Comparing long-term hydrologic records with reconstructions of urban growth provided a powerful means to examine how and when development altered stream flow in urbanizing watersheds. Across the majority of watersheds, there was limited growth between 1900 and 1950, rapid development between 1950 and 1970, and then stabilization of growth after 1970 (Figure 4-4). The onset of development occurred in 1950 in the urban watersheds and in 1950, 1960, or 1965 in the suburban watersheds (Table 4-2). The period of peak development lasted between 10 to 25 years, typically ending in 1965 and 1970 (Table 4-2). After 1970, building and population growth slowed and stabilized (Figure 4-4). However, two Baltimore watersheds Dead Run and Gwynns Falls Villa Nova, experienced a second period of growth between 1980 and 2000, while Abers Creek experienced a decline in population density starting in 1980 (Figure 4-4). Development began earliest in the Boston watersheds, with mean building construction dates of 1945 in the Aberjona River watershed and 1958 in the Neponset River watershed (Table 4-2). Development was youngest in the suburban Baltimore watershed, Little Patuxent River, with a mean building construction date of 1979.

Table 4-2: Comparisons of development patterns in each study watershed.

Watershed	Land Use	Peak Growth Period	Peak Growth Mid-Point	Peak Growth Period (years)	Peak Building Density Change (blg/km^2)	Peak Building Growth Rate (blg/km^2/yr)	Overall Population Growth Rate (ppl/km^2/yr)	Overall Building Density Growth (blg/km^2/yr)	Mean Year Built
Gwynns Falls Villa Nova	Urban	1950 - 1970	1960	20	141.1	7.1	21	5.9	1972
Aberjona River	Urban	1950 - 1960	1955	10	77.7	7.8	10	3.5	1945
Neponset River	Suburb	1950 - 1965	1957.5	15	43.4	2.9	5	1.8	1958
Dead Run	Suburb	1950 - 1965	1957.5	15	236.1	15.7	21	8.0	1963
Abers Creek	Suburb	1955 - 1970	1962.5	15	234.7	15.6	16	6.5	1968
Lt. Patuxent River	Suburb	1965 - 1990	1977.5	25	233.6	9.3	17	5.8	1979

Note: Overall building density and population density growth rates are calculated as changes between 1950 and 2000.

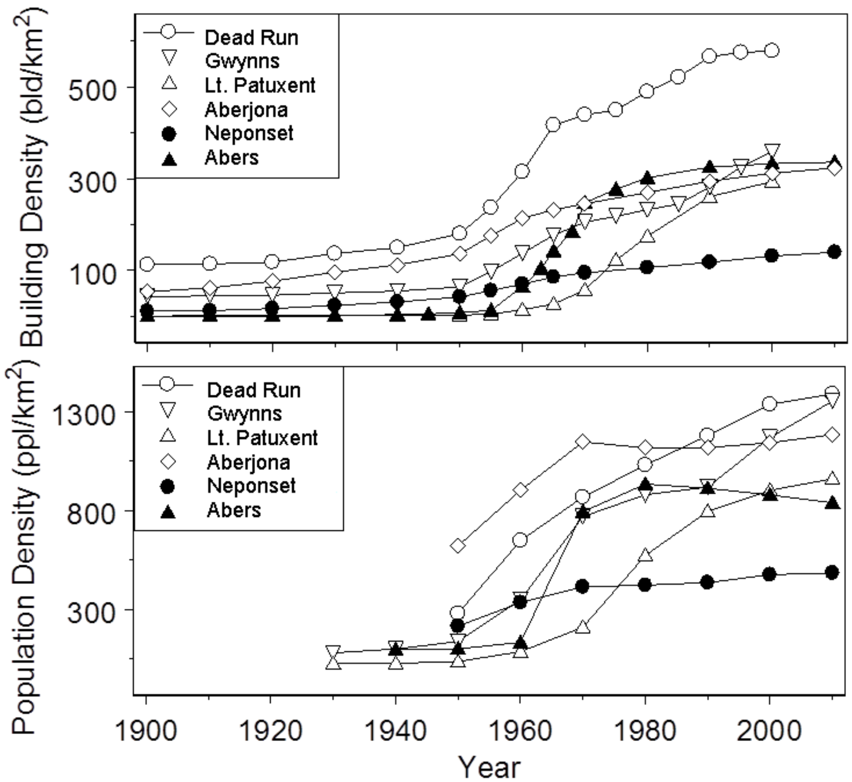

Figure 4-4: Study watershed development histories.

The peak development period indicated differences in the intensity of development among the study watersheds. Peak building density and overall population density growth rates ranged from 2.9 to 15.7 buildings/km^2/yr and 5 to 45 people/km^2/yr, respectively (Table 4-2). Peak building and population growth rates were greatest in Dead Run in Baltimore, Aberjona River in Boston, and Abers Creek in Pittsburgh. Development intensity was lowest in low-density suburban watershed Neponset River. Overall changes in population density between 1950 and 2000 were highest in Dead Run and Gwynns Falls Villa Nova and lowest in the Neponset River (Table 4-2). Watersheds with the highest building density growth rate did not necessarily have the highest population density growth rate.

4.3.2 Historical precipitation patterns

There were no significant ($p < 0.05$) trends in annual precipitation between 1950 and 2012 in the Baltimore, Boston, or Pittsburgh precipitation records (Figure 4-5). Average annual precipitation from 1950 to 2012 in Baltimore, Boston, and Pittsburgh was 108 cm, 110 cm, and 97 cm, respectively. Average annual precipitation as snow in Baltimore, Boston, and Pittsburgh was 5%, 10%, and 12%, respectively.

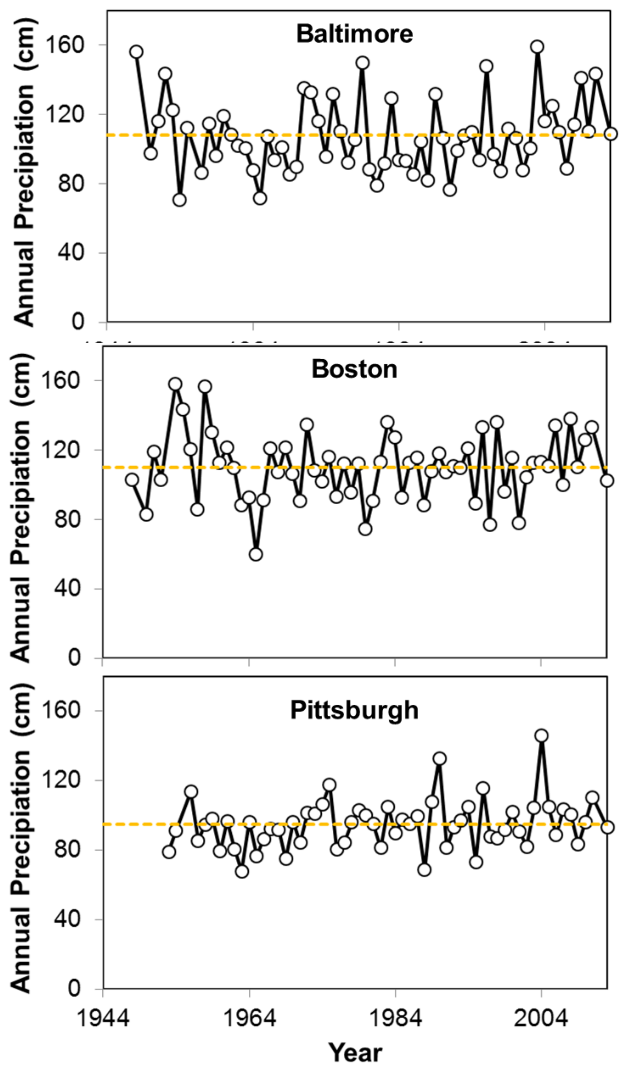

Figure 4-5: Annual precipitation in each study city. Dashed line indicates mean annual precipitation.

4.3.3 Increased frequency of high flow events

Across all study watersheds, there was a significant ($p < 0.05$) increase in the frequency of high flow events with time. Increases in the frequency of high flow events were greatest in the Baltimore watersheds (Figure 4-6). In contrast, the Boston watersheds had less frequent high pulse events compared to similarly developed watersheds in Baltimore and Pittsburgh. Increases in the frequency of high flow events were not always monotonic. In Aberjona River, Abers Creek, and Dead Run, the average annual frequency of high flow events shifted towards more frequent high flow events after 1970 (Figure 4-6). Breakpoints were used to identify the year of high pulse shifts in each study watershed. All high pulse shifts occurred between the years 1960 and 1976 (Table 4-3). High pulse shifts occurred two to eighteen years after the growth midpoint in all study watersheds expect in the Little Patuxent River, where the breakpoint in high pulse frequency occurred seven years before the growth midpoint (Table 4-2). Building densities coincident with the hydrologic breakpoint range from 70 to 260 building/km^2 (Table 4-3).

Hydrologic changes are most evident in the Abers Creek, Dead Run, and Aberjona River watersheds (Figure 4-6). These three watersheds urbanized rapidly during the same time period between 1950 and 1970 and all experienced a sustained increase in the frequency of high flow events between 1960 and 1975. In Dead Run, annual high flow frequency increased from 25 events in 1961 to 50 events in 1970. In Abers Creek, the annual frequency of high flow events increased from 10 events per year in 1963 to 34 events per year in 1974. In the Aberjona River, annual frequency of high flow events continuously increased from 5 events in 1964 to 21 events in 1973. During this ten year period, the frequency of high flow events doubled, tripled, and quadrupled in these watersheds. Once this dramatic increase occurred, the average annual frequency of high flow events shifted and stabilized at a new elevated state (Figure 4-6).

Mean annual high flow frequency during pre- and post-development time periods were also compared (Table 4-4). The mean annual frequency of high flow events during the pre-development time period ranged from 8 to 10 events in Baltimore, 17 events in Pittsburgh, and 21-28 events in Baltimore (Table 4-4). Differences in the mean frequency of high flow events indicated significant increases in the frequency of high flow events during the post-development period in five of the seven study watersheds (Table 4-4). Dead Run had the largest difference with a shift from an average of 28 to 48 high flow events per year. In general, these changes could not be attributed to changing precipitation amounts because the pre- and post-development periods had similar amounts of annual precipitation (Table 4-4). However, due to the limited pre-development record in Dead Run, that was coincident with a period of low annual precipitation, the post-development period had significantly higher annual precipitation (Table 4-4). Mean annual frequency of high flow events in Abers Creek increased from an average of 17 high flow events per year during the pre-development period to an average of 24 events per year during the post-development time period. In the Aberjona River, the most developed Boston watershed, mean high flow events shifted from an average of 10 events during the pre-development to 15 events during post-development. Gwynns Falls Villa Nova was the only watershed with no significant difference between the annual average frequency of high flow events during the pre- and post-development periods, though a substantial gap in the flow record (1989-1996) made precise identification of the hydrologic change challenging.

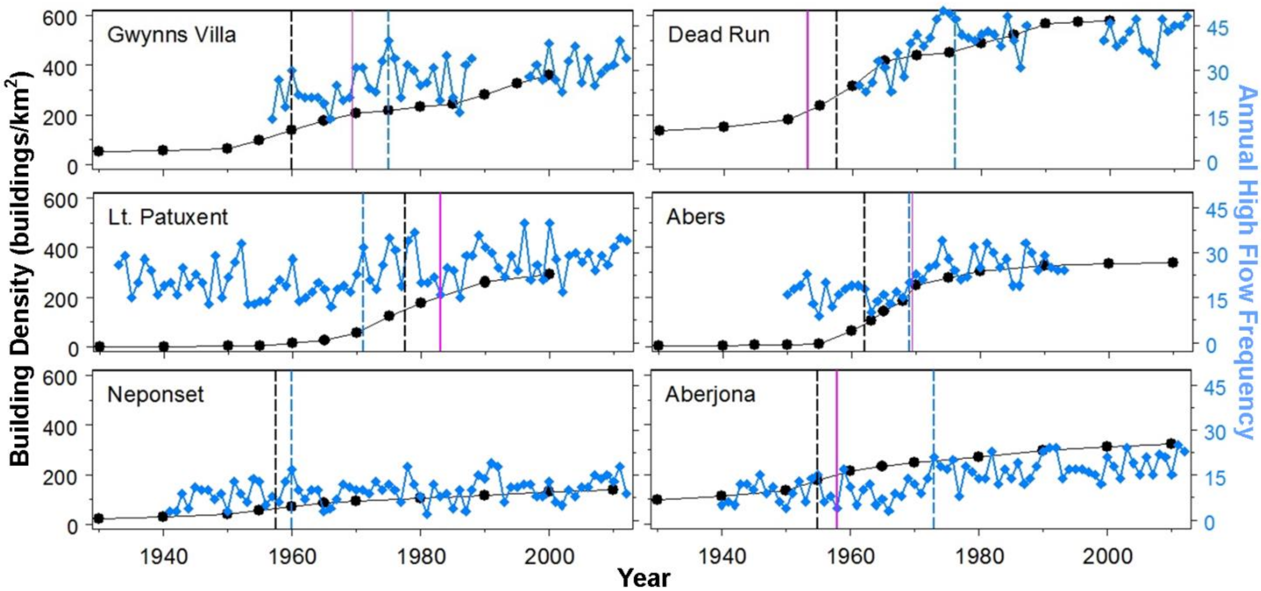

Figure 4-6: Building growth and annual high pulse frequency for each study watershed (1930-2010). Black dashed lines indicate the midpoint of peak growth and solid magenta lines indicate the year building density reached 200 building/km^2. Blue dashed lines indicate the high pulse breakpoint.

Table 4-3: Hydrologic breakpoints for high flow frequency and runoff efficiency.

City	Watershed	High Flow Break-Point	High Flow Lag*	Building Density at Breakpoint	Runoff Efficiency Breakpoint	Runoff Efficiency Lag*	Building Density at Breakpoint	Building Density in 1900 (blg/km^{2})
BES	Dead Run	1976	18	457	1971	13	441	112
BES	Gwynns Falls Villa Nova	1975	15	218	1972	12	210	43
BES	Lt. Patuxent River	1971	-7	70	1971	-7	70	1
BOS	Aberjona River	1973	18	260	1966	11	235	54
BOS	Neponet River	1960	2	71	1968	10	91	11
PIT	Abers Creek	1969	6	216	1975	12	277	1

*Lag times indicate the number of years between the break point and the midpoint of the peak development period.

Table 4-4: Means for hydrologic metrics during pre- and post-urbanization periods.

Watershed	Time Period	Mean Annual High Flow Frequency	Mean Annual Runoff Efficiency	Mean Annual Precipitation (mm)
Dead Run (Baltimore)[ǂ]				
Pre	1960 - 1968	28.1	0.28	992
Post	1969 - 2012	42.2	0.40	1,104
Average Change		14.1*	0.12**	112*
Gwynns Falls at Villa Nova (Baltimore)				
Pre	1957 - 1960	22.3	0.12	1,100
Post	1961 - 2012	27.8	0.19	1,066
Average Change		5.5	0.07	-35
Little Patuxent River (Baltimore)				
Pre	1933 - 1977	20.8	0.13	1,033
Post	1978 - 2012	27.4	0.19	1,078
Average Change		6.6**	0.06**	45
Aberjona River (Boston)				
Pre	1940 - 1955	9.5	0.08	1,067
Post	1958 - 2012	15.1	0.13	1,095
Average Change		5.6**	0.05**	28
Neponset River (Boston)				
Pre	1940 - 1957	8.0	0.08	1,063
Post	1958 - 2012	10.3	0.10	1,095
Average Change		2.3*	0.02**	32
Abers Creek (Pittsburgh)				
Pre	1949 - 1962	16.9	0.20	947
Post	1963 - 1993	23.5	0.20	936
Average Change		6.6**	0.0	-11

** Significant differences pre- and post-urbanization periods $p < 0.01$

* Significant differences pre- and post-urbanization periods $p < 0.05$

[ǂ] Due to limited pre-development stream flow records the development periods were defined by visual interpretation of the time series.

4.3.4 Increased runoff efficiency

Significant ($p < 0.05$) increases in runoff efficiency were observed across the time series in all study watersheds except Abers Creek (Figure 4-7). Runoff efficiency was defined as the proportion of precipitation routed to the stream as storm flow each year. Dead Run had the largest increase in runoff efficiency across the time series and the greatest variability (mean = 0.37 ± s.d. 0.09), whereas the Neponset River had the least annual variability in runoff efficiency across the time series (mean = 0.095 ± s.d. 0.027). In contrast to the high pulse frequency, increases in runoff efficiency were gradual across the time series, with relatively minor shifts (Figure 4-7). Breakpoint analysis indicated relatively minor shifts in runoff efficiency occurred between the years 1966 and 1975 (Table 4-3). Runoff efficiency breakpoints occurred between 1971 and 1972 in all the Baltimore watersheds (Table 4-3). All runoff efficiency breakpoints occurred after the growth midpoint, except in the Little Patuxent River where the breakpoint occurred seven years before the growth midpoint. In the other watersheds, the runoff efficiency breakpoints lagged ten to thirteen years behind the growth midpoint. The year of runoff efficiency breakpoints occurred prior to or in the same year as high pulse frequency breakpoints in Baltimore watersheds and the Aberjona River and after high pulse frequency breakpoints in the Neponset River and Abers Creek (Table 4-3).

Along with overall increases in runoff efficiency, the magnitude of average annual increases in runoff efficiency during pre- and post-development time periods were variable (Table 4-4). Mean annual pre-development runoff efficiency ranged from 0.12 to 0.28 in the Baltimore watersheds, 0.20 in Pittsburgh, and 0.08 in Boston (Table 4-4). Mean differences in runoff efficiency indicated significant increases in runoff efficiency during the post-development period in four of the six long-term watersheds (Table 4-4). Dead Run had the largest increase in the post-development mean runoff efficiency from 0.28 to 0.40, an increase of 0.12. The Aberjona River and Little Patuxent River had mean increases in runoff efficiency of 0.05 and 0.06 during the post-development period, respectively.

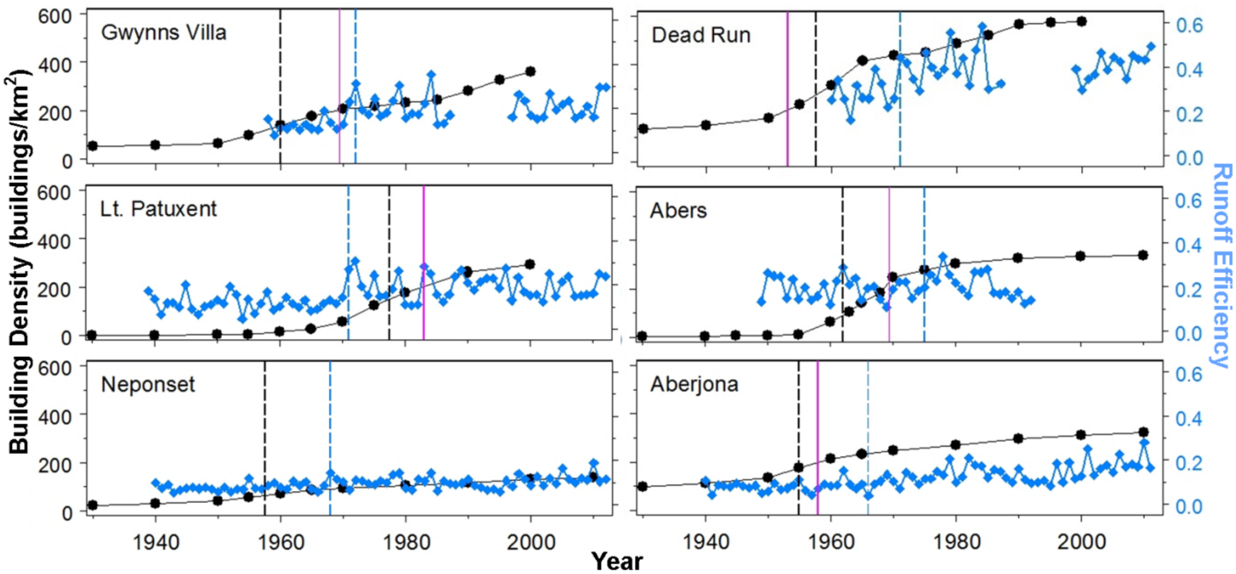

Figure 4-7: Building growth and annual runoff efficiency for each study watershed. Black dashed lines indicate the midpoint of peak growth and solid magenta lines indicate the year building density reached 200 buildings/km^2. Blue dashed lines indicate the runoff efficiency breakpoint.

4.3.5 Development intensity and hydrologic shifts

Results indicated the shift in the mean frequency of high flow events and runoff efficiency from the pre- to post-development period was proportional to the overall change in watershed building density between 1950 and 2000 (Figure 4-8). Overall building density had the strongest association with high flow frequency and runoff efficiency changes among the growth metrics quantified here including, overall population density and peak building density.

This relationship was particularly strong for runoff efficiency when the outlier Abers Creek was excluded. Abers Creek was identified as an outlier because it had lower runoff efficiency than expected given development intensity. In Abers Creek, baseflow seemed to be supplemented by additional water imports leading to lower runoff efficiency than expected. Results suggest the magnitude of hydrologic changes with urbanization is highly dependent on the intensity of development.

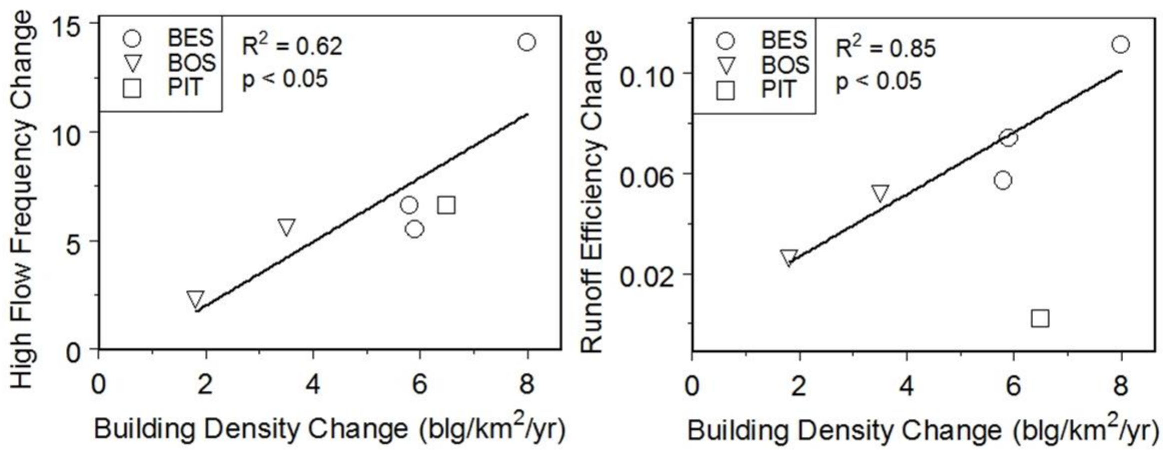

Figure 4-8: The magnitude of the change in mean pre- and post-development hydrologic metrics increased linearly with the change in watershed building density between 1950 and 2000. Abers Creek was excluded from the linear fit for runoff efficiency.

4.4 DISCUSSION

This work reconstructed the timing and intensity of watershed development and identified the timing of long-term hydrologic changes in six urbanizing watersheds in the Eastern U.S. The results identified: (1) significant increases in the frequency of high flow events and runoff efficiency in the majority of the study watersheds; (2) three watersheds that developed rapidly exhibited a significant shift in mean annual high flow frequency and runoff efficiency; (3) the magnitude of hydrologic shifts was proportional to development intensity; and (4) flow shifts typically lagged behind the growth midpoint but coincided with a period a rapid development between 1950 and 1970 and the construction of landscape features such as highways and strip malls and an extreme flood event (e.g., Hurricane Agnes).

4.4.1 Stream flow shifts and inter-city differences

These results demonstrate that rapid urbanization leads to abrupt shifts from one flow regime to another, with the magnitude of the flow shift proportional to development intensity (Figure 4-8). However, current conceptual models of hydrologic changes in urbanizing watersheds assume these changes were coincident with development. This conceptual model arises in part due to the use of urbanization gradients as a study design, which requires fundamental assumptions about temporal dynamics, such as watersheds spanning the rural to urban gradient represent general development stages during watershed urbanization. These stages then serve to represent changes occurring within one watershed during urbanization. However, this approach minimizes transitions in water management and development styles over time. Instead, a long-term approach can be used to overcome some of the limitations of a gradient approach. For example, *DeWalle et al.*, [2000] found urbanization increased mean annual stream flow, with stream flow changes proportional to the change in watershed population density in 39 urbanizing watersheds across the U.S. However, *DeWalle et al.* [2000] did not identify any regional differences in stream flow response to urbanization. The results presented here also report changes in runoff efficiency were related to the change in watershed population density during urbanization (R^2 = 0.66, p = 0.06). However, building density had stronger associations with changes in both high flow frequency and runoff efficiency in the study watersheds. Significant changes in stream flow were also evident in an urbanizing watershed in Annandale, VA that had an increase in watershed impervious cover from 3% to 1949 to 33% in 1994 [*Jennings and Jarnagin*, 2002]. *Jennings and Jarnagin* [2002] identified a significant change in stream flow response between 1963 and 1971, which corresponded with a change from 13% and 21% impervious cover, respectively. The majority of the hydrologic shifts identified in this study corresponded with the time period identified by *Jennings and Jarnagin* [2002] (Table 4-3).

Pre-development baselines varied among the study cities, with lower pre-development runoff efficiency and high flow frequency in the Boston watersheds compared to watersheds in Pittsburgh and Baltimore (Table 4-4). Lower pre-development baselines in Boston compared to Pittsburgh and Baltimore are consistent with findings from Chapter 3 of this dissertation. Lower pre-development baselines in Boston may be due regional differences in physiographic setting such as local topography and soils. The topography of the Boston watersheds is flat with an average watershed slope of approximately 3% and lake density is high compared to the other study watersheds (Table 4-5). In addition, soils in the Aberjona River watershed had an average permeability of 8 in/hr, compared to 1 in/hr in Abers Creek and Dead Run (Table 4-5). These physiographic features in Boston watersheds may buffer high flow events, resulting in lower frequency of high flow events.

Hydrologic changes in the urban watersheds were also smaller in the Aberjona River compared to Dead Run and Abers Creek. One explanation for the lower hydrologic baseline could be the hydrologic buffering capacity of the watershed drainage network, which is related to the extent and geometry of the drainage network [*Benda et al.*, 2004]. The Aberjona River watershed has a series of lakes (1.7% of the watershed area) distributed throughout the catchment and three dams with a total storage capacity of 50 Megaliters/km^2 (Table 4-5). A higher density of lakes and dams and more permeable soils seems to hydrologically buffer the effects of urbanization in the Aberjona River watershed relative to the other watersheds.

Table 4-5: Average physiographic characteristics for study watersheds.

Watershed	City	Basin Slope (%)	Soil Permeability (in/hr)	Dam Storage (Ml/km^2)	Lake Density (#/km^2)	Dominant Soils*
Neponset	BOS	2.7	9	57.9	2.9	Till
Aberjona	BOS	3.3	8	49.9	2.5	Till
Lt. Patuxent	BES	3.2	2	37.2	0.7	Clay residuum
Dead Run	BES	2.7	1	0.0	0.1	Clay residuum
Gywnns Falls	BES	3.6	2	1.1	0.4	Clay residuum
Abers Creek	PIT	8.8	1	0.0	0.9	Sandy & stony colluvium

Soil permeability derived from *Wolock* [1997].
*Dominant soil types derived from [*Clawges and Price*, 1999].

Other studies have also found variability in stream flow response among urban watersheds in different physiographic regions. In Maryland, impervious cover affects high flow events to a greater degree in Coastal Plain streams relative to Piedmont streams [*Utz et al.*, 2011]. *Utz et al.,* [2011] suggest greater hydrologic impact in the Coastal Plain may be due to lower topographic relief and more permeable soils in the Coastal Plain compared to steep gradients, shallow basement rock, and less permeable soils in the Piedmont. Therefore, adding impervious surfaces to the Coast Plain watersheds would induce greater hydrologic impact relative to the Piedmont. The results from Chapter 3 provided a contrasting explanation of the variability in hydrologic metrics among ecoregions (Figure 3-12). Chapter 3 identified distinct flashiness responses to urbanization among physiographic settings, specifically glaciation history may strongly influence hydrologic response to urbanization. Study watersheds with a glacial legacy had twice the soil permeability, twice the lake density and roughly half the slope of non-glaciated watersheds. These landscape features likely buffer small flow events and result in a reduction in the overall frequency of high flow events. Results from this long-term study confirmed these observations, with Boston streams having lower hydrologic baselines at low levels of development (Figure 4-6). However, results also indicated that hydrologic changes relative to the baseline occur to a similar degree across the three study cities, with development intensity as the main driver of hydrologic changes (Figure 4-8). This was evident due to the linear increase identified between the change in hydrologic metrics and the change in building density. Shifts in hydrologic metrics indicated increases relative to the baseline, low-development condition. Therefore, relative to the baseline, the magnitude of the hydrologic shift was dependent on development intensity regardless of location or physiographic setting.

The nature of abrupt hydrologic shifts in the study watersheds has clear implications for stream impairment and stream restoration efforts. The timing of hydrologic shifts in the study watersheds indicate natural flow regimes were modified over 40 years ago. The compounding set of symptoms that these systems experienced for over 40 years will be challenging to address with stream restoration. The results from this synthesis suggest that restoration solutions focused on capturing and infiltrating stormwater at the source would be more effective at reducing the hydrologic effects of urbanization by reducing the volume of stormwater delivered to the stream. In suburban and urban watersheds, placing stormwater management strategies in the headwaters of the watershed before restoration efforts occur in the stream reach will likely provide greater hydrologic benefits than stream restoration alone [*Walsh et al.*, 2005b; *Roy et al.*, 2008]. For example, stream restoration practices using pool and riffle sequences to slow down and dissipate energy will likely have limited success in highly modified urban streams where extremely flashy storm flows can wash out investments along the stream reach [*Bain et al.*, 2014]. Focusing on the catchment to regulate flow in the stream will likely be the solution in most urban systems because in-stream restoration efforts do not directly address stormwater quantity at the watershed scale [*Walsh et al.*, 2005b].

4.4.2 Precipitation variability and flow metrics

Shifting precipitation patterns during the late 20th century seemed to drive stream flow increases in reference watersheds in the Eastern U.S. [*Lins and Slack*, 1999; *McCabe and Wolock*, 2002]. However, in human-dominated watersheds, the expansion, arrangement, and connection of impervious surfaces to the stream networks drive hydrologic changes [*Shuster et al.*, 2005; *Walsh et al.*, 2005b]. Further, urbanization intensifies the underlying precipitation signature as the watershed shifts from infiltration- to runoff-dominated pathways [*Arnold and Gibbons*, 1996]. In the study watersheds, hydrologic shifts were independent of annual variability in precipitation patterns. While annual precipitation varies annually, this study did not identify any significant increases or declines ($p < 0.05$) in annual precipitation amount from 1950 to 2000 any of the study watersheds. In addition, only Dead Run had significantly less annual precipitation during the pre- and post-development periods (Table 4-4). This difference in precipitation amount is likely due to the limited pre-development stream flow record, which coincided with a period of lower annual precipitation.

On an annual basis both high flow frequency and runoff efficiency varied. High flow frequency ranged from no change in annual high flow frequency between consecutive years to an increase of 20 high flow events from one year to the next (Figure 4-6). This variability indicated annual high flow frequency was relatively sensitive to precipitation. In contrast, runoff efficiency normalized total storm flow by annual precipitation and therefore controlled for variability in precipitation. Runoff efficiency ranged from no change to a change of 0.28 from one year to the next (Figure 4-7). The stronger relationship between the change in runoff efficiency and change in building density compared to change in high flow frequency and change in building density was likely because runoff efficiency was less sensitive to annual precipitation patterns (Figure 4-8). Therefore, runoff efficiency was an effective metric for identifying and assessing the degree of long-term stream flow alteration. In addition, runoff efficiency was a more standardized metric for the comparison of watersheds of different sizes and in different climates.

4.4.3 Hydrologic lags

The unique history of watershed development in each study watershed provided a dataset to investigate potential drivers of the hydrologic shifts. Inter-city differences in physiographic setting provided a diverse set of templates for contrasting urbanization processes under different constraints. The timing of peak development in the study watersheds was relatively consistent across the three cities, typically occurring between 1950 and 1970 (Table 4-2). While the magnitude of each hydrologic shift was proportional to the change in watershed building density, the hydrologic breakpoints lagged between 7 years before or 18 years after the growth midpoint (Table 4-3). The variability of hydrologic lags indicated runoff efficiency and high flow frequency were likely affected by different urbanization processes. The timing of hydrologic lags were not clearly linked to growth metrics, therefore other factors along with development seem to drive these changes. In particular, extreme weather events and highway construction may influence the timing of hydrologic changes in the study set.

Hydrologic shifts in runoff efficiency in the three Baltimore study watersheds coincided with the year of an extreme weather event (Figure 4-9). Hurricane Agnes struck the East Coast of the U.S. in June of 1972, dropping more than 25 cm of rain on the Piedmont of Maryland [*DeAngelis and Hodge*, 1972]. In all Baltimore study watersheds, runoff efficiency breakpoints occurred between 1971 and 1972, coincident with Hurricane Agnes (Table 4-3). The timing of runoff efficiency shifts and Hurricane Agnes suggests that this extreme weather event may drive the timing of runoff efficiency shifts, more so than watershed urbanization. The timing of Hurricane Agnes better explains the variability in lag times among Baltimore watersheds. Extreme weather events may amplify the effect of urbanization, by sparking a shift from one hydrologic state to another.

Other studies documented the impacts of Hurricane Agnes on Piedmont watersheds in Maryland. *Costa* [1974], found cross-section changes showing the widening and deepening of the stream channels in a watershed west of Baltimore. However, *Costa*, [1974] suggest that large flood events play a minor role in shaping the Piedmont landscape, because study cross-sections indicated the stream channel accumulated significant amounts of sediment within one year of Agnes. However, results from this study indicate Hurricane Agnes likely had a significant impact of hydrology in these watersheds. None of the Baltimore flow regimes recovered to pre-storm levels after Hurricane Agnes (Figure 4-9). The lack of hydrologic recovery suggests that hydrologic rebound is challenging after such an extreme event that can amplify the impacts of urbanization.

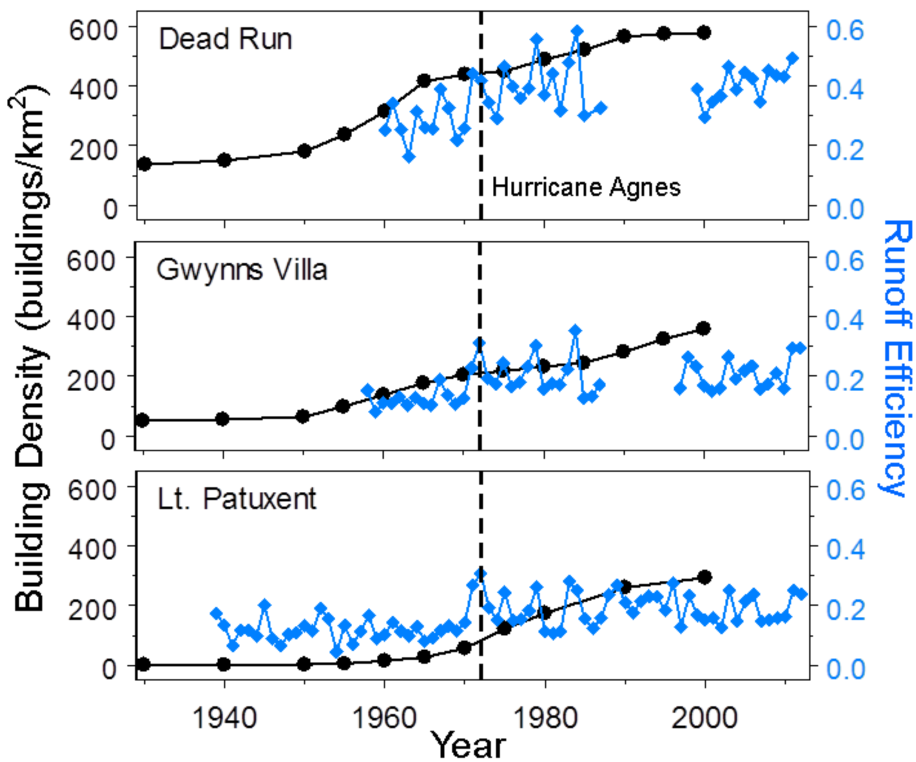

Figure 4-9: Changes in runoff efficiency in the Baltimore watershed coincident with Hurricane Agnes in 1972.

The timing of impervious surfaces growth may also contribute to lags in hydrologic response. Urbanization during the early 20th century was likely similar to current suburban development, with the installation of roads, sewers, and drainage networks first, followed by the construction of residential houses and population growth [Chapter 2]. In some of the study watersheds, the construction of highway interchanges and the connection of these impervious surfaces can explain variability in lag times and stream flow shifts. Abers Creek and Dead Run watersheds were similar in size and in development intensity, with both experiencing growth rates of 16 building/km^2/yr during the period of peak development (Table 4-2). However, Dead Run experienced a larger shift in the average annual frequency of high flow events during the post-development period, 14 events compared to 7 events in Abers Creek (Table 4-4). The larger shift in Dead Run was likely due to the construction of an interstate interchange in the watershed during the late 1960's. The I-695 and I-70 interchange opened in 1969, which added 8.4 km of two- and four-lane highways bisecting the Dead Run watershed [*MSA SC* 1969]. The construction of these highways and associated onramps added 0.3 km^2 of directly connected impervious surfaces (2% of total area) to the watershed, based on the number of lanes, road widths, and state highway standards. The completion of the highway interchange in 1969 and the hydrologic shift in runoff efficiency in 1971 suggests that the construction of the highway coincident with Hurrian Agnes may drive the shift in runoff efficiency.

Nelson et al., [2006] also identified an increase in mean annual discharge during the 1960's and 1970's and a leveling off of flow in the 1980's in Dead Run. However, *Nelson et al.*, [2006] attribute the flow increase during the 1970's to an influx of imported water from leaks in the water distribution system and the leveling off of flows during the 1980's to evapotranspiration in newly constructed detention ponds. However, *Nelson et al.*, [2006] provide little quantitative evidence to support these assertions. While these are a possible explanations for observed flow changes in Dead Run, results from long-term reconstructions suggest the construction of the highway system is the main driver of hydrologic changes in Dead Run. Results indicate the timing of hydrologic lags depends less on the timing of peak watershed development, which was relatively consistent among the study watersheds, and more on interactions with perturbations such as extreme weather events (i.e., Hurricane Agnes) and large construction projects (i.e., highways).

4.5 CONCLUSIONS

Results clarify that urbanization can lead abrupt hydrologic shifts in the frequency of high flow events and runoff efficiency and for the first time demonstrate temporal lags in hydrologic response. The magnitude of shifts in runoff efficiency and high flow frequency during urbanization were proportional to the intensity of development. This relationship indicates that development intensity is the main driver of magnitude of flow regime shifts. However, development patterns were not the dominant driver of the timing of stream flow shifts, which lagged behind growth midpoints in almost all of the study watersheds. Perturbations such as extreme weather events (i.e., Hurricane Agnes) and large construction projects (i.e., highways and strip malls) are the main drivers of hydrologic shifts in the study watersheds. Features such as highways dramatically alter drainage patterns over a relatively period (2-5 years). In addition, results indicate extreme weather events concurrent with watershed development can have lasting hydrologic effects on the stream flow regime.

The current conceptualization of urban stream syndrome does not effectively incorporate the importance of large features, such as highways, or the potential for extreme weather events to amplify per-existing hydrologic shifts. In addition, differences in hydrologic responses to urbanization across physiographic regions are only now being recognized and explored [*Brown et al.*, 2009b; *Utz et al.*, 2011]. The results presented here also illustrate the importance of contrasting hydrologic response across physiographic regions and the variability in hydrologic baselines across watersheds within the same city and among cities. Without a hydrologic baseline, it is challenging to quantify the severity of hydrologic alterations due to urbanization, to identify a target for restoration, or to assess the performance of stormwater management efforts. Refining urban stream syndrome theory to incorporate inter-city variation in baselines and temporal lags in will improve our ability assess and identify mechanisms driving variability in hydrologic response among urban watersheds.

5.0 CONCLUSIONS & SYNTHESIS

The symptoms of urban stream syndrome are well documented in the literature. However, a framework is lacking that allows explanation of the wide variation observed in the symptoms of urban stream syndrome across watersheds and regions. This dissertation identifies additional factors that can be integrated into existing conceptual and mechanistic models when examining hydrologic responses to urbanization. Chapter 2 identifies the roles of arrangement and connectivity of sewer and drainage infrastructure, the age of sewer infrastructure, and the extent of tree canopy in a small urban watershed. Integrating these three factors into hydrologic models will improve our accounting of water inputs and outputs including inter-basin transfer of water and sewage, groundwater subsidies from leaking pipes, and changes in rain interception and evapotranspiration due to expanding or declining urban tree canopy. These factors can provide substantial contributions to the overall water balance; however, they are often neglected in urban studies due to the challenges in quantifying such values. Existing work has shown that both refined urban water balance methods and partnerships with local water and sewer authorities can quantify some of these components [*Bhaskar and Welty*, 2012; *Wollheim et al.*, 2013; *Hopkins et al.*, 2014]. Continued improvements in quantifying these water balance components are essential for the effective remediation and restoration of urban hydrologic systems.

Chapter 3 documented variation in hydrologic alterations among the study cities and explored how natural differences among physiographic regions might influence hydrologic response. In particular, the pre-existing physical template (i.e., glaciation history) influences the magnitude of changes in stream flashiness across study urbanization gradients. Glaciation history imparts specific features on the landscape (i.e., low relief and high water storage capacity), that provide hydrologic buffering that can dampen the severity of high flow events by slowing down and storing more water relative to non-glaciated landscapes. This pre-existing physical template strongly influences the type and magnitude of hydrologic changes within a city and can regulate the contrasting relationships identified here between flashiness response and annual precipitation among glaciated and unglaciated cities. An overarching framework is presented that identifies important physical characteristics of the watershed and urban characteristics that influence the severity of hydrologic change among glaciated and unglaciated regions (Figure 3-12). Overall, results from Chapter 3 provide a unique dataset that facilitates evaluation of hydrologic changes in each city and clarifies of the drivers of inter-city differences in hydrologic response to urbanization.

Results from Chapter 3 can also be used to identify cities and watersheds that are more resistant to hydrologic change and identify both landscape features and infrastructure strategies with higher hydrologic buffering capacity (Figure 3-12). Results highlight the value of landscape features (i.e., lakes and soils) that increase the water storage capacity of the landscape. Replicating the water storage function of large-scale features via a distributed network of stormwater management strategies that improve water infiltration and storage may have a similar impact in urban watersheds. However, given the importance of the physical template that a city is built upon, addressing hydrologic alterations through the installation of new stormwater management strategies will likely require more investment in some cities than others to achieve target conditions. For example, installing stormwater management practices (i.e., rain gardens) in a city such as Pittsburgh, with steeper relief and less permeable soils, will require more investment to amend the soil to increase infiltration and slow down stormwater, than a city such as St. Paul with flat relief and more permeable soils.

The long-term watershed approach utilized in Chapter 4 examined abrupt shifts in runoff efficiency and high flow frequency following watershed urbanization. In particular, temporal lags in hydrologic response are demonstrated for the first time in urban systems. Results indicate the timing of hydrologic lags depends less on the timing of peak watershed development, which was relatively consistent among the study watersheds, and more on the interaction of perturbations such as extreme weather events (i.e., Hurricane Agnes) and large-scale construction projects (i.e., highways). For example, the hydrologic impact of Hurricane Agnes was evident in the runoff efficiency record of all three Baltimore watersheds, with shifts in runoff efficiency all occurring between 1971 and 1972, coincident with Hurricane Agnes (Table 4-3). These results demonstrate that extreme weather events can drive hydrologic shifts and explain the timing of runoff efficiency lag in the Baltimore watersheds. Thus, extreme weather events apparently amplify the effect of urbanization. In addition, none of the flow regimes patterns recovered to pre-storm levels after this extreme event, indicating that hydrologic rebound may be challenging once urbanization occurs.

Along with the timing of hydrologic changes, it is also important to recognize hydrologic baseline conditions in the watershed prior to urbanization. Chapter 4 highlights variability in hydrologic baselines across watersheds within the same city and among cities. Without a hydrologic baseline it is difficult to accurately quantify the severity of hydrologic changes post-urbanization. Paired watershed and urbanization gradient studies provide knowledge of baseline conditions. Results from long-term watershed studies provide a better estimate of watershed-specific baselines, which were variable among the three study cities (Table 4-4). Results highlight the need to refine urban stream syndrome theory to incorporate inter-city variation in baseline conditions upon which symptoms of the syndrome are assessed. Further these baselines provide a potential target for restoration efforts and stormwater management practices assess progress against. Work presented in this dissertation has advanced the field of urban system science by identifying mechanisms driving variability in hydrologic response among cities and suggesting additional components to add to existing conceptual models. Further, this work demonstrates the benefit of spatiotemporal reconstructions of human- and natural-infrastructure during the process of urbanization to clarify potential alterations of specific components of the hydrologic cycle.

Finally, results from this dissertation were used to organize a framework of physical and hydrologic changes associated with different types of human infrastructure common in urban watersheds. Table 5-1 describes the range of physical and hydrologic impacts associated with human infrastructure, as well the major mechanism that drives hydrologic change. In addition, the timing of hydrologic changes and long-term effects of each human infrastructure component are described. For example, the construction stormwater pipe networks (i.e., stormwater and combined sewer) can have numerous hydrologic impacts that vary depending on the physical changes due to stormwater pipe construction (Table 5-1). Stormwater pipe infrastructure that connects impervious surfaces directly to the stream will increase stream flashiness, whereas stormwater pipe infrastructure that connect two adjacent watershed together can divert runoff to an adjacent watershed thereby reducing stream flashiness.

Table 5-1: Physical and hydrologic changes associated with different types of human infrastructure associated with urbanization.

Human Infrastructure	Potential Physical Changes	Mechanism for Hydrologic Change	Major Hydrologic Consequences	Timing of Hydrologic Change	Long-Term Hydrologic Impacts
Stormwater or combined sewer infrastructure	Installation of stormwater or combined sewer pipe networks	Increased effective impervious cover through the direct connection of impervious surfaces to stream network	↑ Frequency of high flow events ↓ Duration of high flow events ↑ Magnitude of extreme events ↑ Runoff efficiency	Activated during construction and intensifies as development expands	Pipe leakage subsidizes groundwater
	Stream culverting and burial	Alteration and simplification of the natural drainage network	↓ Stream baseflow	Activated during construction and intensifies as development expands	Increased erosion and channel incision/widening
	Inter-basin water transfer	Pipe infrastructure connects two adjacent watershed together	↓ Frequency of high flow events ↑ Duration of high flow events ↓ Magnitude of extreme events ↓ Runoff efficiency	Activated during construction and intensifies as development expands	Overall reduction in water yield Reduction in dry weather baseflow
Impervious surfaces	Hard surfaces such as roadways, parking lots, and rooftops	Sealing of the soil surface impervious surfaces that prevent infiltration and general runoff	↑ Frequency of high flow events ↓ Duration of high flow events ↑ Magnitude of extreme events ↑ Runoff efficiency ↓ Baseflow	Activated as impervious surfaces are connected to the stream network via pipe. Extreme weather events coincident with IC expansion can spark flow shifts	Continuous impact
Dams and reservoirs	Large structures that regulate the flow of water and create a large reservoir	Stream flow regulation and stabilization	↓ Frequency of high flow events ↑ Duration of high flow events ↓ Magnitude of extreme events ↑ Baseflow	Activated once construction is completed	Regulating function is reduced over time as sediment accumulates behind the dam

APPENDIX A

DATA TABLES FOR CHAPTER 2

Table A 1: Panther Hollow watershed population data.

Year	Total Population	Total Houses	Impervious Cover (%)	Residential Water Use (m^3/year)	Sewer Leakage (%)	Sewer Leakage (m^3/year)	Sewer Leakage (mm/yr)
1910	1,458	179	11.4%	201,477	NA	NA	NA
1920	2,024	352	14.6%	279,606	0.5%	1,398	1
1930	3,792	600	20.2%	523,955	1.0%	5,240	4
1940	4,669	653	21.2%	645,065	1.5%	9,676	7
1950	4,603	697	21.3%	635,932	2.0%	12,719	9
1960	4,192	735	21.4%	579,186	2.5%	14,480	10
1970	3,736	817	21.8%	516,260	3.0%	15,488	11
1980	3,338	841	22.1%	461,211	3.5%	16,142	11
1990	3,164	872	22.5%	437,135	4.0%	17,485	12
2000	3,048	898	22.9%	421,127	4.5%	18,951	13
2010	3,397	ND	23.2%	469,311	5.0%	23,466	16

Table A 2: Panther Hollow watershed infrastructure data.

Year	Sewers (km)	Roads (km)	Streams (km)	Tree Canopy (%)
1872	0.0	3.1	4.9	ND
1890	0.0	4.5	4.9	ND
1989	4.4	ND	4.9	ND
1904	9.3	8.7	2.7	ND
1911	16.7	15.0	2.1	ND
1923	ND	16.4	2.1	ND
1938	ND	17.2	2.1	20%
1956	ND	ND	ND	24%
1967	ND	16.1	2.1	26%
2010	16.8	13.7	2.1	36%

Table A 3: Panther Hollow watershed yield reconstructions.

Year	Annual Precipitation (mm)	Impervious Cover (%)	Ric	Impervious Yield (mm)	Rhist	Infra. Yield	Additional ET (mm)	Additional Leakage (mm)
1872	811	2.5%	0.35	284	0.21	341	ND	ND
1873	1052	2.6%	0.35	369	0.21	442	ND	ND
1874	1001	2.6%	0.35	351	0.21	421	ND	ND
1875	865	2.7%	0.35	303	0.21	363	ND	ND
1876	940	2.7%	0.35	330	0.21	395	ND	ND
1877	882	2.8%	0.35	309	0.21	371	ND	ND
1878	985	2.8%	0.35	346	0.21	414	ND	ND
1879	940	2.9%	0.35	330	0.21	395	ND	ND
1880	812	2.9%	0.35	285	0.21	341	ND	ND
1881	947	3.0%	0.35	333	0.21	398	ND	ND
1882	981	3.0%	0.35	345	0.21	412	ND	ND
1883	1097	3.1%	0.35	386	0.21	461	ND	ND
1884	884	3.2%	0.35	311	0.21	372	ND	ND
1885	867	3.2%	0.35	305	0.21	364	ND	ND
1886	996	3.3%	0.35	351	0.21	419	ND	ND
1887	1066	3.3%	0.35	376	0.21	448	ND	ND
1888	1013	3.4%	0.35	357	0.21	426	ND	ND
1889	1051	3.4%	0.35	371	0.21	442	ND	ND
1890	1285	3.5%	0.35	454	0.21	540	ND	ND
1891	972	3.7%	0.35	344	0.21	409	ND	ND
1892	830	3.9%	0.35	294	0.21	349	ND	ND
1893	961	4.1%	0.36	341	0.21	404	ND	ND
1894	716	4.4%	0.36	255	0.21	301	ND	ND
1895	699	4.6%	0.36	249	0.21	294	ND	ND
1896	1126	4.8%	0.36	403	0.21	473	ND	ND
1897	891	5.0%	0.36	319	0.21	374	ND	ND
1898	908	5.3%	0.36	326	0.21	382	ND	ND
1899	860	5.5%	0.36	309	0.21	361	ND	ND
1900	654	5.7%	0.36	236	0.21	275	ND	ND
1901	1035	5.9%	0.36	374	0.21	413	ND	ND
1902	818	6.2%	0.36	296	0.21	310	ND	ND
1903	986	6.4%	0.36	357	0.21	352	ND	ND
1904	858	6.6%	0.36	311	0.21	288	ND	ND
1905	894	7.4%	0.37	327	0.21	282	ND	ND
1906	795	8.2%	0.37	293	0.21	234	ND	ND

Year	Annual Precipitation (mm)	Impervious Cover (%)	Ric	Impervious Yield (mm)	Rhist	Infra. Yield	Additional ET (mm)	Additional Leakage (mm)
1907	885	9.0%	0.37	328	0.21	242	ND	ND
1908	766	9.8%	0.37	286	0.21	193	ND	ND
1909	843	10.6%	0.38	317	0.21	195	ND	ND
1910	808	11.4%	0.38	306	0.21	170	ND	ND
1911	1047	12.2%	0.38	399	0.21	220	ND	ND
1912	973	12.4%	0.38	372	0.21	204	ND	ND
1913	978	12.7%	0.38	374	0.21	205	ND	ND
1914	850	13.0%	0.38	326	0.21	179	ND	ND
1915	902	13.2%	0.38	347	0.21	189	ND	ND
1916	885	13.5%	0.39	341	0.21	186	ND	ND
1917	836	13.8%	0.39	323	0.21	175	ND	ND
1918	828	14.0%	0.39	321	0.21	174	ND	ND
1919	1105	14.3%	0.39	429	0.21	232	ND	ND
1920	855	14.6%	0.39	333	0.21	180	ND	1
1921	980	15.1%	0.39	383	0.21	206	ND	1
1922	758	15.7%	0.39	297	0.21	159	ND	1
1923	1055	16.3%	0.39	416	0.21	221	ND	2
1924	958	16.8%	0.40	379	0.21	201	ND	2
1925	716	17.4%	0.40	285	0.21	150	ND	2
1926	900	17.9%	0.40	360	0.21	189	ND	3
1927	1096	18.5%	0.40	440	0.21	230	ND	3
1928	885	19.0%	0.40	357	0.21	186	ND	3
1929	938	19.6%	0.40	380	0.21	197	ND	3
1930	575	20.2%	0.41	234	0.21	121	ND	4
1931	990	20.3%	0.41	403	0.21	208	ND	4
1932	658	20.4%	0.41	268	0.21	138	ND	4
1933	1023	20.5%	0.41	417	0.21	215	ND	4
1934	804	20.6%	0.41	328	0.21	169	ND	5
1935	845	20.7%	0.41	345	0.21	177	ND	5
1936	977	20.8%	0.41	399	0.21	205	ND	5
1937	957	20.9%	0.41	391	0.21	201	ND	6
1938	844	21.0%	0.41	345	0.21	177	0	6
1939	802	21.1%	0.41	329	0.21	169	0	6
1940	1057	21.2%	0.41	433	0.21	222	1	7
1941	873	21.2%	0.41	358	0.21	183	1	7
1942	1064	21.3%	0.41	437	0.21	223	2	7
1943	881	21.3%	0.41	362	0.21	185	2	7
1944	1029	21.3%	0.41	422	0.21	216	3	7
1945	1224	21.3%	0.41	502	0.21	257	3	8

Year	Annual Precipitation (mm)	Impervious Cover (%)	Ric	Impervious Yield (mm)	Rhist	Infra. Yield	Additional ET (mm)	Additional Leakage (mm)
1946	743	21.3%	0.41	305	0.21	156	3	8
1947	762	21.3%	0.41	313	0.21	160	4	8
1948	987	21.3%	0.41	405	0.21	207	4	8
1949	858	21.3%	0.41	352	0.21	180	5	8
1950	1229	21.3%	0.41	504	0.21	258	5	9
1951	1147	21.3%	0.41	471	0.21	241	5	9
1952	958	21.3%	0.41	393	0.21	201	6	9
1953	793	21.3%	0.41	325	0.21	166	6	9
1954	914	21.4%	0.41	375	0.21	192	7	9
1955	886	21.4%	0.41	364	0.21	186	7	9
1956	1135	21.4%	0.41	466	0.21	238	8	9
1957	855	21.4%	0.41	351	0.21	180	8	9
1958	948	21.4%	0.41	389	0.21	199	8	10
1959	981	21.4%	0.41	403	0.21	206	9	10
1960	795	21.4%	0.41	326	0.21	167	9	10
1961	968	21.4%	0.41	398	0.21	203	10	10
1962	803	21.5%	0.41	330	0.21	169	10	10
1963	680	21.5%	0.41	280	0.21	143	11	10
1964	962	21.6%	0.41	396	0.21	202	11	10
1965	768	21.6%	0.41	316	0.21	161	12	10
1966	865	21.6%	0.41	356	0.21	182	12	10
1967	924	21.7%	0.41	380	0.21	194	13	10
1968	916	21.7%	0.41	377	0.21	192	13	10
1969	751	21.7%	0.41	309	0.21	158	14	10
1970	962	21.8%	0.41	396	0.21	202	14	11
1971	844	21.8%	0.41	348	0.21	177	15	11
1972	1018	21.8%	0.41	419	0.21	214	15	11
1973	1009	21.9%	0.41	416	0.21	212	16	11
1974	1062	21.9%	0.41	438	0.21	223	17	11
1975	1179	21.9%	0.41	486	0.21	248	17	11
1976	807	22.0%	0.41	333	0.21	170	18	11
1977	843	22.0%	0.41	348	0.21	177	18	11
1978	960	22.1%	0.41	396	0.21	202	19	11
1979	1030	22.1%	0.41	425	0.21	216	19	11
1980	1002	22.1%	0.41	414	0.21	210	20	11
1981	953	22.2%	0.41	393	0.21	200	20	11
1982	813	22.2%	0.41	336	0.21	171	21	11
1983	1052	22.2%	0.41	435	0.21	221	21	11
1984	897	22.3%	0.41	371	0.21	188	22	11

Year	Annual Precipitation (mm)	Impervious Cover (%)	Ric	Impervious Yield (mm)	Rhist	Infra. Yield	Additional ET (mm)	Additional Leakage (mm)
1985	978	22.3%	0.41	405	0.21	205	23	11
1986	950	22.3%	0.41	393	0.21	199	23	12
1987	996	22.4%	0.41	412	0.21	209	24	12
1988	688	22.4%	0.41	285	0.21	144	24	12
1989	1080	22.5%	0.41	447	0.21	227	25	12
1990	1327	22.5%	0.41	550	0.21	279	25	12
1991	813	22.5%	0.41	337	0.21	171	26	12
1992	931	22.6%	0.41	386	0.21	195	26	12
1993	972	22.6%	0.41	403	0.21	204	27	12
1994	1050	22.6%	0.41	435	0.21	221	28	12
1995	734	22.7%	0.41	304	0.21	154	28	12
1996	1155	22.7%	0.41	479	0.21	243	29	12
1997	878	22.7%	0.41	364	0.21	184	29	13
1998	869	22.8%	0.42	361	0.21	182	30	13
1999	920	22.8%	0.42	382	0.21	193	30	13
2000	1019	22.9%	0.42	423	0.21	214	31	13
2001	908	22.9%	0.42	377	0.21	191	31	13
2002	821	22.9%	0.42	341	0.21	172	32	13
2003	1042	23.0%	0.42	433	0.21	219	33	14
2004	1458	23.0%	0.42	606	0.21	306	33	14
2005	1047	23.0%	0.42	436	0.21	220	34	14
2006	886	23.1%	0.42	369	0.21	186	34	15
2007	1034	23.1%	0.42	430	0.21	217	35	15
2008	1008	23.1%	0.42	420	0.21	212	35	15
2009	834	23.2%	0.42	347	0.21	175	36	16
2010	961	23.2%	0.42	400	0.21	202	36	16
2011	1265	23.2%	0.42	527	0.21	266	36	16
2012	1060	23.2%	0.42	442	0.21	223	36	17

APPENDIX B

DATA TABLES FOR CHAPTER 3

Table B 1: Urbanization gradient hydrologic metrics.

Site and Gage Name	USGS Gage Number	Drainage Area (km^2)	Baseflow Index	High Flow Frequency	High Flow Length (Days)	Maximum Flow ($m^3/sec/km^2$)
ATLbigCrk	02335700	190.6	0.16	21.5	2.1	0.26
ATLfallCrk	02212600	188.0	0.01	11.8	3.5	0.21
ATLnancyCrk	02336410	96.5	0.18	30.9	2.0	0.35
ATLnoonday	02392950	65.5	0.08	27.4	2.0	0.53
ATLnosesCrk	02336968	114.5	0.08	21.4	2.3	0.30
ATLsnakeCrk	02337500	92.3	0.24	7.2	4.0	0.27
ATLsopeCrk	02335870	79.5	0.11	30.2	1.6	0.48
ATLsuwanee	02334885	122.1	0.14	25.2	2.1	0.30
ATLtworun	02395120	84.0	0.24	10.8	2.7	0.24
BESbaisman	01583580	3.9	0.23	15.4	1.8	0.12
BESdeadrun	01589330	14.2	0.06	42.1	1.8	0.61
BESgwynDel	01589197	10.6	0.23	31.1	1.7	0.39
BESgwynGly	01589180	0.8	0.03	31.2	1.8	0.45
BESgwynVill	01589300	84.5	0.18	31.6	2.0	0.35
BESgwynWash	01589352	159.1	0.19	35.1	2.0	0.38
BESherbert	01589100	6.4	0.14	40.0	1.5	0.40
BESjones	01589440	65.1	0.23	21.3	1.7	0.30
BESltpatuxen	01593500	98.0	0.12	29.3	1.9	0.30
BESmooresRad	01585230	9.1	0.08	43.4	1.3	0.47
BESpondb	01583570	0.4	0.28	16.2	1.7	0.07
BESsawmill	01589500	12.6	0.48	23.9	2.1	0.15
BESsfork	01589795	2.5	0.32	23.2	2.1	0.41

Site and Gage Name	USGS Gage Number	Drainage Area (km^2)	Baseflow Index	High Flow Frequency	High Flow Length (Days)	Maximum Flow ($m^3/sec/km^2$)
BESwestbr	01585200	6.0	0.09	41.5	1.3	0.34
BESwhitmar	01585100	19.7	0.06	38.3	2.0	0.61
BOSaberjon	01102500	59.7	0.10	19.5	2.9	0.27
BOSipswichSmid	01101500	115.3	0.03	7.4	9.5	0.16
BOSnashoba	01097300	30.9	0.03	14.7	3.2	0.21
BOSneponset	01105000	84.9	0.09	11.4	4.3	0.16
BOSneponsetEbr	01105500	60.7	0.13	13.8	3.5	0.21
BOSoyster	01073000	31.3	0.03	14.2	3.5	0.33
BOSparker	01101000	55.5	0.03	6.7	10.7	0.18
BOSsegreg	01109070	27.2	0.01	14.8	4.5	0.36
BOSsquann	01096000	173.1	0.10	11.7	4.1	0.27
BOSstillwtr	01095220	78.7	0.04	12.0	4.0	0.26
BOStownbrk	01105585	11.1	0.18	25.8	1.2	0.13
BOSwading	01109000	112.7	0.06	9.6	5.8	0.15
CAPcavecrk	09512280	188.7	0.00	4.8	3.9	0.10
CAPindian	09512162	212.4	0.00	6.8	2.7	0.03
CAPnewriver	09513780	177.5	0.00	3.3	21.7	0.14
CAPskunk	09513860	170.1	0.00	3.5	1.6	0.03
CAPsycam	09510200	425.3	0.00	4.5	8.6	0.09
DETepond	04164100	55.0	0.19	11.2	5.0	0.07
DETpaint	04161540	186.0	0.21	14.2	3.0	0.07
DETplum	04163400	47.0	0.09	23.6	2.5	0.17
DETrouge	04166000	85.8	0.18	20.7	2.4	0.12
DETstone	04161580	64.3	0.17	11.6	3.8	0.05
DETuroug	04166300	45.6	0.22	22.9	3.2	0.15
PDXbeaver	14142800	28.8	0.02	18.0	2.7	0.36
PDXbullwilh	14198400	1.8	0.03	8.8	7.3	0.48
PDXfanno56	14206900	6.2	0.04	26.0	1.8	0.29
PDXfannodur	14206950	80.7	0.06	21.0	1.5	0.26
PDXfircrk	14138870	14.0	0.08	14.6	4.7	0.85
PDXjohnmilw	14211550	137.3	0.20	12.8	4.0	0.19
PDXjohnregn	14211400	39.8	0.03	12.1	4.8	0.33
PDXjohnsyc	14211500	68.5	0.03	12.8	4.1	0.30
PDXltsandy	14141500	59.9	0.10	14.2	4.3	0.68
PDXnforkBull	14138900	21.7	0.16	15.2	4.2	1.06
PITltpine	03049800	14.9	0.05	19.5	3.2	0.32
PITmontour	03085956	67.1	0.12	27.9	1.9	0.31
PITninemile	03085049	15.8	0.14	37.3	1.3	0.23

Site and Gage Name	USGS Gage Number	Drainage Area (km^2)	Baseflow Index	High Flow Frequency	High Flow Length (Days)	Maximum Flow ($m^3/sec/km^2$)
PITredston	03074500	191.1	0.18	15.8	3.0	0.19
PITsawmill	03085213	46.5	0.23	39.3	1.0	0.22
PITthomp	03084800	40.1	0.34	25.0	1.2	0.20
RALmarsh	0208732885	17.8	0.07	38.2	2.0	0.43
RALmount	0208524090	20.7	0.02	17.1	2.4	0.30
RALnecreek	0209741955	54.6	0.21	27.2	2.5	0.34
RALnewhope	02097314	197.3	0.13	18.8	3.2	0.29
RALrocky	0208735012	3.1	0.07	40.3	1.2	0.65
RALwalnut	02087359	77.0	0.10	31.1	2.3	0.29
RALwhiteoak	0209782609	31.1	0.00	22.8	2.2	0.37
STPkitts	NA	4.5	0.13	33.3	1.5	0.29
STPphalen	NA	5.8	0.40	24.0	1.3	0.21
STPshingle	05288705	73.0	0.06	9.2	4.1	0.05
STPstant	NA	13.8	0.31	20.7	1.3	0.15
STPtroutE	NA	3.3	0.43	24.0	2.0	0.18
STPtroutW	NA	21.0	0.24	17.2	1.5	0.12

Table B 2: Urbanization gradient urban characteristics.

Site and Gage Name	Population Density (ppl/km^2)	Road Density (km/km^2)	Impervious Cover (%)	Developed Land (%)	Septic Households (%)	Sewer Households (%)
ATLbigCrk	302	3.8	14.5	50.3	52.0%	47.4%
ATLfallCrk	2	0.8	0.1	3.8	96.3%	1.6%
ATLnancyCrk	885	6.7	24.0	74.2	6.3%	93.6%
ATLnoonday	443	5.1	26.6	72.9	12.3%	87.7%
ATLnosesCrk	507	4.6	11.0	49.4	25.3%	74.4%
ATLsnakeCrk	54	2.0	1.4	8.0	77.2%	21.7%
ATLsopeCrk	891	7.2	20.3	76.7	11.2%	88.8%
ATLsuwanee	264	3.6	17.8	56.8	50.1%	49.4%
ATLtworun	48	1.9	1.9	11.8	93.2%	3.9%
BESbaisman	98	1.5	1.0	25.1	98.7%	0.1%
BESdeadrun	1,086	8.9	39.1	95.2	0.5%	99.4%
BESgwynDel	1,585	8.4	16.9	78.4	6.2%	93.4%
BESgwynGly	1,064	8.6	19.6	74.4	7.0%	93.0%
BESgwynVill	1,207	7.0	19.1	65.8	4.4%	95.3%
BESgwynWash	1,867	8.6	26.4	75.7	1.6%	97.7%
BESherbert	1,825	9.9	38.4	91.3	0.1%	99.8%
BESjones	284	3.8	4.9	33.9	34.4%	65.0%
BESltpatuxen	874	5.9	13.6	58.7	3.9%	96.0%
BESmooresRad	2,953	12.6	32.4	97.6	0.3%	99.5%
BESpondb	78	0.0	0.0	0.0	98.7%	0.0%
BESsawmill	331	5.1	21.2	66.6	33.3%	66.8%
BESsfork	104	3.7	7.2	35.6	95.1%	4.9%
BESwestbr	1,882	9.6	24.2	86.6	0.6%	99.4%
BESwhitmar	1,629	8.0	27.8	84.8	1.9%	98.0%
BOSaberjon	1,096	7.9	41.9	81.5	3.9%	96.0%
BOSipswichSmid	461	4.9	19.6	54.7	63.8%	35.9%
BOSnashoba	171	2.8	11.0	31.7	72.1%	24.4%
BOSneponset	460	4.2	16.9	46.7	30.6%	69.3%
BOSneponsetEbr	609	5.2	21.5	55.6	34.7%	65.0%
BOSoyster	74	2.1	2.2	11.5	77.3%	22.7%
BOSparker	165	2.8	4.7	17.9	89.3%	10.3%
BOSsegreg	99	1.8	4.3	14.7	91.9%	7.9%
BOSsquann	77	2.0	2.2	8.8	89.1%	10.4%
BOSstillwtr	52	1.7	1.6	7.6	91.9%	7.9%
BOStownbrk	1,415	9.6	51.3	86.8	0.4%	99.6%
BOSwading	229	2.9	10.5	30.7	77.0%	22.6%
CAPcavecrk	0	0.5	0.2	0.1	93.2%	5.8%

Site and Gage Name	Population Density (ppl/km^2)	Road Density (km/km^2)	Impervious Cover (%)	Developed Land (%)	Septic Households (%)	Sewer Households (%)
CAPindian	627	5.7	21.0	53.2	6.7%	93.2%
CAPnewriver	0	0.3	0.1	0.0	94.9%	4.9%
CAPskunk	24	1.8	1.9	14.5	94.5%	3.7%
CAPsycam	0	0.5	0.2	0.8	77.3%	7.8%
DETepond	51	2.5	2.6	17.6	89.5%	10.5%
DETpaint	332	3.9	10.2	41.6	29.5%	70.0%
DETplum	937	7.0	29.5	92.2	5.3%	94.7%
DETrouge	656	7.3	23.6	90.2	12.4%	87.6%
DETstone	88	2.4	1.8	11.8	85.4%	14.6%
DETuroug	818	6.9	29.2	79.7	8.0%	92.0%
PDXbeaver	843	5.9	24.1	56.1	9.8%	90.3%
PDXbullwilh	0	0.0	0.0	0.0	100.0%	0.0%
PDXfanno56	1,522	12.9	31.0	85.6	0.9%	99.0%
PDXfannodur	1,484	10.0	39.5	89.0	5.5%	94.5%
PDXfircrk	0	0.2	0.0	0.0	68.1%	31.9%
PDXjohnmilw	1,245	8.0	30.3	66.6	39.3%	60.3%
PDXjohnregn	191	3.8	9.4	33.0	60.9%	38.7%
PDXjohnsyc	458	4.8	14.6	42.7	30.5%	69.2%
PDXltsandy	1	1.6	0.0	0.0	91.0%	7.1%
PDXnforkBull	0	1.4	0.0	0.0	ND	ND
PITltpine	204	3.2	4.6	28.2	34.3%	64.5%
PITmontour	212	3.4	21.0	56.4	11.9%	87.8%
PITninemile	2,397	14.1	40.5	83.8	0.3%	99.3%
PITredston	207	3.2	7.5	24.1	24.8%	74.6%
PITsawmill	2,194	13.4	33.5	90.5	0.4%	99.6%
PITthomp	909	6.9	28.9	71.3	3.8%	96.2%
RALmarsh	1,003	6.8	29.6	94.8	6.0%	93.8%
RALmount	45	2.0	1.4	9.4	94.9%	0.1%
RALnecreek	255	3.7	14.4	57.2	18.1%	81.7%
RALnewhope	439	4.3	8.8	40.4	10.2%	89.4%
RALrocky	971	9.4	37.5	99.0	0.5%	99.5%
RALwalnut	1,054	7.2	21.3	81.3	3.2%	96.5%
RALwhiteoak	317	3.8	7.7	32.6	83.1%	13.4%
STPkitts	2,438	15.3	56.0	99.5	0.0%	99.9%
STPphalen	3,176	15.3	59.0	98.2	0.1%	99.9%
STPshingle	1,026	7.1	34.2	80.6	0.4%	99.6%
STPstant	1,356	10.6	55.0	97.0	0.0%	99.9%
STPtroutE	2,959	13.1	45.0	96.0	0.4%	99.5%
STPtroutW	1,774	9.6	37.0	90.8	0.3%	99.5%

Table B 3: Urbanization gradient watershed characteristics.

Site and Gage Name	Dam Storage (Ml/km^2)	Lake Density (no./km^2)	Permeability (in/hr)	Mean Slope (%)	Annual Precipitation (cm)	Snow as Precip (%)
ATLbigCrk	48.4	1.3	1.7	4.3	140	4.2
ATLfallCrk	16.0	0.3	1.8	4.8	122	1.0
ATLnancyCrk	29.3	0.8	1.6	4.4	136	3.0
ATLnoonday	50.5	1.4	1.6	4.3	137	4.0
ATLnosesCrk	12.0	1.5	1.6	3.8	139	3.8
ATLsnakeCrk	17.5	0.7	1.8	5.1	136	2.0
ATLsopeCrk	15.1	1.2	1.6	4.1	137	4.0
ATLsuwanee	3.8	1.2	1.8	4.4	139	3.9
ATLtworun	7.1	1.3	1.0	3.8	135	3.5
BESbaisman	0.0	0.3	2.0	6.6	116	12.5
BESdeadrun	0.0	0.1	1.2	2.7	115	11.5
BESgwynDel	0.0	0.7	1.8	3.2	115	13.1
BESgwynGly	0.0	0.0	1.6	9.7	115	13.1
BESgwynVill	1.1	0.4	1.7	3.6	116	12.9
BESgwynWash	7.5	0.3	1.5	3.7	115	12.0
BESherbert	0.0	1.1	2.3	3.5	113	11.0
BESjones	0.2	1.0	1.8	5.1	117	12.3
BESltpatuxen	37.2	0.7	1.6	3.2	114	12.7
BESmooresRad	0.0	0.0	1.8	3.0	120	11.0
BESpondb	0.0	0.0	2.0	12	116	12.5
BESsawmill	0.0	0.2	10.7	1.5	109	11.0
BESsfork	0.0	0.0	6.3	1.9	112	11.0
BESwestbr	16.3	0.5	2.5	3.4	121	11.1
BESwhitmar	0.0	0.7	3.1	3.8	120	11.3
BOSaberjon	49.9	2.5	7.8	3.3	121	26.6
BOSipswichSmid	73.1	2.0	8.1	2.0	120	26.7
BOSnashoba	2.8	2.6	7.8	2.9	117	27.0
BOSneponset	62.2	2.9	8.6	2.7	122	26.0
BOSneponsetEbr	62.8	2.3	9.9	2.3	124	24.7
BOSoyster	0.0	0.7	5.9	3.0	112	30.4
BOSparker	29.6	2.5	5.6	3.1	120	26.0
BOSsegreg	1.7	2.5	2.3	1.6	124	24.0
BOSsquann	35.0	1.4	5.2	5.8	122	29.1
BOSstillwtr	27.6	0.7	3.8	6.5	128	28.8
BOStownbrk	60.9	0.9	6.4	3.9	122	24.2
BOSwading	38.7	2.7	7.3	1.6	125	24.8
CAPcavecrk	0.0	0.1	5.2	21.1	51	0.5

Site and Gage Name	Dam Storage (Ml/km^2)	Lake Density (no./km^2)	Permeability (in/hr)	Mean Slope (%)	Annual Precipitation (cm)	Snow as Precip (%)
CAPindian	0.0	0.2	2.6	4.6	30	0.0
CAPnewriver	0.0	0.2	3.5	22.5	53	0.8
CAPskunk	0.0	0.1	1.5	9.8	35	0.0
CAPsycam	0.0	0.0	4.1	21.4	61	2.1
DETepond	20.9	1.1	3.0	2.1	81	22.0
DETpaint	44.1	1.7	5.6	1.8	80	21.4
DETplum	0.0	0.7	2.8	0.6	82	21.0
DETrouge	12.8	2.0	3.8	1.7	80	21.2
DETstone	42.2	1.2	3.2	1.9	80	21.8
DETuroug	0.0	1.6	1.9	1.8	81	21.9
PDXbeaver	7.6	0.6	1.8	4.1	146	11.3
PDXbullwilh	0.0	0.0	2.3	36.1	227	22.7
PDXfanno56	0.0	0.0	1.0	11.4	116	9.4
PDXfannodur	0.0	0.7	1.0	5.9	107	9.9
PDXfircrk	0.0	0.4	3.3	27.1	312	36.0
PDXjohnmilw	0.4	0.8	1.9	5.5	134	10.0
PDXjohnregn	0.0	1.4	0.9	7.3	156	11.3
PDXjohnsyc	0.5	1.2	1.2	7.7	149	10.8
PDXltsandy	0.0	0.3	2.3	18.2	273	28.8
PDXnforkBull	0.0	0.6	2.7	19.0	332	32.0
PITltpine	0.0	0.3	1.8	11.7	101	16.4
PITmontour	31.8	0.7	2.8	7.2	97	17.6
PITninemile	0.0	0.1	1.7	8.5	99	15.5
PITredston	0.6	0.6	2.6	9.8	114	19.0
PITsawmill	0.0	0.2	2.0	10.3	98	17.0
PITthomp	0.0	0.3	2.0	9.6	101	16.7
RALmarsh	10.9	1.4	1.5	1.9	118	4.0
RALmount	9.6	1.1	1.4	4.1	119	5.7
RALnecreek	21.5	1.6	1.3	2.2	118	4.0
RALnewhope	2.4	1.2	1.2	3.5	121	4.8
RALrocky	0.0	0.3	1.4	2.1	119	3.2
RALwalnut	66.1	1.1	1.4	2.4	119	3.3
RALwhiteoak	2.3	3.3	1.3	2.5	119	4.0
STPkitts	0.0	0.0	8.1	1.2	80	17.4
STPphalen	0.0	0.0	2.3	1.2	81	17.4
STPshingle	0.0	2.0	7.0	1.2	80	17.4
STPstant	0.0	0.1	4.7	1.2	80	17.4
STPtroutE	0.0	0.3	6.8	1.2	81	17.4
STPtroutW	0.0	0.6	8.4	1.2	81	17.4

APPENDIX C

DATA TABLES FOR CHAPTER 4

Table C 1: Building density reconstructions.

Year	Building Density (bld/km^2)					
	Little Patuxent River	Gywnns Falls Villa	Dead Run	Abers Creek	Aberjona River	Neponset River
1900	0.6	42.9	112.3	0.8	53.7	10.9
1910	0.6	44.4	113.9	1.2	62.0	12.8
1920	0.8	46.2	118.1	2.0	76.7	16.9
1930	1.0	51.0	136.9	2.4	96.6	23.8
1940	1.5	54.8	149.4	3.8	111.9	31.2
1950	2.6	64.1	180.1	8.4	135.9	42.1
1960	14.7	137.2	314.6	65.0	213.6	70.6
1970	57.1	205.2	438.9	247.5	245.6	95.0
1980	174.4	232.5	489.0	301.9	269.6	106.1
1990	260.6	281.9	565.6	324.8	294.3	117.8
2000	293.6	359.2	577.8	332.5	311.9	131.1
2010	ND	ND	ND	335.9	322.8	139.8

Table C 2: **Hydrologic records for long-term watersheds.**

Dead Run, Baltimore, MD					
Year	Annual High Flow Frequency	Total Annual Flow (mm)	Total Annual Baseflow (mm)	Total Annual Precipitation (mm)	Runoff Efficiency
1960	ND	422	122	1190	0.25
1961	25	529	159	1087	0.34
1962	23	340	80	1023	0.25
1963	26	218	56	1006	0.16
1964	33	386	108	882	0.31
1965	31	261	74	717	0.26
1966	23	356	79	1077	0.26
1967	36	476	110	939	0.39
1968	28	423	93	1012	0.33
1969	39	267	81	854	0.22
1970	42	343	112	900	0.26
1971	38	761	162	1355	0.44
1972	41	753	198	1330	0.42
1973	47	552	152	1164	0.34
1974	50	401	122	959	0.29
1975	49	799	187	1317	0.47
1976	47	573	134	1104	0.40
1977	42	447	114	925	0.36
1978	41	564	151	1055	0.39
1979	40	1040	210	1499	0.55
1980	42	438	111	883	0.37
1981	43	444	95	793	0.44
1982	42	406	114	920	0.32
1983	38	761	141	1297	0.48
1984	48	699	150	939	0.58
1985	40	379	98	935	0.30
1986	31	ND	ND	ND	ND
1987	45	395	116	856	0.33
1999	40	536	100	1117	0.39
2000	46	440	125	1065	0.30
2001	38	395	91	879	0.35
2002	40	446	76	1006	0.37
2003	43	946	207	1592	0.46
2004	47	579	130	1161	0.39
2005	37	708	152	1248	0.45
2006	36	605	138	1099	0.42

Year	Annual High Flow Frequency	Total Annual Flow (mm)	Total Annual Baseflow (mm)	Total Annual Precipitation (mm)	Runoff Efficiency
2007	32	390	83	889	0.35
2008	47	614	98	1143	0.45
2009	43	750	134	1412	0.44
2010	45	624	148	1105	0.43
2011	45	849	139	1436	0.49
2012	48	ND	ND	ND	ND
Gwynns Falls Villa Nova, Baltimore, MD					
Year	Annual High Flow Frequency	Total Annual Flow (mm)	Total Annual Baseflow (mm)	Total Annual Precipitation (mm)	Runoff Efficiency
1957	14	ND	ND	ND	ND
1958	27	486	311	1148	0.15
1959	18	220	143	964	0.08
1960	30	337	205	1190	0.11
1961	22	330	212	1087	0.11
1962	21	319	186	1023	0.13
1963	21	253	149	1006	0.10
1964	21	304	191	882	0.13
1965	19	235	157	717	0.11
1966	14	243	133	1077	0.10
1967	25	355	177	939	0.19
1968	20	330	191	1012	0.14
1969	21	242	151	854	0.11
1970	31	305	192	900	0.13
1971	31	580	271	1355	0.23
1972	24	818	403	1330	0.31
1973	23	560	336	1164	0.19
1974	33	394	227	959	0.17
1975	40	637	315	1317	0.24
1976	34	438	255	1104	0.17
1977	21	362	195	925	0.18
1978	32	539	293	1055	0.23
1979	30	835	379	1499	0.30
1980	25	389	251	883	0.16
1981	26	291	151	793	0.18
1982	31	346	187	920	0.17
1983	20	575	284	1297	0.22
1984	35	654	322	939	0.35
1985	21	288	168	935	0.13

Year	Annual High Flow Frequency	Total Annual Flow (mm)	Total Annual Baseflow (mm)	Total Annual Precipitation (mm)	Runoff Efficiency
1986	16	259	146	856	0.13
1987	32	387	209	1043	0.17
1988	34	ND	ND	ND	ND
1997	28	415	259	974	0.16
1998	32	497	266	874	0.26
1999	27	550	290	1117	0.23
2000	39	410	230	1065	0.17
2001	27	320	187	879	0.15
2002	23	303	143	1006	0.16
2003	33	806	383	1592	0.27
2004	38	499	276	1161	0.19
2005	26	500	228	1248	0.22
2006	34	500	243	1099	0.23
2007	25	334	196	889	0.15
2008	29	378	180	1143	0.17
2009	31	534	236	1412	0.21
2010	32	438	262	1105	0.16
2011	40	667	244	1436	0.29
2012	34	489	207	951	0.30
Little Patuxent River, Baltimore, MD					
Year	Annual High Flow Frequency	Total Annual Flow (mm)	Total Annual Baseflow (mm)	Total Annual Precipitation (mm)	Runoff Efficiency
1933	26	468	291	ND	ND
1934	29	415	252	ND	ND
1935	15	465	302	ND	ND
1936	20	431	274	ND	ND
1937	28	542	321	ND	ND
1938	24	255	207	ND	ND
1939	16	290	214	437	0.17
1940	19	363	220	1067	0.13
1941	20	239	186	803	0.07
1942	16	300	171	1105	0.12
1943	25	335	229	888	0.12
1944	19	273	172	1017	0.10
1945	23	459	242	1073	0.20
1946	20	301	223	882	0.09
1947	13	225	152	1089	0.07
1948	29	413	252	1559	0.10

1949	15	383	282	923	0.11
1950	22	367	239	978	0.13
1951	27	415	281	1164	0.12
1952	33	602	326	1438	0.19
1953	13	525	334	1226	0.16
1954	13	191	159	709	0.04
1955	14	325	173	1122	0.13
1956	14	272	201	1005	0.07
1957	18	281	182	863	0.11
1958	21	491	299	1148	0.17
1959	19	254	169	964	0.09
1960	28	353	232	1190	0.10
1961	14	430	273	1087	0.14
1962	15	328	210	1023	0.12
1963	17	256	155	1006	0.10
1964	20	329	215	882	0.13
1965	18	240	182	717	0.08
1966	12	259	160	1077	0.09
1967	18	320	211	939	0.12
1968	19	321	189	1012	0.13
1969	17	252	154	854	0.11
1970	23	339	210	900	0.14
1971	32	673	308	1355	0.27
1972	21	856	447	1330	0.31
1973	18	580	356	1164	0.19
1974	26	357	212	959	0.15
1975	35	632	310	1317	0.24
1976	31	413	247	1104	0.15
1977	19	318	176	925	0.15
1978	34	455	263	1055	0.18
1979	37	774	380	1499	0.26
1980	20	332	234	883	0.11
1981	20	220	135	793	0.11
1982	22	264	160	920	0.11
1983	16	614	248	1297	0.28
1984	25	537	301	939	0.25
1985	24	313	167	935	0.16
1986	15	245	139	856	0.12
1987	29	369	205	1043	0.16
1988	29	391	196	821	0.24
1989	36	635	281	1319	0.27

1990	32	448	224	1064	0.21
1991	30	315	179	767	0.18
1992	25	391	178	990	0.22
1993	22	532	282	1080	0.23
1994	29	504	250	1101	0.23
1995	24	351	178	940	0.18
1996	40	732	322	1481	0.28
1997	21	365	239	974	0.13
1998	26	439	235	874	0.23
1999	21	348	160	1117	0.17
2000	40	366	204	1065	0.15
2001	28	307	169	879	0.16
2002	17	247	122	1006	0.12
2003	29	749	347	1592	0.25
2004	30	430	259	1161	0.15
2005	27	492	224	1248	0.21
2006	30	473	212	1099	0.24
2007	24	307	176	889	0.15
2008	29	352	178	1143	0.15
2009	26	433	211	1412	0.16
2010	32	424	247	1105	0.16
2011	35	594	232	1436	0.25
2012	34	416	188	951	0.24
Aberjona River, Boston, MA					
Year	Annual High Flow Frequency	Total Annual Flow (mm)	Total Annual Baseflow (mm)	Total Annual Precipitation (mm)	Runoff Efficiency
1940	5	376	279	915	0.11
1941	6	186	153	785	0.04
1942	5	296	204	1079	0.09
1943	12	309	243	820	0.08
1944	12	279	205	942	0.08
1945	10	450	335	1221	0.09
1946	15	397	316	968	0.08
1947	9	289	219	963	0.07
1948	11	415	328	1030	0.08
1949	6	220	182	800	0.05
1950	4	231	184	831	0.06
1951	9	518	406	1194	0.09
1952	13	439	372	1032	0.07
1953	6	507	402	1467	0.07
1954	14	625	487	1584	0.09

Year	Annual High Flow Frequency	Total Annual Flow (mm)	Total Annual Baseflow (mm)	Total Annual Precipitation (mm)	Runoff Efficiency
1955	15	608	450	1436	0.11
1956	6	485	410	1204	0.06
1957	8	216	179	862	0.04
1958	4	562	450	1567	0.07
1959	17	380	263	1306	0.09
1960	11	366	273	1130	0.08
1961	5	461	354	1217	0.09
1962	10	567	398	1099	0.15
1963	12	356	278	886	0.09
1964	5	335	269	928	0.07
1965	7	146	91	603	0.09
1966	3	128	92	915	0.04
1967	9	381	271	1209	0.09
1968	8	370	257	1075	0.11
1969	14	492	330	1214	0.13
1970	12	399	291	1065	0.10
1971	9	290	226	906	0.07
1972	14	638	444	1350	0.14
1973	21	473	337	1087	0.13
1974	18	361	269	1023	0.09
1975	17	428	293	1164	0.12
1976	20	346	238	934	0.12
1977	8	497	331	1123	0.15
1978	18	382	255	957	0.13
1979	16	544	314	1123	0.21
1980	14	212	138	747	0.10
1981	14	291	177	908	0.13
1982	23	583	347	1134	0.21
1983	12	725	483	1362	0.18
1984	17	679	460	1276	0.17
1985	14	329	216	930	0.12
1986	19	451	275	1127	0.16
1987	12	529	356	1156	0.15
1988	14	353	247	884	0.12
1989	18	334	226	1078	0.10
1990	23	548	358	1182	0.16
1991	24	414	296	1074	0.11
1992	24	393	288	1112	0.09
1993	14	465	357	1099	0.10

Year	Annual High Flow Frequency	Total Annual Flow (mm)	Total Annual Baseflow (mm)	Total Annual Precipitation (mm)	Runoff Efficiency
1994	17	489	359	1211	0.11
1995	17	324	249	893	0.08
1996	17	697	450	1335	0.19
1997	16	363	286	773	0.10
1998	15	699	440	1363	0.19
1999	12	378	266	964	0.12
2000	21	488	341	1159	0.13
2001	18	513	317	781	0.25
2002	14	394	257	1044	0.13
2003	24	584	401	1128	0.16
2004	19	546	346	1133	0.18
2005	15	627	465	1110	0.15
2006	21	797	494	1344	0.23
2007	15	475	307	1003	0.17
2008	22	763	512	1385	0.18
2009	21	638	452	1106	0.17
2010	15	782	431	1262	0.28
2011	25	720	503	1331	0.16
2012	23	ND	ND	ND	ND
Neponset River, Boston, MA					
Year	Annual High Flow Frequency	Total Annual Flow (mm)	Total Annual Baseflow (mm)	Total Annual Precipitation (mm)	Runoff Efficiency
1940	ND	439	349	915	0.10
1941	3	269	211	785	0.07
1942	3	392	296	1079	0.09
1943	9	388	343	820	0.06
1944	4	308	246	942	0.07
1945	11	590	502	1221	0.07
1946	10	545	471	968	0.08
1947	10	407	337	963	0.07
1948	7	609	529	1030	0.08
1949	9	315	258	800	0.07
1950	3	330	281	831	0.06
1951	13	556	464	1194	0.08
1952	9	461	400	1032	0.06
1953	6	669	567	1467	0.07
1954	14	701	593	1584	0.07
1955	13	903	732	1436	0.12

Year	Annual High Flow Frequency	Total Annual Flow (mm)	Total Annual Baseflow (mm)	Total Annual Precipitation (mm)	Runoff Efficiency
1956	5	675	585	1204	0.08
1957	8	362	302	862	0.07
1958	6	753	618	1567	0.09
1959	13	609	477	1306	0.10
1960	17	593	505	1130	0.08
1961	10	674	588	1217	0.07
1962	7	604	488	1099	0.11
1963	10	446	369	886	0.09
1964	10	489	394	928	0.10
1965	3	243	201	603	0.07
1966	4	255	202	915	0.06
1967	7	570	464	1209	0.09
1968	12	589	433	1075	0.15
1969	11	649	509	1214	0.11
1970	10	602	490	1065	0.10
1971	10	413	354	906	0.07
1972	9	798	648	1350	0.11
1973	13	587	471	1087	0.11
1974	10	568	470	1023	0.10
1975	12	629	525	1164	0.09
1976	10	520	420	934	0.11
1977	6	607	497	1123	0.10
1978	18	650	521	957	0.13
1979	12	745	585	1123	0.14
1980	8	319	263	747	0.08
1981	2	320	260	908	0.07
1982	12	724	594	1134	0.11
1983	8	842	698	1362	0.11
1984	9	933	751	1276	0.14
1985	4	292	234	930	0.06
1986	10	593	473	1127	0.11
1987	3	727	619	1156	0.09
1988	10	501	422	884	0.09
1989	15	608	504	1078	0.10
1990	14	673	538	1182	0.11
1991	19	514	422	1074	0.09
1992	18	498	412	1112	0.08
1993	6	561	489	1099	0.07
1994	11	590	507	1211	0.07

Year	Annual High Flow Frequency	Total Annual Flow (mm)	Total Annual Baseflow (mm)	Total Annual Precipitation (mm)	Runoff Efficiency
1995	11	377	325	893	0.06
1996	12	887	742	1335	0.11
1997	12	491	426	773	0.08
1998	8	944	752	1363	0.14
1999	8	582	471	964	0.11
2000	13	554	454	1159	0.09
2001	6	529	431	781	0.13
2002	5	400	312	1044	0.08
2003	10	776	641	1128	0.12
2004	8	565	460	1133	0.09
2005	11	945	765	1110	0.16
2006	11	874	721	1344	0.11
2007	15	549	451	1003	0.10
2008	14	806	643	1385	0.12
2009	15	752	628	1106	0.11
2010	13	814	577	1262	0.19
2011	18	840	701	1331	0.10
2012	9	411	303	934	0.12
Abers Creek, Pittsburgh, PA					
Year	Annual High Flow Frequency	Total Annual Flow (mm)	Total Annual Baseflow (mm)	Total Annual Precipitation (mm)	Runoff Efficiency
1949	ND	355	243	841	0.13
1950	16	627	303	1230	0.26
1951	18	649	364	1147	0.25
1952	19	478	241	959	0.25
1953	23	330	214	794	0.15
1954	13	395	182	915	0.23
1955	9	357	230	887	0.14
1956	20	566	344	1134	0.20
1957	12	330	211	856	0.14
1958	16	391	240	949	0.16
1959	18	468	259	982	0.21
1960	19	309	214	796	0.12
1961	19	560	339	969	0.23
1962	18	493	262	804	0.29
1963	10	306	164	682	0.21
1964	14	448	220	964	0.24
1965	16	321	213	769	0.14

Year	Annual High Flow Frequency	Total Annual Flow (mm)	Total Annual Baseflow (mm)	Total Annual Precipitation (mm)	Runoff Efficiency
1966	13	352	184	866	0.19
1967	17	423	236	924	0.20
1968	15	308	176	917	0.14
1969	20	220	138	753	0.11
1970	23	420	239	964	0.19
1971	21	391	203	845	0.22
1972	25	610	385	1019	0.22
1973	26	399	249	1011	0.15
1974	34	449	256	1064	0.18
1975	28	534	300	1181	0.20
1976	24	400	193	809	0.26
1977	21	365	174	844	0.23
1978	22	511	189	961	0.34
1979	32	575	313	1031	0.25
1980	25	475	257	1003	0.22
1981	33	420	239	954	0.19
1982	30	346	215	814	0.16
1983	25	490	209	1052	0.27
1984	28	542	303	899	0.27
1985	19	506	232	979	0.28
1986	19	351	187	951	0.17
1987	33	410	243	997	0.17
1988	30	239	118	689	0.18
1989	24	411	249	1081	0.15
1990	29	514	280	1328	0.18
1991	25	255	153	814	0.13
1992	24	345	213	932	0.14
1993	24	ND	ND	ND	ND

BIBLIOGRAPHY

Alberti, M., D. Booth, K. Hill, B. Coburn, C. Avolio, S. Coe, and D. Spirandelli (2007), The impact of urban patterns on aquatic ecosystems: An empirical analysis in Puget lowland sub-basins, *Landscape and Urban Planning*, *80*(4), 345–361.

ALCOSAN, Allegheny County Sanitary Authority (2010), *Annual Combined Sewer Overflow Status Report*, Allegheny County Sanitary Authority, Pittsburgh, PA.

Alley, W. M., and J. E. Veenhuis (1983), Effective impervious area in urban runoff modeling, *Journal of Hydraulic Engineering*, *109*(2), 313–319.

Arnold, C. L., and C. J. Gibbons (1996), Impervious surface coverage: the emergence of a key environmental indicator, *Journal of the American Planning Association*, *62*(2), 243–258.

Bain, D. et al. (2014), Characterizing Major Urban Stream Restoration Projects: Nine Mile Run (Pittsburgh, PA, USA), *Journal of the American Water Resources Association*.

Bain, D. J., and G. S. Brush (2008), Gradients, property templates, and land use change, *The Professional Geographer*, *60*(2), 224–237.

Bain, D. J., J. A. . Arrigo, M. B. Green, B. A. Pellerin, and C. J. Vörösmarty (2011), Historical Legacies, Information and Contemporary Water Science and Management, *Water*, *3*(2), 566–575.

Bain, D. J., M. B. Green, J. L. Campbell, J. F. Chamblee, S. Chaoka, J. M. Fraterrigo, S. S. Kaushal, S. L. Martin, T. E. Jordan, and A. J. Parolari (2012a), Legacy effects in material flux: Structural catchment changes predate long-term studies, *BioScience*, *62*(6), 575–584.

Bain, D. J., R. L. Hale, and W. M. Wollheim (2012b), Hotbeds of Biogeochemical Diversity: Insights from Urban Long-Term Ecological Research Sites, *Elements*, *8*(6), 435–438.

Barringer, T. H., R. G. Reiser, and C. V. Price (1994), Potential effects of development on flow characteristics of two New Jersey streams, *Journal of the American Water Resources Association*, *30*(2), 283–295.

Benda, L., K. Andras, D. Miller, and P. Bigelow (2004), Confluence effects in rivers: interactions of basin scale, network geometry, and disturbance regimes, *Water Resources Research*, *40*(5).

Bernhardt, E. S., and M. A. Palmer (2007), Restoring streams in an urbanizing world, *Freshwater Biology*, *52*(4), 738–751.

Bhaskar, A. S., and C. Welty (2012), Water Balances along an Urban-to-Rural Gradient of Metropolitan Baltimore, 2001–2009, *Environmental & Engineering Geoscience*, *18*(1), 37–50.

Booth, D. B., and L. E. Reinelt (1993), Consequences of urbanization on aquatic systems-measured effects, degradation thresholds, and corrective strategies, in *Proceedings Watersheds ‘93*, pp. 545–550, U.S. Environmental Protection Agency, Alexandria, Virginia.

Booth, D. B., and C. R. Jackson (1997), Urbanization of aquatic systems: degradation thresholds, stormwater detection, and the limits of mitigation, *Journal of the American Water Resources Association*, *33*(5), 1077–1090.

Brandes, D., G. J. Cavallo, and M. L. Nilson (2005), Base flow trends in urbanizing watersheds of the Delaware River basin, *Journal of the American Water Resources Association*, *41*(6), 1377–1391.

Brown, R., N. Keath, and T. Wong (2009a), Urban water management in cities: historical, current and future regimes, *Water Science & Technology*, *59*(5), 847–855.

Brown, L. R., T. F. Cuffney, J. F. Coles, F. Fitzpatrick, G. McMahon, J. Steuer, A. H. Bell, and J. T. May (2009b), Urban streams across the USA: lessons learned from studies in 9 metropolitan areas, *Journal of the North American Benthological Society*, *28*(4), 1051–1069.

Buchan, J. (1948), *Reid's Practical Sanitation, 24th Edition*, Charles Griffen & Company, London, England.

Bürgi, M., A. M. Hersperger, and N. Schneeberger (2004), Driving forces of landscape change—current and new directions, *Landscape ecology*, *19*(8), 857–868.

Carter, T., C. R. Jackson, A. Rosemond, C. Pringle, D. Radcliffe, W. Tollner, J. Maerz, D. Leigh, and A. Trice (2009), Beyond the urban gradient: barriers and opportunities for timely studies of urbanization effects on aquatic ecosystems, *Journal of the North American Benthological Society*, *28*(4), 1038–1050.

Claessens, L., C. Hopkinson, E. Rastetter, and J. Vallino (2006), Effect of historical changes in land use and climate on the water budget of an urbanizing watershed, *Water Resources Research*, *42*(W03426), doi:10.1029/2005WR004131.

Clawges, R., and C. Price (1999), *Digital data set describing surficial geology in the conterminous US*, U.S. Geological Survey, Reston, VA.

Collins, S. L., S. R. Carpenter, S. M. Swinton, D. E. Orenstein, D. L. Childers, T. L. Gragson, N. B. Grimm, J. M. Grove, S. L. Harlan, and J. P. Kaye (2011), An integrated conceptual framework for long-term social-ecological research, *Frontiers in Ecology and the Environment*, *9*(6), 351–357.

Costa, J. E. (1974), Response and recovery of a Piedmont watershed from tropical storm Agnes, June 1972, *Water Resources Research*, *10*(1), 106–112.

Cuo, L., D. P. Lettenmaier, M. Alberti, and J. E. Richey (2009), Effects of a century of land cover and climate change on the hydrology of the Puget Sound basin, *Hydrological Processes*, *23*(6), 907–933.

DeAngelis, R., and W. T. Hodge (1972), *Preliminary Climatic Data Report Hurricane Agnes, June 14-23*, National Oceanic and Atmospheric Administration, Environmental Data Service, Ashville, NC.

DeGasperi, C. L., H. B. Berge, K. R. Whiting, J. J. Burkey, J. L. Cassin, and R. R. Fuerstenberg (2009), Linking Hydrologic Alteration to Biological Impairment in Urbanizing Streams of the Puget Lowland, Washington, USA, *Journal of the American Water Resources Association*, *45*(2), 512–533.

Deletic, A. (1998), The first flush load of urban surface runoff, *Water Research*, *32*(8), 2462–2470.

DeWalle, D. R., B. R. Swistock, T. E. Johnson, and K. J. McGuire (2000), Potential effects of climate change and urbanization on mean annual streamflow in the United States, *Water Resources Research*, *36*(9), 2655–2664.

Divers, M., E. Elliott, and D. Bain (2013), Constraining nitrogen inputs to urban streams from leaking sewers using inverse modeling: Implications for DIN retention in urban environments, *Environmental Science & Technology*, *47*(4), 1816–1823.

Driscoll, C. T., D. Whitall, J. Aber, E. Boyer, M. Castro, C. Cronan, C. L. Goodale, P. Groffman, C. Hopkinson, and K. Lambert (2003), Nitrogen pollution in the northeastern United States: Sources, effects, and management options, *BioScience*, *53*(4), 357–374.

Driver, N. E., and B. M. Troutman (1989), Regression models for estimating urban storm-runoff quality and quantity in the United States, *Journal of Hydrology*, *109*(3), 221–236.

Ellis, J. B., D. M. Revitt, D. J. Blackwood, and D. J. Gilmour (2004), Leaky sewers: assessing the hydrology and impact of exfiltration in urban sewers, *Hydrology: Science & Practices for the 21st Century, Volume II*.

Falcone, J. (2011), *GAGES II: Geospatial attributes of gages for evaluating streamflow*, NSDI Node, U. S. Geological Survey, Reston, VA.

Fitzpatrick, F. A., M. W. Diebel, M. A. Harris, T. L. Arnold, M. A. Lutz, and K. D. Richards (2005), Effects of urbanization on the geomorphology, habitat, hydrology, and fish index of biotic integrity of streams in the Chicago area, Illinois and Wisconsin, in *American Fisheries Society Symposium*, vol. 47, pp. 87–115.

Gleick, P. H. (1996), Basic water requirements for human activities: Meeting basic needs, *Water International*, *21*(2), 83–92.

Gregory, J. H., M. D. Dukes, P. H. Jones, and G. L. Miller (2006), Effect of urban soil compaction on infiltration rate, *Journal of soil and water conservation*, *61*(3), 117–124.

Grimm, N. B., S. H. Faeth, N. E. Golubiewski, C. L. Redman, J. Wu, X. Bai, and J. M. Briggs (2008), Global change and the ecology of cities, *Science*, *319*(5864), 756.

Grimm, N. B., F. S. Chapin III, B. Bierwagen, P. Gonzalez, P. M. Groffman, Y. Luo, F. Melton, K. Nadelhoffer, A. Pairis, and P. A. Raymond (2013), The impacts of climate change on ecosystem structure and function, *Frontiers in Ecology and the Environment*, *11*(9), 474–482.

Groffman, P. M., D. J. Bain, L. E. Band, K. T. Belt, G. S. Brush, J. M. Grove, R. V. Pouyat, I. C. Yesilonis, and W. C. Zipperer (2003), Down by the riverside: urban riparian ecology, *Frontiers in Ecology and the Environment*, *1*(6), 315–321.

Groffman, P. M., J. Cavender-Bares, N. D. Bettez, J. M. Grove, S. J. Hall, J. B. Heffernan, S. E. Hobbie, K. L. Larson, J. L. Morse, and C. Neill (2014), Ecological homogenization of urban USA, *Frontiers in Ecology and the Environment*, *12*(1), 74–81.

Grove, J. M., A. R. Troy, J. P. M. O'Neil-Dunne, W. R. Burch Jr, M. L. Cadenasso, and S. T. A. Pickett (2006a), Characterization of households and its implications for the vegetation of urban ecosystems, *Ecosystems*, *9*(4), 578–597.

Grove, J. M., M. L. Cadenasso, W. R. Burch Jr, S. T. Pickett, K. Schwarz, J. O'Neil-Dunne, M. Wilson, A. Troy, and C. Boone (2006b), Data and methods comparing social structure and vegetation structure of urban neighborhoods in Baltimore, Maryland, *Society and Natural Resources*, *19*(2), 117–136.

Heath, R. (1984), *Ground-water regions of the United States*, Water Supply Paper 2242, United State Geological Survey, Washington, DC.

Hibbert, A. R. (1966), *Forest treatment effects on water yield*, Pergamon Press, Oxford, NY.

Hopkins, G. M. (1911), Real estate plat-book for the city of Pittsburgh, *Historic Pittsburgh*. Available from: http://digital.library.pitt.edu/maps (Accessed 19 July 2012).

Hopkins, K. G., D. J. Bain, and E. M. Copeland (2014), Reconstruction of a century of landscape modification and hydrologic change in a small urban watershed in Pittsburgh, PA, *Landscape Ecology*, *29*(3), 413–424.

Horton, R. E. (1945), Erosional development of streams and their drainage basins; hydrophysical approach to quantitative morphology, *Geological society of America bulletin*, *56*(3), 275–370.

Janke, B. D., J. C. Finlay, S. E. Hobbie, L. A. Baker, R. W. Sterner, D. Nidzgorski, and B. N. Wilson (2013), Contrasting influences of stormflow and baseflow pathways on nitrogen and phosphorus export from an urban watershed, *Biogeochemistry*, 1–20.

Jennings, D., and T. Jarnagin (2002), Changes in anthropogenic impervious surfaces, precipitation and daily streamflow discharge: a historical perspective in a mid-Atlantic subwatershed, *Landscape Ecology*, *17*(5), 471–489.

Kaushal, S. S., and K. T. Belt (2012), The urban watershed continuum: evolving spatial and temporal dimensions, *Urban Ecosystems*, *15*(2), 409–435.

Kendall, M. G. (1938), A new measure of rank correlation, *Biometrika*, *30*(1-2), 81–89.

Klein, R. D. (1979), Urbanization and stream quality impairment, *Journal of the American Water Resources Association*, *15*(4), 948–963.

Konrad, C. P., and D. B. Booth (2005), Hydrologic changes in urban streams and their ecological significance, in *American Fisheries Society Symposium*, vol. 47, pp. 157–177.

Lavendel, B. (2002), The business of ecological restoration, *Ecological Restoration*, *20*(3), 173–178.

Lee, J. G., and J. P. Hearney (2003), Estimation of urban imperviousness and its impacts on storm water systems, *Journal of Water Resources Planning and Management*, *129*(5), 419–426.

Leopold, L. B., R. Huppman, and A. Miller (2005), Geomorphic effects of urbanization in forty-one years of observation, *Proceedings of the American Philosophical Society*, *149*(3), 349–371.

Lerner, D. N. (2002), Identifying and quantifying urban recharge: a review, *Hydrogeology Journal*, *10*(1), 143–152.

Lins, H. F., and J. R. Slack (1999), Streamflow trends in the United States, *Geophysical Research Letters*, *26*(2), 227–230.

Lookingbill, T. R., S. S. Kaushal, A. J. Elmore, R. Gardner, K. N. Eshleman, R. H. Hilderbrand, R. P. Morgan, W. R. Boynton, M. A. Palmer, and W. C. Dennison (2009), Altered ecological flows blur boundaries in urbanizing watersheds, *Ecology and Society*, *14*(2), 10.

Markewich, H. W., M. J. Pavich, and G. R. Buell (1990), Contrasting soils and landscapes of the Piedmont and Coastal Plain, eastern United States, *Geomorphology*, *3*(3), 417–447.

Mathews, R., and B. D. Richter (2007), Application of the Indicators of Hydrologic Alteration Software in Environmental Flow Setting, *Journal of the American Water Resources Association*, *43*(6), 1400–1413.

McCabe, G., and D. Wolock (2002), A step increase in streamflow in the conterminous United States, *Geophysical Research Letters*, *29*(24), 38–1–38–4.

McDonnell, M. J., and S. T. Pickett (1990), Ecosystem structure and function along urban-rural gradients: an unexploited opportunity for ecology, *Ecology*, *71*(4), 1232–1237.

McShane, C. (1979), Transforming the Use of Urban Space: A Look at the Revolution in Street Pavements, 1880-1924, *Journal of Urban History*, *5*(3), 279–307.

Meyer, G. (2007), *Surficial geology of the Twin Cities Metropolitan Area, Minnesota*, Minnesota Geological Survey, Minneapolis, MN.

Meyer, J. L., M. J. Paul, and W. K. Taulbee (2005), Stream ecosystem function in urbanizing landscapes, *Journal of the North American Benthological Society*, *24*(3), 602–612.

Micevski, T., G. Kuczera, and P. Coombes (2002), Markov model for storm water pipe deterioration, *Journal of Infrastructure Systems*, *8*(2), 49–56.

Minnesota Population Center (2011), *National Historical Geographic Information System: Version 2.0*, University of Minnesota, Minneapolis, MN.

MSA SC, State Roads Commission of Maryland (1969), *State of Maryland: State Highway Systems and Connections*, 4409-2-42, State Roads Commission of Maryland, Brooklandville, MD.

Muggeo, V. (2003), Estimating regression models with unknown break-points, *Stastics in Medicine*, *22*(19), 3055–3071.

Nelson, P. A., J. A. Smith, and A. J. Miller (2006), Evolution of channel morphology and hydrologic response in an urbanizing drainage basin, *Earth Surface Processes and Landforms*, *31*(9), 1063–1079.

Newbury, R. I., D. J. Belz, and R. G. Crubb (1981), Soil Survey of Allegheny County, Pennsylvania,

O'Driscoll, M., S. Clinton, A. Jefferson, A. Manda, and S. McMillan (2010), Urbanization effects on watershed hydrology and in-stream processes in the southern United States, *Water*, *2*(3), 605–648.

Ogle, M. (1996), *All the modern conveniences : American household plumbing, 1840-1890*, Johns Hopkins University Press, Baltimore, MD.

Olson, S. H. (1979), Baltimore imitates the spider, *Annals of the Association of American Geographers*, *69*(4), 557–574.

Paul, M. J., and J. L. Meyer (2001), Streams in the urban landscape, *Annual Review of Ecology and Systematics*, *32*, 333–365.

Poff, N. L., and J. K. Zimmerman (2010), Ecological responses to altered flow regimes: a literature review to inform the science and management of environmental flows, *Freshwater Biology*, *55*(1), 194–205.

Poff, N. L. ., J. D. Allan, M. B. Bain, J. R. Karr, K. L. Prestegaard, B. D. Richter, R. E. Sparks, and J. C. Stromberg (1997), The natural flow regime, *BioScience*, *47*(11), 769–784.

Poff, N. L. ., B. P. Bledsoe, and C. O. Cuhaciyan (2006), Hydrologic variation with land use across the contiguous United States: geomorphic and ecological consequences for stream ecosystems, *Geomorphology*, *79*(3-4), 264–285.

Poff, N. L., J. D. Olden, D. M. Merritt, and D. M. Pepin (2007), Homogenization of regional river dynamics by dams and global biodiversity implications, *Proceedings of the National Academy of Sciences*, *104*(14), 5732–5737.

Power, M. E., A. Sun, G. Parker, W. E. Dietrich, and J. T. Wootton (1995), Hydraulic food-chain models, *BioScience, 45*(3), 159–167.

PPC, Pittsburgh Parks Conservancy (2011), *Restoring the health of Panther Hollow: A plan for watershed restoration*, Meliora, Andropogon, and Rothschild Doyno Collaborative, Pittsburgh, PA.

Price, K. (2011), Effects of watershed topography, soils, land use, and climate on baseflow hydrology in humid regions: A review, *Progress in Physical Geography*, *35*(4), 465–492.

Richter, B. D., J. V. Baumgartner, J. Powell, and D. P. Braun (1996), A method for assessing hydrologic alteration within ecosystems, *Conservation Biology*, *10*(4), 1163–1174.

Roy, A. H., S. J. Wenger, T. D. Fletcher, C. J. Walsh, A. R. Ladson, W. D. Shuster, H. W. Thurston, and R. R. Brown (2008), Impediments and solutions to sustainable, watershed-scale urban stormwater management: lessons from Australia and the United States, *Environmental Management*, *42*(2), 344–359.

Roy, A. H., A. H. Purcell, C. J. Walsh, and S. J. Wenger (2009), Urbanization and stream ecology: five years later, *Journal of the North American Benthological Society*, *28*(4), 908–910.

Sanders, R. A. (1986), Urban vegetation impacts on the hydrology of Dayton, Ohio, *Urban Ecology*, *9*(3-4), 361–376.

Scalenghe, R., and F. A. Marsan (2009), The anthropogenic sealing of soils in urban areas, *Landscape and Urban Planning*, *90*(1), 1–10.

Schneider, A., and C. E. Woodcock (2008), Compact, dispersed, fragmented, extensive? A comparison of urban growth in twenty-five global cities using remotely sensed data, pattern metrics and census information, *Urban Studies*, *45*(3), 659–692.

Schueler, T. R. (1994), The importance of imperviousness, *Watershed protection techniques*, *1*(3), 100–111.

Schueler, T. R., L. Fraley-McNeal, and K. Cappiella (2009), Is impervious cover still important? review of recent research, *Journal of Hydrologic Engineering*, *14*(4), 309–315.

Seto, K. C., R. Sánchez-Rodríguez, and M. Fragkias (2010), The new geography of contemporary urbanization and the environment, *Annual Review of Environment and Resources*, *35*, 167–194.

Seto, K. C., B. Güneralp, and L. R. Hutyra (2012), Global forecasts of urban expansion to 2030 and direct impacts on biodiversity and carbon pools, *Proceedings of the National Academy of Sciences*, *109*(40), 16083–16088.

Shuster, W. D., J. Bonta, H. Thurston, E. Warnemuende, and D. R. Smith (2005), Impacts of impervious surface on watershed hydrology: A review, *Urban Water*, *2*(4), 263–275.

Shuster, W. D., S. Dadio, P. Drohan, R. Losco, and J. Shaffer (2014), Residential demolition and its impact on vacant lot hydrology: Implications for the management of stormwater and sewer system overflows, *Landscape and Urban Planning*, *125*, 48–56.

Steele, M. K., J. B. Heffernan, N. Bettez, J. Cavender-Bares, P. M. Groffman, J. M. Grove, S. Hall, S. E. Hobbie, K. Larson, and J. L. Morse (2014), Convergent surface water distributions in US cities, *Ecosystems*, *17*(4), 685–697.

Tarr, J. A., J. McCurley, F. C. McMichael, and T. Yosie (1984), Water and wastes: a retrospective assessment of wastewater technology in the United States, 1800-1932, *Technology and Culture*, *25*(2), 226–263.

Tarr, J. A. (2005), *Devastation and renewal: An environmental history of Pittsburgh and its region*, University of Pittsburgh Press, Pittsburgh, PA.

Thomas, M. A. (2000), Tthe effect of residential development on ground-water quality near Detroit, Michigan, *Journal of the American Water Resources Association*, *36*(5), 1023–1038.

United Nations Population Division (UNDP) (2009), *World Population Prospects: The 2008 Revision and World Urbanization Prospects: The 2009 Revision*, Population Division of the Department of Economic and Social Affairs of the United Nations Secretariat.

University of Pittsburgh's Digital Research Library (2012a), G. M. Hopkins Company Maps, 1872-1940, *Historic Pittsburgh*. Available from: http://digital.library.pitt.edu/maps (Accessed 19 July 2012).

University of Pittsburgh (2012b), Historic Pittsburgh Image Collection, *Archives Service Center at the University of Pittsburgh*. Available from: http://digital.library.pitt.edu/images (Accessed 19 July 2012).

UTC (2012), *Urban Tree Canopy (UTC) Assessment for Pittsburgh*, University of Vermont Spatial Analysis Laboratory, Burlingon, VT.

Utz, R. M., K. N. Eshleman, and R. H. Hilderbrand (2011), Variation in physicochemical responses to urbanization in streams between two Mid-Atlantic physiographic regions, *Ecological Applications*, *21*(2), 402–415.

VanBriessen, J., and M. Schoen (2007), *Panther Hollow E Coli Sampling Report*, Carnegie Mellon University, Water Quest Program.

Wagner, W. (1970), *Geology of the Pittsburgh Area*, Pittsburgh Geological Society, Commonwealth of Pennsylvania, Pittsburgh, PA.

Walsh, C. J., A. H. Roy, J. W. Feminella, P. D. Cottingham, P. M. Groffman, and R. P. Morgan II (2005a), The urban stream syndrome: current knowledge and the search for a cure, *Journal of the North American Benthological Society*, *24*(3), 706–723.

Walsh, C. J., T. D. Fletcher, and A. R. Ladson (2005b), Stream restoration in urban catchments through redesigning stormwater systems: looking to the catchment to save the stream, *Journal of the North American Benthological Society*, *24*(3), 690–705.

Wenger, S. J., A. H. Roy, C. R. Jackson, E. S. Bernhardt, T. L. Carter, S. Filoso, C. A. Gibson, W. C. Hession, S. S. Kaushal, and E. Martí (2009), Twenty-six key research questions in urban stream ecology: an assessment of the state of the science, *Journal of the North American Benthological Society*, *28*(4), 1080–1098.

Williams, G. P., and M. G. Wolman (1984), *Downstream effects of dams on alluvial rivers*, Geological Survey Professional Paper 1286, US Government Printing Office, Washington, DC.

Wirahadikusumah, R., D. Abraham, and T. Iseley (2001), Challenging issues in modeling deterioration of combined sewers, *Journal of infrastructure systems*, *7*(2), 77–84.

Wollheim, W. M., M. B. Green, B. A. Pellerin, N. B. Morse, and C. S. Hopkinson (2013), Causes and Consequences of Ecosystem Service Regionalization in a Coastal Suburban Watershed, *Estuaries and Coasts*, 1–16.

Wolman, M. G. (1967), A cycle of sedimentation and erosion in urban river channels, *Geografiska Annaler. Series A. Physical Geography*, 385–395.

Wolock, D. (1997), *STATSGO soil characteristics for the conterminous United States*, U.S. Geological Survey, Lawrence, KS.

Xiao, Q., E. G. McPherson, J. R. Simpson, and S. L. Ustin (1998), Rainfall interception by Sacramento's urban forest, *Journal of Arboriculture*, *24*, 235–244.